10-25-2012

Mechanisms of Chloroperoxidase-catalyzed Enantioselective Reactions as Probed by Site-directed Mutagenesis and Isotopic Labeling

Lin Jiang
Florida International University, ljian002@fiu.edu

FLORIDA INTERNATIONAL UNIVERSITY

Miami, Florida

MECHANISMS OF CHLOROPEROXIDASE-CATALYZED ENANTIOSELECTIVE

REACTIONS AS PROBED BY SITE-DIRECTED MUTAGENESIS AND ISOTOPIC

LABELING

A dissertation submitted in partial fulfillment of the

requirements for the degree of

DOCTOR OF PHILOSOPHY

in

CHEMISTRY

by

Lin Jiang

2012

To: Dean Kenneth Furton
      College of Arts and Sciences

This dissertation, written by Lin Jiang, and entitled Mechanisms of Chloroperoxidase-catalyzed Enantioselective Reactions as Probed by Site-directed Mutagenesis and Isotopic Labeling, having been approved in respect to style and intellectual content, is referred to you for judgment.

We have read this dissertation and recommend that it be approved.

_____
David Chatfield

_____
Kevin O'Shea

_____
Jaroslava Miksovska

_____
Lou Kim

_____
Xiaotang Wang, Major Professor

Date of Defense: October 25, 2012

The dissertation of Lin Jiang is approved.

_____
Dean Kenneth Furton
College of Arts and Sciences

_____
Dean Lakshmi Reddi
University Graduate School

Florida International University, 2012

DEDICATION

I dedicate this dissertation to my mother Yanhong Miao and my father Peizhong Jiang. Without their understanding, encouragement, support, and most of all love, the completion of this work would not have been possible.

ACKNOWLEDGMENTS

ABSTRACT OF THE DISSERTATION

MECHANISMS OF CHLOROPEROXIDASE-CATALYZED ENANTIOSELECTIVE

REACTIONS AS PROBED BY SITE-DIRECTED MUTAGENESIS AND ISOTOPIC

LABELING

by

Lin Jiang

Florida International University, 2012

Miami, Florida

Professor Xiaotang Wang, Major Professor

Chloroperoxidase (CPO) is a heme-containing glycoprotein secreted by the marine fungus *Caldariomyces fumago*. Chloroperoxidase contains one ferriprotoporphyrin IX prosthetic group per molecule and catalyzes a variety of reactions, such as halogenation, peroxidation and epoxidation. The versatile catalytic activities of CPO coupled with the increasing demands for chiral synthesis have attracted an escalating interest in understanding the mechanistic and structural properties of this enzyme.

In order to better understand the mechanisms of CPO-catalyzed enantioselective reactions and to fine-tune the catalytic properties of chloroperoxidase, asparagine 74 (N74) located in the narrow substrate access channel of CPO was replaced by a bulky, nonpolar valine and a polar glutamine using site-directed mutagenesis. The CPO N74 mutants displayed significantly enhanced activity toward nonpolar substrates compared to wild-type CPO as a result of changes in space and polarity of the heme distal environment. More interestingly, N74 mutants showed dramatically decreased chlorination and catalase activity but significantly enhanced epoxidation activity as a

consequence of improved kinetic perfection introduced by the mutation as reflected by the favorable changes in k_{cat} and k_{cat}/K_M of these reactions. It is also noted that the N74V mutant is capable of decomposing cyanide, the most notorious poison for many hemoproteins, as judged by the unique binding behavior of N74V with potassium cyanide.

Histidine 105 (H105) was replaced by a nonpolar amino acid alanine using site-directed mutagenesis. The CPO H105 mutant (H105A) displayed dramatically decreased chlorination and catalase activity possibly because of the decreased polarity in the heme distal environment and loss of the hydrogen bonds between histidine 105 and glutamic acid 183. However, significantly increased enantioselectivity was observed for the epoxidation of bulky styrene derivatives. Furthermore, my study provides strong evidence for the proposed histidine/cysteine ligand switch in chloroperoxidase, providing experimental support for the structure of the 420-nm absorption maximum for a number of carbon monoxide complexes of heme-thiolate proteins.

For the NMR study, [dCPO(heme)] was produced using 90% deuterated growth medium with excess heme precursors and [dCPO(Phe)] was grown in the same highly deuterated medium that had been supplemented with excess natural phenylalanine. To make complete heme proton assignments, NMR spectroscopy has been performed for high-resolution structural characterization of [dCPO(heme)] and [dCPO(Phe)] to achieve unambiguous and complete heme proton assignments, which also allows important amino acids close to the heme active center to be determined.

TABLE OF CONTENT

LIST OF TABLES

LIST OF FIGURES

LIST OF ABBREVIATIONS AND ACRONYMS

ABBREVIATION	FULL NAME
ABTS	2,2'-azino-bis-3-ethyl-benzthiazoline-6-sulfonic acid
ALA	δ-Aminolevulinic acid
Ala/A	Alanine
A.niger	*Aspergillus niger*
Asn/N	Asparagine
ATCC	American type culture collection
C*c*O	Cytochrome *c* oxidase
C*c*P	Cytochrome *c* peroxidase
CD	Circular dichroism spectra
C. fumago	*Caldariomyces fumago*
CN	Cyanide
CooA	CO-sensing transcriptional activator
COSY	Correlation spectroscopy
CPD	Cyclopentanedione
Cpd I	Compound I
Cpd II	Compound II
CPO	Chloroperoxidase
Cys/C	Cysteine
DEAE	Diethylaminoethyl (cellulose)
DMF	*N,N*-dimethylformamide

DMSO	Dimethyl sulfoxide
DNA	Deoxyribonucleic acid
ε	Extinction coefficient
ee	Enantiomeric excess
ER	Endoplasmic reticulum
GLA	Glucoamylase
Gln/Q	Glutamine
His/H	Histidine
HPLC	High performance liquid chromatography
HRP	Horseradish peroxidase
KCN	Potassium cyanide
MCD	Monochlorodimedone
NADH	Nicotinamide adenine dinucleotide, reduced
NADPH	Nicotinamide adenine dinucleotide phosphate, reduced
NMR	Nuclear magnetic resonance spectroscopy
NOE	Nuclear overhauser effect
NOESY	Nuclear overhauser enhancement spectroscopy
P450	Cytochrome P450 mono-oxygenase
PCR	Polymerase chain reaction
Phe/F	Phenylalanine
pI	Isoelectric point
rCPO	Recombinant chloroperoxidase

Rz value	Reinheitzahl value
SDS-PAGE	Sodium dodecyl sulfate polyacrylamide gel electrophoresis
T1	Spin-lattice relation time
UV-Vis	Ultraviolet-Visible
Val/V	Valine
Wt CPO	Wild-type chloroperoxidase

CHAPTER I

INTRODUCTION

1.1 Overview of hemoproteins

Hemoproteins are one of the largest classes of metalloproteins and in most cases contain a unique prosthetic group of iron-protoporphyrin IX in the active site (Montellano 1987). Ferriprotoporphyrin IX is composed of four pyrrole rings joined by methyne bridges with a ferric iron at the center, replacing the two hydrogen atoms that are attached to the pyrrole nitrogens. The carbon atoms of the methene bridges are symbolized as α, β, γ, and δ characters (Dunford 1999). The eight side chains in the ferriprotoporphyrin IX are four methyl groups at the 1, 3, 5, and 8 positions, two vinyl groups at the 2 and 4 positions, and two propionate groups at the 6 and 7 positions. The structure of the six coordinated heme iron allows histidine, cysteine or other amino acids in the enzyme to serve as the fifth ligand and external substrates to covalently bind to the heme iron as the sixth ligand (Williams 1987; Bertini 1994; Lu 2009).

There are four main types of heme prothetic groups that contain a planar iron-tetrapyrrole ring system with different side chains (Figure 1.1). Heme a can function as a cofactor for the cytochrome aa_3 in the respiratory protein cytochrome c oxidase (CcO). Heme b (ferriprotoporphyrin IX) is the most abundant and important prothetic group among these four heme species, since heme b serves as the catalytic center for chloroperoxidase, catalase, hemoglobin, myoglobin, heme peroxidases, b-type cytochromes, and cytochrome P450s. Heme c is the prosthetic group for the extensively studied c-type electron transfer cytochromes. Heme d_1 normally exists in the heme-

containing nitrite reductases designated to carry out the reduction of nitrite (Silvestrini 1994; Malatesta 1995; Scott 1996).

Hemoproteins are involved in a wide range of biological processes and carry out many essential metabolic functions (Sono 1996; Dunford 1999). It is concluded that the type of heme groups and the amino acid arrangment around the central heme are important to direct the heme to a prescribed function specifically and efficiently. The most familiar category is oxygen transport proteins, which are multisubunit and circulating molecules that provide an efficient supply of oxygen to metabolically active metazoans, including hemoglobin and myoglobin. Cytochromes, another class of heme-containing proteins, are generally found either as monomeric proteins or as subunits of bigger enzymatic complexes that function as parts of the active membrane and electron transfer components to catalyze redox reactions. In addition to these traditional heme-containing proteins, a new class of hemoproteins termed the heme-based sensor proteins has been reported recently such as guanylyl cyclase, FixL, and CO-sensing transcriptional activator (CooA), in which the heme acts as a sensor of an effector molecule (Lippard 1994; Dunford 1999; Lu 2001).

1.2 Imidazole- and thiolate-ligated hemoproteins

Enzymatic functions of hemoproteins are significantly affected by the polarity of the heme binding site and axial coordination to the central iron, especially the nature of the proximal ligand attached to the heme. In most heme peroxidases, the proximal heme ligand is a histidine nitrogen, while in catalase, tyrosine oxygen serves as the fifth heme iron ligand (Frew 1984; Dunford 1999). However, in cytochromes P450 and CPO, the cysteine sulphor is involved in covalent binding to the heme iron (Moore 1990).
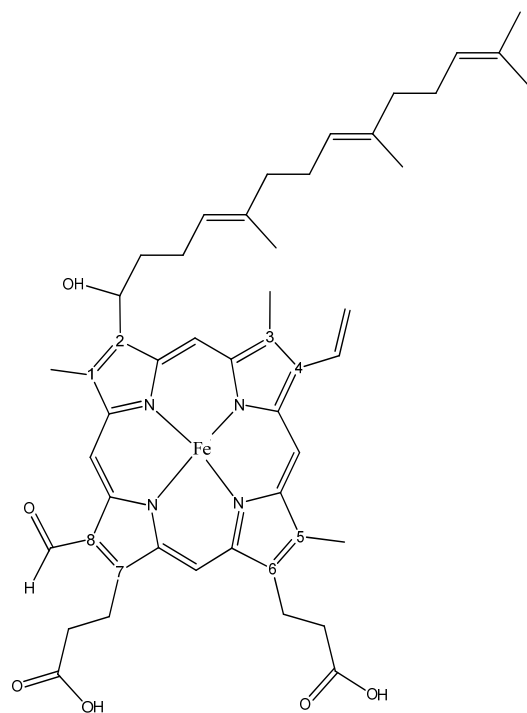
A. Heme *a*
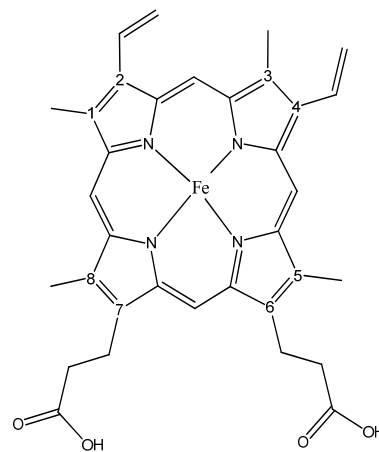
B. Heme *b*
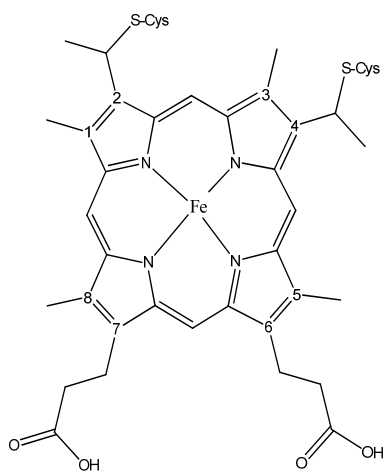
C. Heme *c*
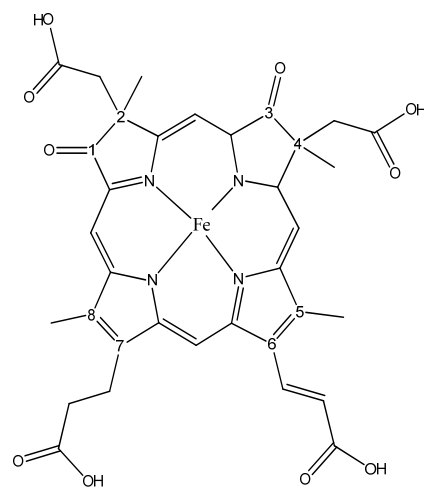
D. Heme d_1

Fig 1.1 Structure of the iron protoporphyrin IX (Heme *b*) and its derivatives usually found in hemoproteins.

Therefore, depending on the type of the proximal ligands bound to the heme iron, hemoproteins are separated into two different classes (Frew 1984). The first one is the imidazole-ligated protein with an imidazole group from histidine as the proximal ligand, including myoglobin, horseradish peroxidase and cytochrome c peroxidase. The other class is the thiolate-ligated protein that uses cysteine as the fifth ligand. The heme thiolate proteins include chloroperoxidase, cytochrome P450 and nitric oxide synthase. The histidine-ligated proteins are able to bind dioxygen reversibly and carry out their specific functions depending on amino acids near the heme center. However, the heme-thiolate proteins normally function as enzymes that catalyze the breakage of the oxygen-oxygen bond (Li 1994; Lu 2001; Omura 2005). The explanation for the reactivity differences between the thiolate- and imidazole-ligated heme proteins is that the proximal thiolate is more electron rich and pushes electrons more strongly to the central iron, thus making it more powerful to catalyze the related cleavage of O-O bond (Auclair 2001; Omura 2005).

The imidazole and thiolate ligated heme proteins also show dramatic differences in their spectral properties in their carbon monoxide complexes. When the proximal ligand is a histidine, the Soret absorption peak of the ferrous hemoprotein-CO complex is located at 420 nm (Choudhury and M. F. 1994). However, the proximal cysteine gives a Soret peak at 450 nm for the ferrous protein (Dawson 1988; Hofrichter 2006). Therefore, carbon monoxide is an efficient substrate to identify the proximal ligands of hemoproteins (Sono 1996; Ortiz de Montellano 1998; Omura 2005).
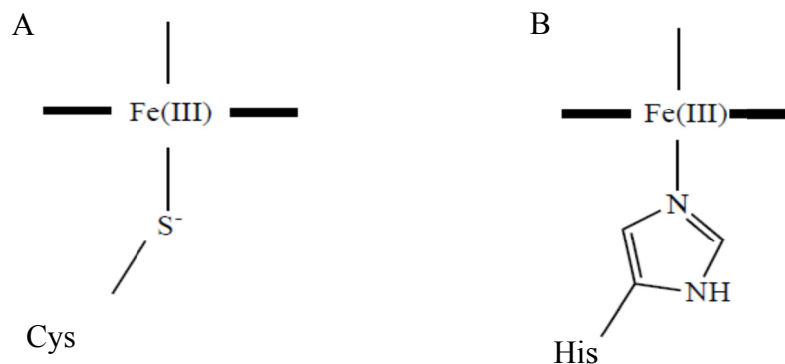
Fig 1.2 Structure of cysteine-(A) and histidine-(B) ligated heme active center.

1.3 Heme thiolate proteins

Heme thiolate proteins are a group of hemoproteins in which the prosthetic group is a protoheme with the thiolate anion of a cysteine residue as the axial ligand (Omura 2005). When carbon monoxide binds to the reduced heme iron, heme thiolate proteins exhibit a characteristic optical absorption spectrum with a prominent Soret peak around 450 nm. Cytochrome P450 was the first hemoprotein discovered to exhibit a 450-nm absorption peak in comparison with many other known hemoproteins that showed a 420-nm absorption peak when bound to carbon monoxide. The highly conserved amino acide sequence "FXXGXRXCXG" around the proximal cysteine residue in cytochromes P450 is named "heme-binding region", which has been confirmed by X-ray crystallographic analysis (Poulos 1987).

The second heme thiolate protein discovered is chloroperoxidase, an extracellular enzyme isolated from the growth media of a marine fungus *Caldaryomyces fumago*. Chloroperoxidase also display a P450-like optical absorbance when bound with carbon monoxide (Dawson 1987). The proximal heme binding ligand of chloroperoxidase has

been confirmed to be a thiolate anion (Dawson 1976), but the P450-like "heme-binding region" has not been identified in CPO's primary sequence (Fang 1986).

The third and fourth members of the heme thiolate protein family are cystathionine β-synthase (H-450) and nitric oxide synthase (NOS) because their carbon monoxide bound spectrum show P450-type peaks at 450 nm and 443 nm, respectively (Omura 1984; White 1992). The heme-containing domains of H-450 and NOS elucidated in the 1990s showed no sequence homology with cytochrome P450 enzymes, although the amino acid sequence of NOS structurally resembled cytochrome P450 reductase (Ishihara 1990; Bredt 1991).

In recent years, CooA of bacterium *Rhodospirillum rubrum* and heme-regulated eIF2α kinase of animals joined the heme thiolate protein family (Aono 1998; Igarawshi 2004). The protein CooA is a carbon monoxide sensor and transcriptional regulator, which activates the expression of a variety of enzymes participating in the oxidation of carbon monoxide. Heme-regulated eIF2α kinase regulates protein synthesis in reticulocytes by phosphorylating eIF2α factor when activated by nitric oxide. Both CooA and heme-regulated eIF2α kinase employ a thiolate anion as the proximal ligand in the oxidized form, but the axial ligand of the heme prosthetic group can be displaced when the heme is reduced and bound to either carbon monoxide or nitric oxide (Aono 1998; Igarawshi 2004).

1.4 Engineering of hemoproteins

Well-studied hemoproteins are primary targets of enzyme engineering because of their distinct activities and versatile functions with almost the same heme prosthetic

group. For protein engineering, there are two basic methods: rational design and directed evolution (Lu 2009).

In rational design, such as site-directed mutagenesis, replacement of specific amino acid in the sequence is carried out by examing the detailed structure of the target protein. Therefore, rational design is not applicable to some new proteins without detailed structural knowledge. Furthermore, it is very difficult to predict the results of certain mutations in the protein structure. Computational protein design is another rational method to pre-specify the structure by finding out the lowest energy to stabilize the structure of proteins. However, inaccuracy of the predicted protein structure is an apparent drawback for the application of computational protein design (Voigt 2001; Dantas 2003) .

In directed evolution, random mutagenesis at a selected sequence region is carried out, which mimics natural evolution (Voigt 2001). The advantage of directed evolution technique is that it is applicable to all proteins without detailed structure. Also it is not necessary to predict the effects of random mutation. However, directed evolution requires large amounts of recombinant DNA for screening and is not applicable for some proteins (Antonini 1971; Dawson 1988; Adachi 1993).

Hemoproteins have special structural components and binding properties around the heme prosthetic group, which give them the diversity of functions and unique spectroscopic characteristics. The unique identity in the proximal site and the catalytic residues in the distal heme pocket are two features that have led to extensive study of hemoproteins. The ultimate goal of these studies is to solve the structures of target proteins and to evaluate the functions of certain residues in enzyme catalysis. With

detailed crystallographic structures of hemoproteins, the site-directed mutagenesis technique has been widely used to study structural-functional relationships of target proteins and to explore more efficient catalytic enzymes (Frandsen 1994). Replacement of a certain amino acid in the heme proximal or distal site can greatly change the interaction of the enzyme with substrates and therefore affect the catalytic efficiency of the enzyme, which provides the chance to discover novel enzymes with improved properties (Dawson 1988; White 1992; Sigman 1999; Lu 2001; Denisov 2005; Lu 2009).

The axial ligands play dominant roles in modulation of structure and functions of hemoproteins. Therefore, changing the axial ligand is apparently an effective way to redesign hemoproteins. For example, the bis-His cytochrome b_5 (Sligar 1987) and cytochrome c_3 (Dolla 1994) have been converted to His-Met cytochromes by the replacement of the proximal histidine ligand with a methionine, which resulted in a 160-180 mV increase in the redox potential. Mutation of His to Cys in the proximal ligand of cytochrome c leads to a 650 mV decrease in the reduction potential, which is the largest decrease of reduction potentials from axial ligand mutations so far (Sorrell 1989). In addition, by replacing the Met ligand to a noncoordinationg amino acid such as Ala using site-directed mutagenesis, cytochrome c has been converted into an oxygen-binding protein, which possesses a similar substrate-binding site for dioxygen and other exogenous ligands like myoglobin (Lu 1993). Interestingly, redesign can also be done in the reverse direction. For example, myoglobin has been mutated to the bis-His cytochrome b_5 when the distal valine was replaced by a histidine residue (Qin 1994).

The proximal thiolate ligation from cysteine is essential for the reactivity and spectral characteristics of many enzymes such as cytochrome P450s, NOS, CPO and

CooA hemoproteins. To study the role of the thiolate ligation, the axial ligand histidine has been mutated to a cysteine in both human (Adachi 1993) and horse heart myoglobins (Hildebrand 1995). Simililarly, the proximal histidine to cysteine mutation was also successfully carried out in heme oxygenase (Liu 1999). In a redesign in the reverse direction to the above work, the proximal cysteine ligand in CPO (Yi 1999) and cytochrome P450 (Auclair 2001) was replaced by a histidine residue. However, mutation of the axial cysteine to histidine in cytochrome $P450_{cam}$ led to a decreased camphor oxidation rate, increased uncoupling rate, slower electron transfer rate and enhanced peroxidase activity. The results indicate that the function of the proximal cysteine is essential for electron transfer, protein folding, and substrate binding (Auclair 2001).

1.5 Characterization of chloroperoxidase

Among thiolate-ligated hemoproteins, chloroperoxidase is one of the most versatile enzymes in the heme peroxidase family. The enzyme was discovered several decades ago by Hager and coworkers in the marine fungus *Calduriomyces fumago* (Hager 1966). Chloroperoxidase is a glycosylated heme-containing protein with a molecular weight of 42 kilodaltons (Morris 1966). The biological function of CPO has been postulated to catalyze the biosysthesis of antibiotic caldariomycin.

As is the case for many other hemoproteins, the active center of CPO is composed of one protoporphyrin IX group. Although CPO is a member of the heme peroxidase family, the proximal ligand is cysteine, which is identical to that of cytochromes P450. Chloroperoxidase can catalyze a variety of reactions, such as halogenation, peroxidation, oxygen insertion reactions, and decomposition of hydrogen peroxide to oxygen and water. Importantly, CPO can catalyze the epoxidation of olefins with high stereoselectivity. On

the basis of these functions and properties, CPO has been considered as a potential candidate for industrial application.

1.5 Structure of chloroperoxidase

Chloroperoxidase has a single polypeptide chain composed of 299 amino acids folded into eight helical segments (Fig 1.3). Structurally CPO has been considered as a P450-peroxidase hybrid because of the cysteinate proximal ligand and the peroxide-binding site in the distal heme environment. However, the catalytic diversity of CPO is derived from its unique active site, which is distinguished from cytochromes P450 and other peroxidases. In the distal pocket of CPO, a glutamic acid instead of a histidine residue is involved in catalysis and responsible for the cleavage of the O-O bond in the formation of Cpd I complex (Sundaramoorthy 1995; Wang 2003; Kuhnel 2006).

The crystallographic structure of CPO was published in 1995 (Sundaramoorthy 1995). The prosthetic group of the CPO active site was revealed to be a high-spin protoporphyrin IX molecule. The iron atom is penta-coordinated to the four nitrogens of the pyrrole ring and ligated to the sulphur of cysteine residue instead of the imidazole group of histidine. The entire heme is sandwiched between the C-terminal and N-terminal helices and positioned on their surface. The complete structure of CPO is composed of eight α-helices, named A – H. The distal residues of CPO are located in helix F. On the proximal side, helix A is perpendicular to the heme plane and close to the N-terminal, which is quite different from other peroxidases and cytochrome P450s (CYP450s). The mechanism by which this arrangement affects the properties of CPO is still unknown (Kuhnel 2006).
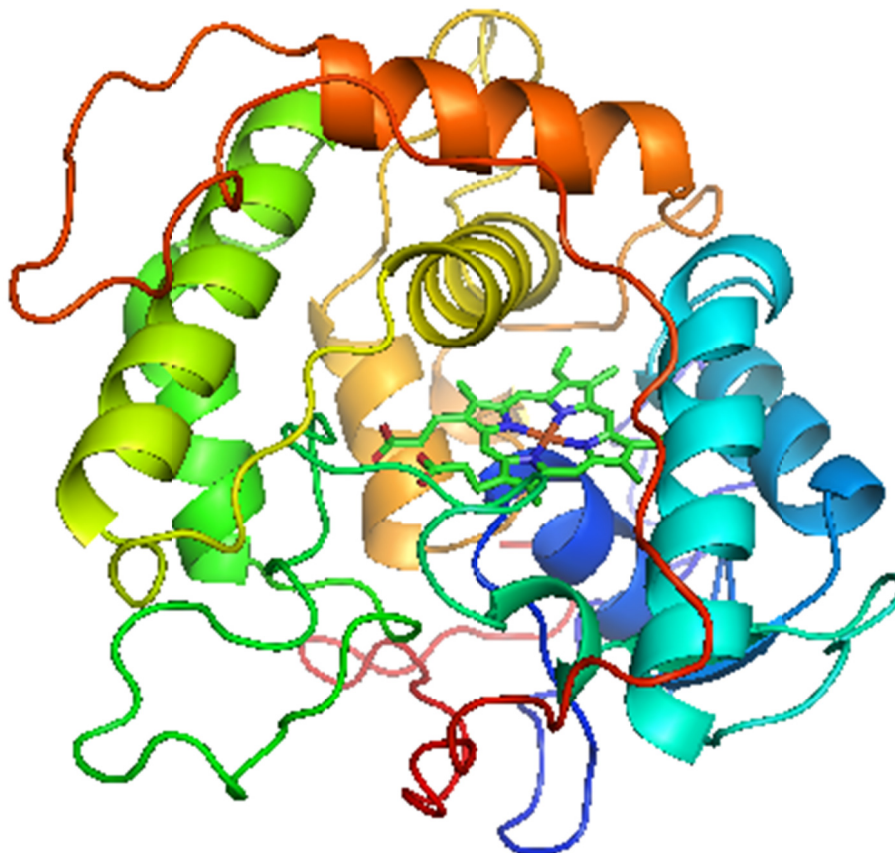
Fig 1.3 Crystal structure of CPO with key elements of the secondary structure shown in different colors. The manganese close to the central heme is shown in purple (PDB code: 1CPO) (Sundaramoorthy 1995).

Similar to other peroxidases, the proximal ligand to the heme is stabilized by the protein environment. Specifically, the cysteine sulphur CPO is stabilized by a positive electrostatic environment, which is considered to be related to the increase of the redox potential in the heme iron (Adachi 1993). Redox potentials of CPO are dependent upon the pH values, and is - 140 mV at pH 5.9 and + 150 mV at pH 2.7. Formation of the initial compound I is relatively insensitive to pH. However, the rate of compound I reduction shows an increasing redox potential as the pH decreases (Makino R 1976).
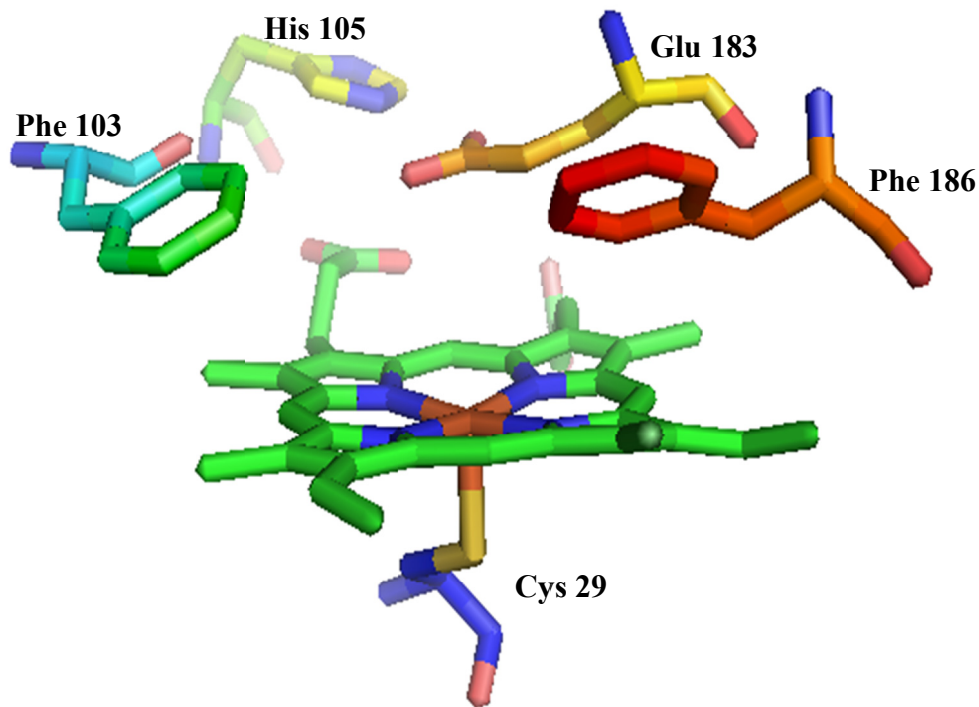
Fig 1.4 Side view of CPO heme active site with important amino acids labeled. Glu 183 can form hydrogen bond with His 105 and function as an acid-base catalyst. Two Phe residues may interact with hydrophobic substrates.

Remniscent of other peroxidases, the distal pocket of CPO is polar, with a glutamic acid instead of a histidine responsible for the cleavage of O-O bond in the formation of coupound I. However, commonly reserved histidine and arginine in other peroxidases are absent in the distal site of CPO. Glutamic acid 183 functions as a general acid-base catalyst. It is interesting to note that histidine 105 is 3.5Å away from the heme propionate and hydrogen bonded to glumatic acid 183, which is also a ligand for manganese (Yi 1999; Yi 2003). Therefore, histidine 105 was proposed to be crucial for CPO catalyzed reactions.

There are two substrate access channels extending from the heme active center to the surface of the enzyme: a narrow channel and a wide channel, simply depending on their

physical dimensions (Fig 1.5). Most halide binding sites are located in the narrow

channel, which indicates the access pathway for the halides to the active oxoferryl center.
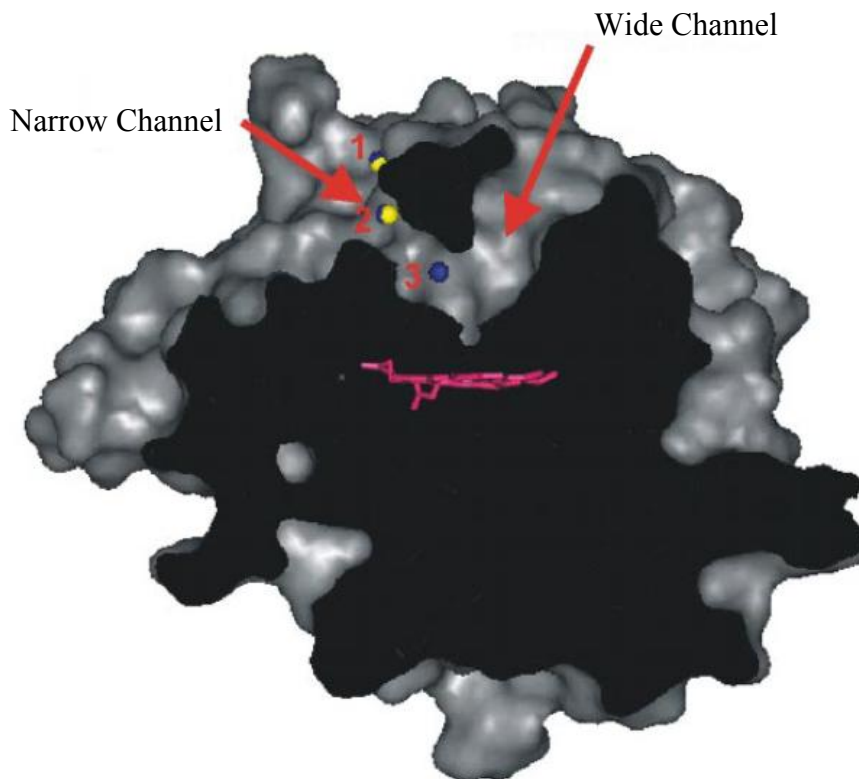
Fig 1.5 Slice through a surface representation of CPO (including sugars attached to the protein). The two channels leading to the active site are marked by arrows, and the heme is shown in magenta. The halide binding site 2 (yellow, bromide; blue, iodide) is located within the narrow channel and the iodide specific binding site 3 at the end of the channel implicating a pathway for halide access from the surface to the heme though this narrow channel (Kuhnel 2006).

The narrow channel is composed of very bulky and hydrophobic residues near the

heme center, but is made of small and polar residues far away from the active center.

Such a structure can facilitate the access and orientation of certain substrates to the heme

active site. The propionate edge of the heme group is not accessible for substrates,

although a substrate pocket is close to the heme. Therefore, the structure of CPO active

center allows substrates to interact with the heme iron in a unique location for stereoselective catalysis (Kuhnel 2006).

1.6 CPO-catalyzed reactions

Of all heme peroxidase known to date, CPO is believed to be the most versatile enzyme on the basis of many types of reactions it catalyzes. The first type of reaction is halogenation in which hydrogen peroxide or other hydroperoxides is used as the initiator, halides (except fluoride) and compound susceptible to halogenation reactions serve as the substrates (Fig 1.6) (Hallenberg 1978). The second category is very similar to the first one, except that the substrate is the uric acid. These two reactions may form a similar chlorinated intermediate in the initial step, therefore they have optimum acidic pH values (Hallenberg 1978; Shahangian 1981; Libby 1982). The third one is a typical peroxidation reaction with the pH optimum between4 and 7 depending on the nature of organic substrates involved.(Sun 1994). Chloroperoxidase can also catalyze the disproportionation of hydrogen peroxidase, a reaction specific to catalases.. Recent studies show that CPO is able to catalyze P450-like monooxygenase reactions (Fig 1.7) (Sundaramoorthy 1995). Finally, CPO has been shown to catalyze the dehalogenation of selected halogenated aromatic compounds (Dawson 1976).

In recent years, CPO has attracted significant interests for its great industrial potential to synthesize enantioselective products. It has been reported that CPO can catalyze chiral epoxidation, sulfoxidation, and hydroxylation with good yield (Allain 1993; Dexter 1995; Zaks 1995).
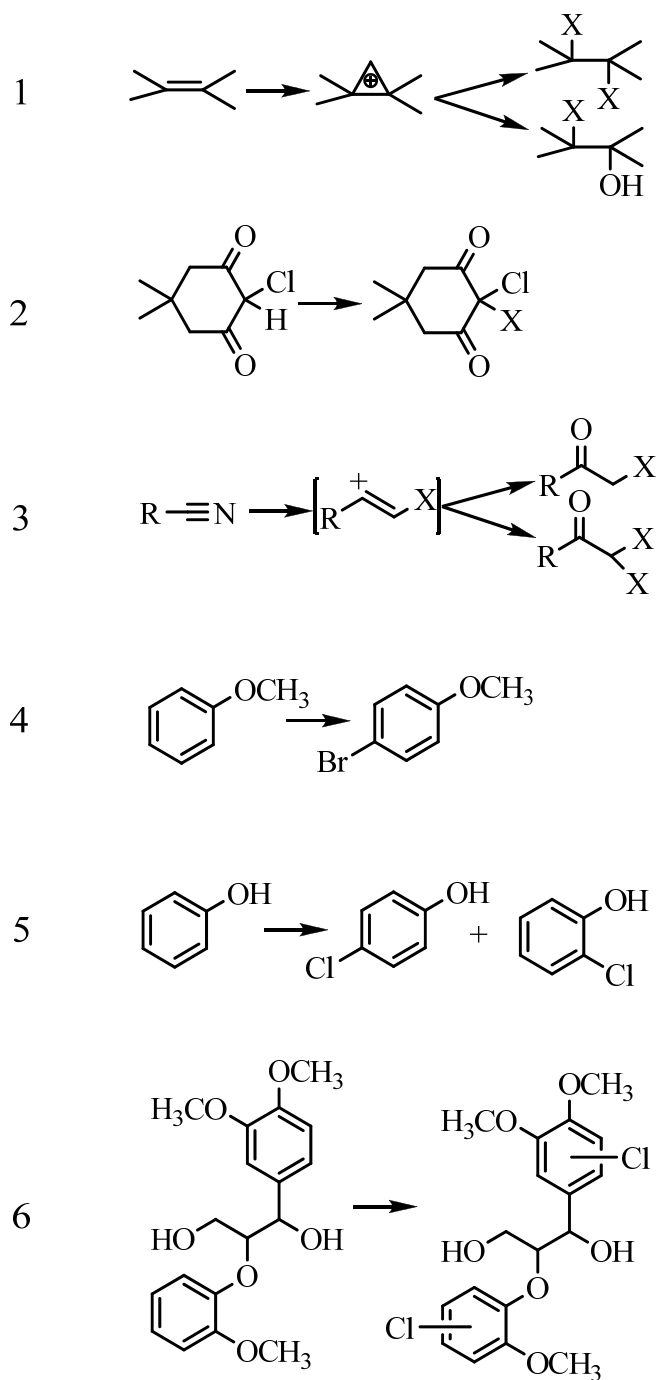
Fig 1.6 Halogenations catalyzed by chloroperoxidase. The substrates are:1 alkenes; 2 β-diketones such as monochlorodimedone (MCD); 3 alkynes; 4 anisole; 5 phenol; 6 non-phenolic lignin model compound. X stands for halide.
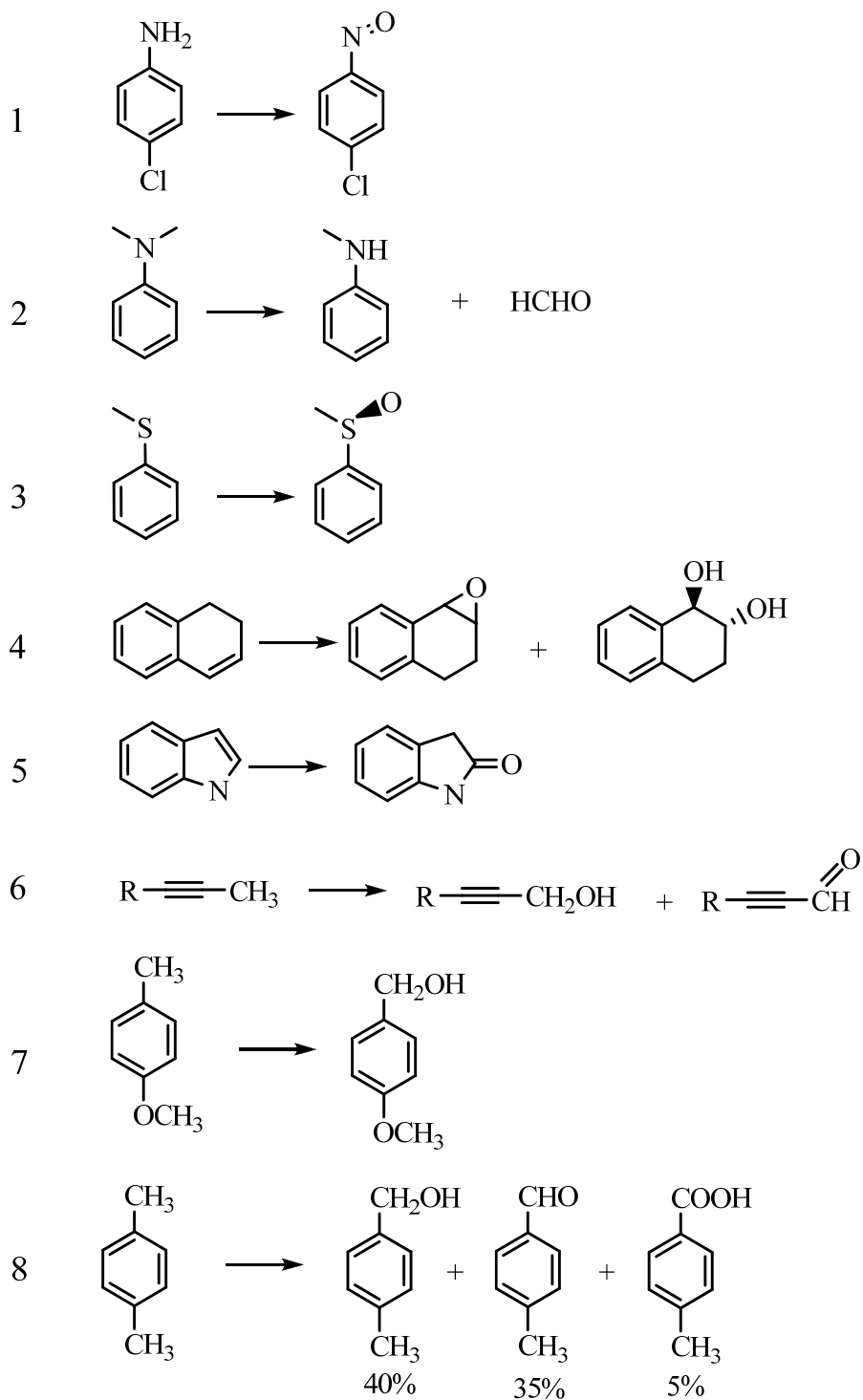
Fig 1.7 Oxidations catalyzed by by chloroperoxidase. The substrates are: 1 chloroaniline; 2 N-dealkylation, e.g., demethylation of N,N-dimethylaniline; 3 thioanisole; 4 1,2-dihydronaphthalene; 5 indole; 6 propargylic hydroxylation; 7 p-methylanisole; 8 pxylene. These reactions are initiated by hydrogen peroxide.

The advantage of CPO catalyzed chiral reactions is that there is no need to supply NAD(P)H or other electron donor as in cytochrome P450 catalyzed reactions. These properties give CPO a bright future in industrial applications, especially in chiral drug synthesis, oil purification and agrochemical production (Dexter 1995; Miller 1995; Hager 1998).

1.7 Mechanism of CPO-catalyzed reactions

The unique active site structure makes CPO adept in catalyzing a variety of reactions and become a promising candidate for industrial applications. The general mechanism of CPO catalyzed reactions is summarized in Fig 1.8. The resting state of the enzyme contains a ferricheme center. Binding of hydrogen peroxide at the heme iron initiates the reaction. Two electrons are then transferred from the heme center to hydrogen peroxidase, resulting in the heterolytic cleavageof the peroxide bond and the formation of a water molecule and activated heme intermediate compound I.

It has been reported that compound I is a common intermediate involved in most heme peroxidase catalyzed reactions. The chemical structure of compound I has been experimentally determined to be an oxo-ferryl porphyrin cation-radical [heme $(Fe^{4+}=O)^{\cdot+}$]. Depending on the nature of proteins, compound I of heme proteins can participate in dramatically different chemical reactions. In the catalase reactions, compound I will interact with the second molecule of hydrogen peroxide, to form dioxygen and reduce heme iron to the ferric resting state. In peroxidation reactions, compound I can convert organic molecules (HA) to radical products (A·) and be reduced to compound II by transferring one electron to the organic substrate (Hager 1972; Palcic 1980; Nakajima 1985). The structure of compound II is assumed to be in the form of $Fe^{IV}=O$. Oxidation
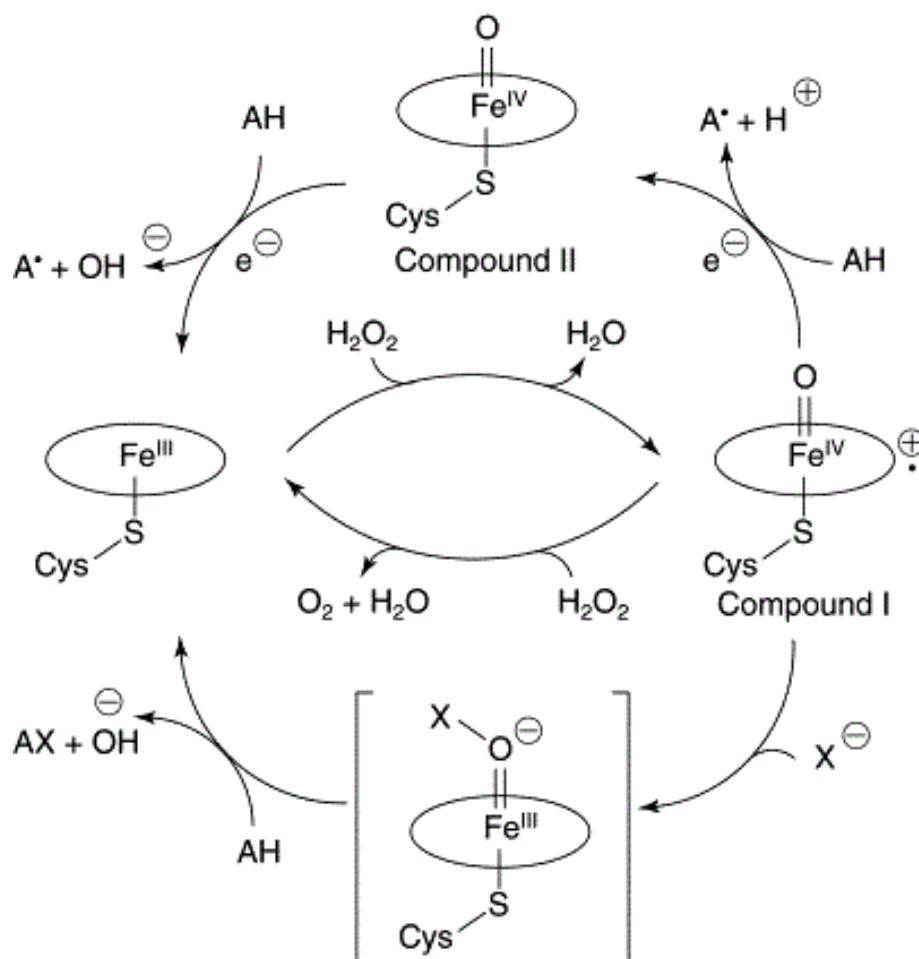
Fig 1.8 Mechanism of CPO-catalyzed reactions. AH represents the substrate and the oval represents the heme plane. Compounds I and II represent the ferryl intermediates; X represents halides involved in the halogenation pathway.

of a second substrate can also regenerate the ferric resting state for the following cycles of the reactions. However, in the chlorination reactions, compound I can interact with chloride ion to form a ferric complex named compound X (heme Fe^{3+}–O–X), which is unstable and can easily decompose to result in the resting state of the enzyme, halonium ion (X^+) and hydroxyl ion (OH^-). They can further react to form the hypohalous acid

18

(HOX). The mechanism for the chlorination of hydrocarbons by CPO is still a puzzle, as well as the detailed structure of compound X formed in the chlorination reaction (Stefano Colonna 2000; Hofrichter 2006).

1.8 Heterologous expression of CPO

Controlled heterologous expression of target genes has become a very useful technique in biochemistry and molecular biology. For characterization of CPO, an efficient heterologous expression system is necessary for site-directed mutagenesis because CPO has many post-translational modifications during protein synthesis, e.g., glycosylation, disulfide bond formation, and prosthetic group incorporation. Therefore, prokaryotic hosts, such as *Escherichia coli* expression systems, are not applicable for synthesis of the active form of chloroperoxidase (Frandsen 1994; Visser 1995; Inoue 1996; Sriprang 2006). It was reported that a non-glycosylated apoprotein had been expressed in an *E. coli* (Zong 1995; Conesa 2001). Therefore, eukaryotic expression systems are the ones suitable for expression of CPO mutants. The baculovirus expression system was also studied to explore the possibility of synthesizing CPO with post-translational modifications. However, inactive enzyme was isolated that could not be converted to functional protein (Conesa 2001). The *Saccharomyces cerevisiae* and *Pichia pastoris* systems both failed to express active CPO mutant (Zong 1997; Sigle 1993). Another strategy for CPO expression was to express the protein in the parental host *Caldariomyces fumago*. However, the presence of wild-type CPO in the background hampered this because of the impossibility of separating the native enzyme from the specific recombinant protein (Zong 1995; Yi 1999).
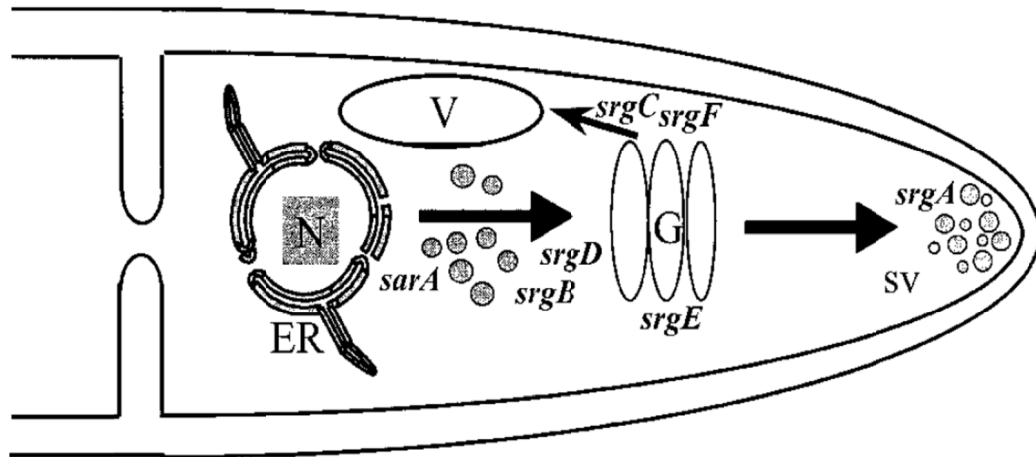
Fig 1.9 Secretion pathway in filamentous fungi. Cloned secretion related GTPases (srgA–F), involved in vesicular trafficking, are indicated. N, nucleus; V, vacuole; ER, endoplasmic reticulum; G, Golgi apparatus; sv, secretion vesicles.

Fortunately, in recent years, a filamentous fungi expression system has been developed as a reliable host for the production of metalloproteins. It has great potential to secret heterologous proteins into the extracellular medium with a well-studied genetic system (Punt 1994; Punt 2002; Liu 2003). Since gene transformation and expression have already been developed for these species, the filamentous fungi expression systems provide great tools for the production of recombinant metalloproteins (Conesa 2001). Recently, expression of the encoding *cpo* gene was tested in the filamentous fungi *Aspergillus niger* and the results showed that the active recombinant protein could be secreted into the culture medium with almost identical catalytic activities compared to the wild-type CPO. Furthermore, there is no extracellular and intracellular peroxidase detected in *A. niger*, which makes it much easier to handle compared with a *C. fumago* expression system because screening for CPO producing transformants will not be complicated by the presence of the endogenous oxidizing activities. Expression of metalloproteins in the filamentous fungi system has been studied for decades (Daboussi

1989). However, the yield of the active recombinant enzymes is still far from expectation (Conesa 2001), which makes the reconstruction and culturing of metalloproteins still a challenging research subject.

1.9 Expression of deuterated CPO

In recent years, deuteration techniques have become a powerful method in studying proteins or other biological systems using NMR spectroscopy (Savenkova 2001). Deuteration of the solvent or the culturing medium provides the chance to simplify the proton NMR spectrum and to suppress the signals of background noise, such as water protons. The estimated deuteration level can be evaluated and optimized for high-resolution proton NMR study.

It has been reported that deuterium-labeled proteins can be overexpressed in bacteria culturing media containing D_2O and either protonated or deuterated carbon sources, depending on the aim of different deuterium incorporations (Gardner and Kay, 1998). Although many bacteria and eukaryotic cells can tolerate culturing media containing a certain concentration of D_2O, the reduction of cell growth rates and lower protein yields are still widely observed in deuterated culturing media (Katz and Crespi, 1970). The reason for the depressing effects of deuterium on expression systems is probably that the deuterated solvent can cause severe isotope effects and replacement of hydrogen by deuterium can damage C-H bond formation. It is widely known that the deuterium isotope effects can decrease the rates of enzyme-catalyzed reactions, influence ionic equilibrium, weaken the strength of hydrogen bonds, and damage the stability of protein structures (Saur et al., 1968a, b; Katz and Crespi, 1970; Schowen, 1977; Schowen and Schowen, 1982).

In 2001, cytochrome *c* peroxidase was overexpressed in *E. coli* using 97-99.9% deuterated medium with excess histidine at natural proton isotope abundance (Savenkova 2001). The results showed that histidine was incorporated into the deuterated recombinant enzyme without degradation. Therefore, this technique can be applied to obtain the complete set of heme proton assignments as well as the assignments of certain amino acids close to the active site. However, the fungi expression systems have never been tested in deuterated medium.

CHAPTER II

ENGINEERING THE NARROW SUBSTRATE CHANNEL IN CPO

2.1 Background

2.1.1 Location of asparagine 74

The most important function of CPO is to bind halides and catalyze chlorination, bromination and iodination reactions (Thomas 1970; Sono 1986). The crystal structure of CPO bound to bromide/iodide instead of chloride has been published as a result of the K-edge of chloride at 4.39 Å (Kuhnel 2006). The bromide/iodide binding site (I/Br1) is located on the surface of CPO, and is occupied 60% by bromide and 30% by iodide in the crystal structure (Fig 2.1). The function of this site is probably to serve as the docking position for halide anions, to stabilize the hydrogen bond with the backbone amino acids and to participate in the interaction with water molecules. The second binding site (I/Br2) located within the narrow channel is 8 Å away from I/Br1 binding position. The second site has a low occupancy with 20% of iodide and 30% of bromide because it is also involved in a hydrogen bonding network with water molecules instead of interacting with bound anions. The third binding site is specific for iodide (I3) with an occupancy of 40% iodide. The I3 binding site is located 6 Å away from halide binding site 2 and 8.8 Å away from the heme iron at the end of the narrow channel. The iodide specific binding site I3 can form hydrogen bonds with the amide group of Asn 74 and water molecules in the middle of the wide channel (Fig 2.2). However, the surrounding environment of I3 is hydrophobic and close to the amino acids leucine 70, phenylalanine 103, isoleucine 179, and alanine 267. The three halide binding sites mentioned above indicate that the narrow channel is the pathway for halides to enter the heme active center. The other four halide

binding sites with different halide occupations are positioned on the surface of the enzyme where anions replace water molecules from the solvent. The halide anions are involved in the formation of hydrogen bonds with side chains of the protein backbone and the ion pairs with positively charged basic residues. Although the surface binding sites can also interact with some symmetry-related amino acids, they are too far away from the narrow channel to be relevant to the enzyme catalysis. The ends of the narrow channel and the wide channel are mainly composed of hydrophobic amino acids except glumatic acid 183 and asparagine 74. Below the two channels, Phe 186 and Phe 103 are 6.2 Å away from the heme iron and are almost parallel to the top of the heme plane to shield the active center from the solvent.
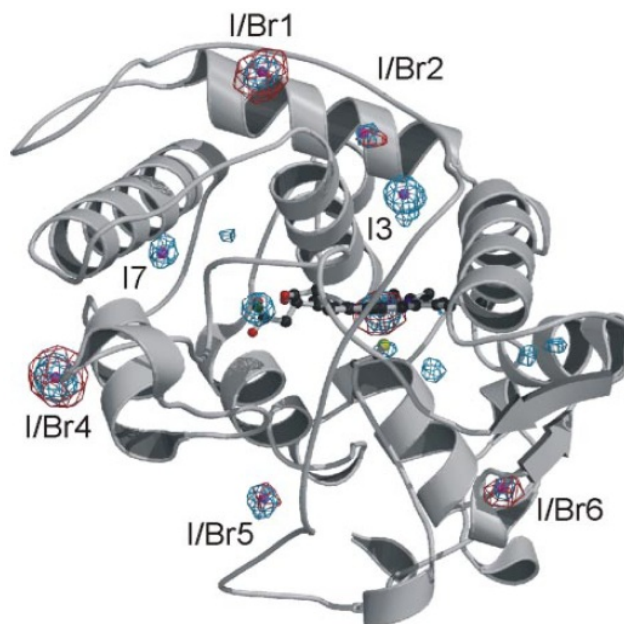
Fig 2.1 Binding of halides to chloroperoxidase. The anomalous difference maps are calculated from iodide (*blue*) and bromide data (*red*). Besides the halide binding sites, the heme iron located next to the heme also show anomalous signals. The weaker peaks visible in the iodide anomalous difference map are caused by the sulfur atoms of methioanine and cystidine.
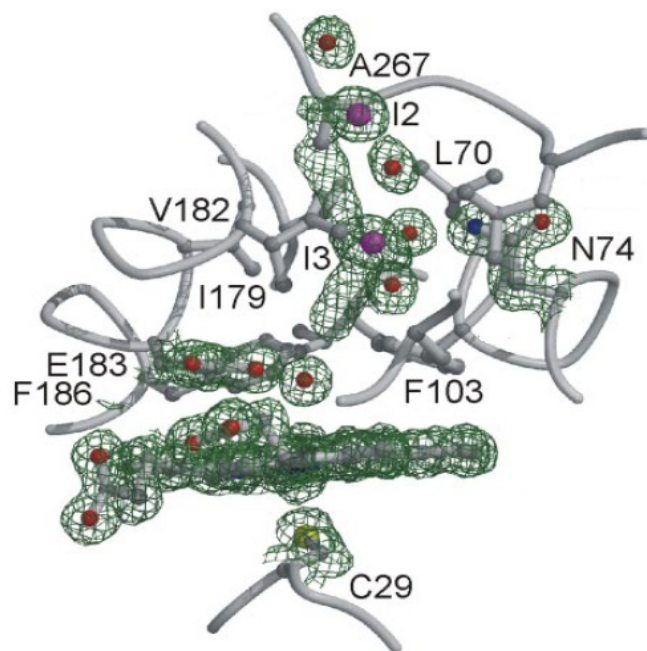
Fig 2.2 Stereoview of the active site with bound iodide. The 1.15-Å electron density map is shown for selected residues, including the iodide (*magenta*).

2.1.2 Function of asparagine 74

The natural function of CPO is to catalyze the chlorination of cyclopentanedione (CPD) during the biosynthesis of caldariomycin. When CPD binds at the heme center, it is sandwiched between phenylalanine 103 and phenylalanine 186. The carbonyl oxygen of CPD forms hydrogen bonds with two water molecules, one of which in turn forms a hydrogen bond with Asn 74 at the iodide specific binding site (Fig 2.3). The iodide binding site is also a binding position for other polar compounds, including dimethyl sulfoxide (DMSO), acetate and ethylene glycol (Fig 2.4). The function of the iodide binding site (I3) may serve as an intermediate site for the substrates to be oriented at the heme center. Asparagine 74 can form hydrogen bonds with these polar substrates, which makes this position favorable for substrate binding. Therefore, the position and polarity of Asn 74 may affect the stereoselectivity of CPO-catalyzed reactions (Kuhnel 2006).
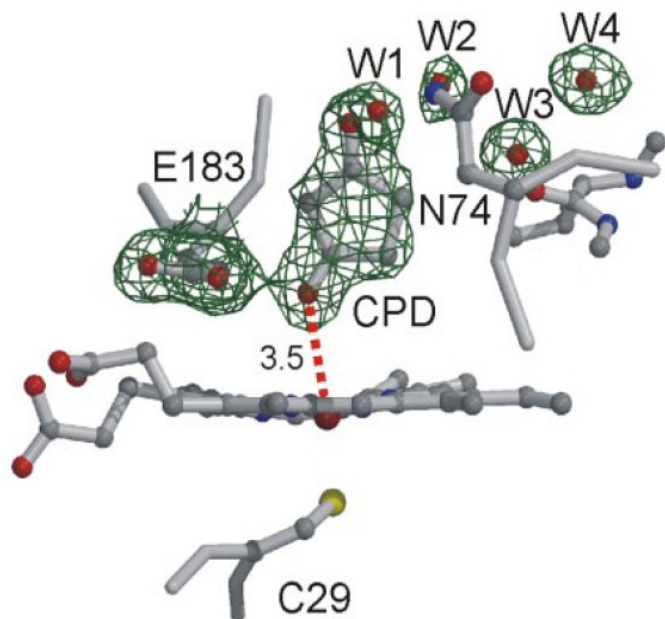
Fig 2.3 Structure of CPO complexed with cyclopentanedione.
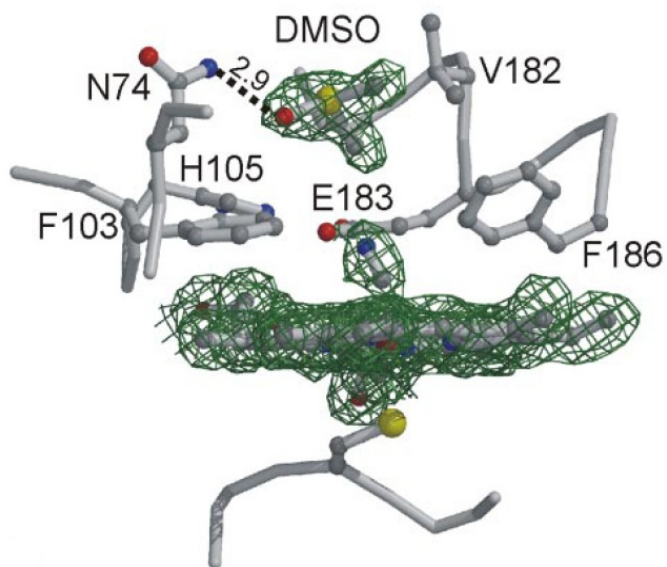
Fig 2.4 Structure of CPO complexed with cyanide and dimethyl sulfoxide.

2.1.3 Aim of this study

To verify the effects of Asn 74 on the stereoselectivity of CPO-catalyzed reactions, the site can be mutated to an aliphatic residue with a similar size (N74V) or a polar amino acid with a bigger size (N74Q). These substitutions are chosen because valine is similar in size to asparagine but is much more hydrophobic. On the other hand, glutamine is polar but bigger compared with asparagine. Site-directed mutagenesis can be carried out to produce these mutants.

2.2 Material and Methods

2.2.1 Materials

Marine fungi *Caldariomyces fumago* and filamentous fungi *Aspergillus niger* (MGG029) were purchased from American Type Culture Collection (ATCC) (Manassas, VA). Gene expression vector pCPO3.I-Amds and co-transformation plasmid pAB4.1 with a selection marker (GenBank accession no. AJ300448) were kindly provided by Dr. Punt (TNO Nutrition and Food Research Institute, Netherlands). Restriction enzymes were purchased from New England Biolabs (Beverly, MA). Ultra-*Pfu* DNA polymerase with relatively high fidelity was obtained from Stratagene (San Diego, CA). Purified oligonucleotide primers were obtained from MWG-Biotech (Ebersberg, Germany). The QuickChange site-directed mutagenesis kit was purchased from Stratagene (La Jolla, CA). De-ionized water for all the experiments were prepared freshly by Milli-Q Biocel (Millipore, Billerica, MA). The JASCO J-720 spectropolarimeter was used to record far UV-CD spectra from 190 to 250 nm. Ultraviolet-Visible absorption was monitored using a VARIAN Cary 300 spectrophotometer.

2.2.2 Gene construction of the CPO mutants

Protocols of N74V/N74Q site-directed mutagenesis were from Stratagene Quikchange Kit and PCR amplification. Expression vector pCPO3.I-AmdS with the complete set of the *cpo* gene encoded was used as the template. The plasmid was designed to use *A. niger* glucoamylase as the promoter and *A. nidulans trpC* as the terminator. A selection marker *AmdS* gene was inserted into the Not I restriction enzyme digestion site (Fig 2.5).
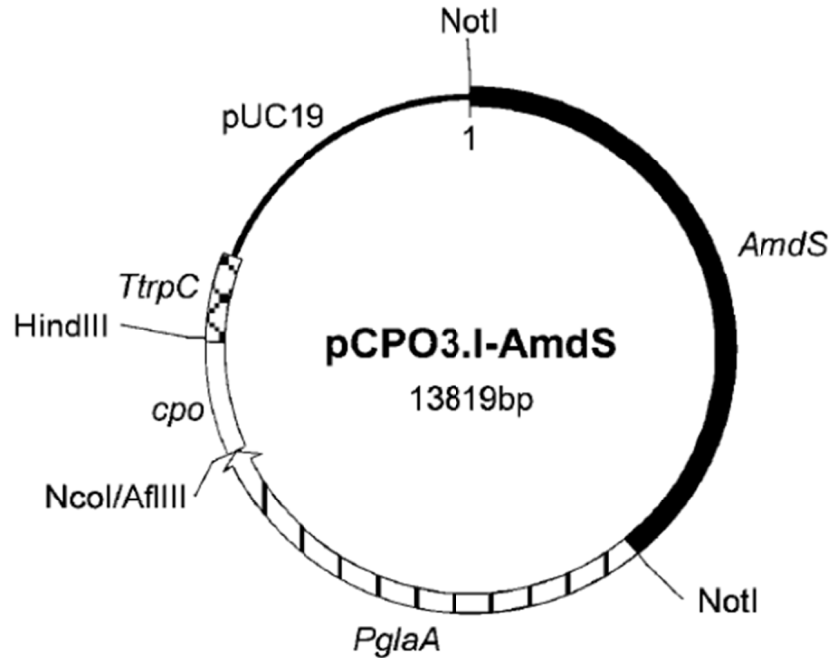
Fig 2.5 Expression vector for co-transformation of *A. niger* strain. Inserted *cpo* and *AmdS* gene are shown in white and black, respectively (Conesa, van De Velde et al. 2001).

Encoded primers for the N74V/N74Q mutants were 5'-gca gac gac gaa ggc gac ggt cag agc aag c-3' with the melting temperature of 79.7°C and 5'-gag ctt gct ctg acc cag gcc ttc gtc gtc tgc g-3' with a melting temperature of 82.3 degrees Celsius. The PCR reactions were carried out by using the following steps: initial denaturation at 94 °C for 1

min followed by 34 cycles of 94 ºC for 30 secs (denaturation) and 68 ºC for 6–9 mins (annealing and extension). The desired mutation was confirmed by DNA sequencing and the expression vector pCPO3.I-AmdS containing the N74V/N74Q mutation was named as pCPO-N74V/N74Q-AmdS. The high fidelity Ultra-*pfu* DNA polymerase was employed in the reactions (Fig 2.6).
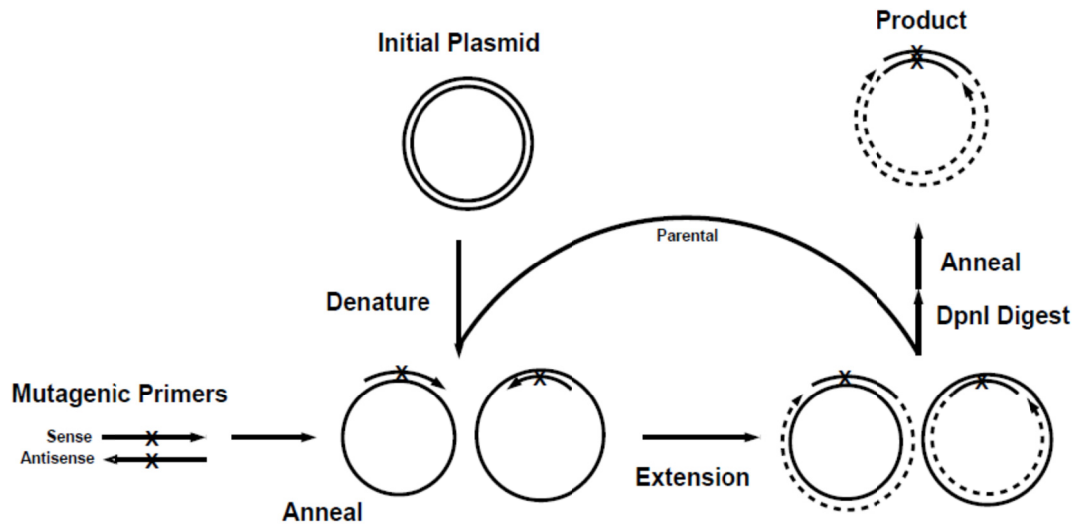
Fig 2.6 Steps of site-directed mutagenesis for the targeted amino acid.

2.2.3 Mutant DNA sequencing and restriction endonuclease digestion

Results of N74V/N74Q single mutations were identified by DNA sequencing and construction of a restriction enzyme digestion map. The mutant DNA was extracted from the transformed *E.coli* strain following the instruction of QIAGEN DNA extraction mini kit (QIAGEN, CA). The plasmid DNA of N74V/N74Q mutants was further examined by restriction endonuclease HpyCH4 III/BstN I, respectively. The restriction endonucleases cleaved the mutant *cpo* gene at the specific location shown below, which did not exist in

the plasmid containing the gene for wild-type chloroperoxidase. The results were examined by SDS-PAGE electrophoresis (Fig 2.7).
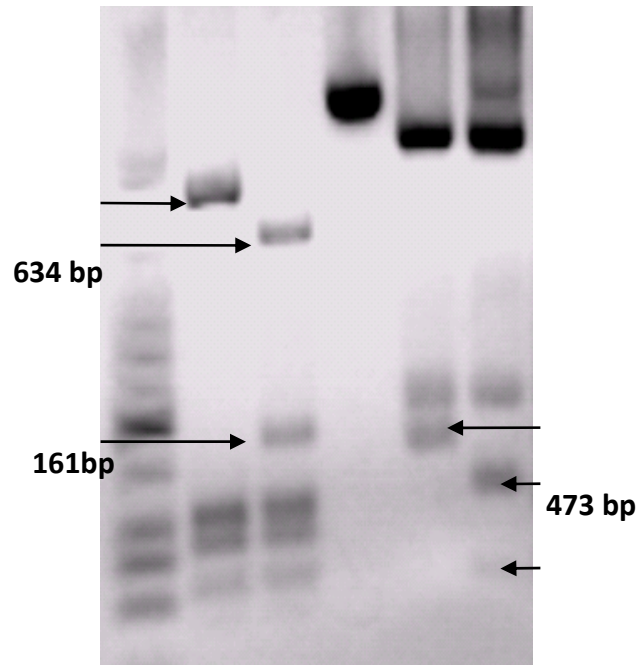
Fig 2.7 Restriction map of CPO mutant coding region. Lane 1. Low molecular weight ladder; lane 2. Wt CPO (digested by BstN I); lane 3. N74Q (digested byBstN I); lane 4. Wt CPO (no digestion); lane 5. Wt CPO (digested by HpyCH4 III); lane 6. N74V (digested by HpyCH4 III).

2.2.4 Gene transformation of the CPO mutants

Filamentous fungus MGG029 strain was inoculated in 125 mL of minimal media with 10 mM uridine and 0.1 mg/mL carbonicilin and cultured for 7 days at 30 degrees Celsius. Mycelia from the fungi were disrupted by using a homogenizer for 20 secs, disruption by homogenization was repeated twice and the contents were then transferred to 2 L of minimal media. The cultures were incubated for 20 hours at 250 rpm and 30 degrees Celsius. Mycelia were filtered through the sterile myracloth and resuspended in 1.7 Osm (0.27 M $CaCl_2$, 0.6 M NaCl) buffer. Protoplasts were then treated with 7.5

mg/mL lysing enzyme (Interspex, Sigma L-1412) for 4 hours at 150 rpm and 37 degrees Celsius. Digested protoplasts were resuspended and incubated on ice for 20 minutes. After centrifugation (3500 rpm, 15 minutes, 0 ºC), samples were washed twice with STC 1700 (1.2 M sorbitol, 10 mM Tris-HCl at pH 7.5, 50 mM CaCl$_2$, 35 mM NaCl), and the protoplasts were resuspended in STC1700 and mixed with 10 μg pCPO3.I-Amds mutant plasmid and 1 μg pAB4.1 co-transformation plasmid, then incubated at 25 ºC for 25 minutes. In three steps, 60% PEG4000 in 10 mM Tris-HCl at pH 7.5 and 50 mM CaCl$_2$ were carefully mixed with the treated protoplast mixture and diluted by addition of 5~10 mL of STC1700 to spread on 1.2 M sorbitol selective agar medium plates (Fig 2.8).
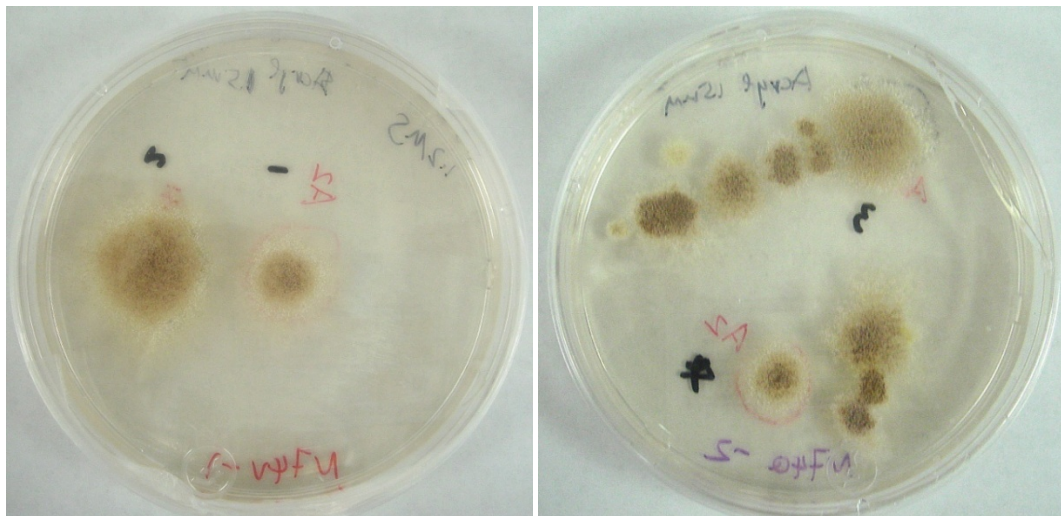
Fig 2.8 Single mutants N74V (left) and N74Q (right) grown on 1.2 M sorbitol selective agar plates after transformation.

2.2.5 Expression of the N74V/N74Q mutant protein

Filamentous fungi were cultured in *A. niger* minimal growth medium containing 50 g/L maltose, 10 g/L glucose, 5 g/L casamino acid, 6 g/L NaNO$_3$, 0.5 g/L KCl, 0.8 g/L KH$_2$PO$_4$, 1 g/L K$_2$HPO$_4$, 0.25 g/L MgSO$_4$, 0.1 mM heme precursor and 100 mg/L carbenicillin. After culturing in a rotary shaker at 250 rpm, 25 ºC for 24 hours, the fungi

were continued to grow at 22 ºC for an additional 6 days. Chlorination activity of the culturing medium was examined daily for the yield of the mutant protein using the MCD assay.

2.2.6 Purification of the mutant protein

Collection of culturing medium was carried out by filtering through Myracloth and a 0.8 μm membrane to remove the fungi and mycelium. After that, a high output ultrafiltration cell with 30 kDa molecular weight cut off membrane was used to condense the large volume of crude medium. About 100 mL samples were collected and dialyzed in 4 L buffer containing 25 mM potassium phosphate at pH 5.9 for 24 hours with at least one buffer exchange. For protein purification, diethylaminoethyl (DEAE) sepharose fast flow column (Amersham, 2.6 × 20 cm) and sephadex G-75 column (Amersham, 2.6 × 100 cm) were applied. Ion exchange chromatography was used to separate the desired protein from others by ionic strength gradient difference (0-0.5 M NaCl) at pH 5.9 in 25 mM potassium phosphate buffer. All experiments were carried out at 4 ºC to keep the mutant protein stable. Reinheitzahl (Rz) value was employed to examine the purity of enzymes and fractions of Rz > 1.0 were collected and condensed by using Centriprep-YM30 (Amicon) for further kinetic studies.

2.2.7 Protein kinetic activity assay

The absorption spectra were taken at pH 5.9 and 25 ºC in 25 mM potassium phosphate buffer. The cyanide and thiocyanate complexes were obtained by adding 2000-fold excess of KCN and KSCN at room temperature. The reduced forms of CPO and its mutants were formed by adding a 1000-fold excess of sodium dithionite, after which the solution were saturated with carbon monoxide (CO) to form the CO complexes.

Chlorination capability of CPO was measured by the transformation of monochlorodimedone (MCD) to dichlorodimedone (DCD). The reaction system contained 20 mM KCl, 0.17 mM MCD, appropriate amounts of the enzyme in 100 mM phosphate buffer at pH 2.75 and the reaction was initiated by addition of 30 μl of 0.67% stock solution of hydrogen peroxide. The rate of formation of DCD product was determined from the decrease in the absorbance at 278 nm during the first 20 seconds.

Epoxidation reaction was carried out in 100 mM sodium acetate buffer at pH 4.5, containing 0.2 mM *p*-nitrostyrene as the substrate and 2 mM Wt CPO or CPO mutants. The decrease in the absorbance at 312 nm as a function of time was monitored for the rate of formation of *p*-nitrostyrene oxide. The reaction was initiated by addition of 30 μl of 0.67% stock solution of hydrogen peroxide.

Catalase activity was measured by the rate of absorbance change of H_2O_2 in 50mM phosphate citrate buffer at pH 5.0. The reaction was initiated by the addition of 2 nM Wt CPO or CPO mutants. The initial rate of the reaction was determined by measuring the decrease in the absorbance at 240 nm during the first 20 seconds.

In the peroxidation activity assay, 2, 2'-azino-bis-3-ethy-benzthiazoline-6-sulfonic acid (ABTS) was used as the electron donor. The reaction mixture was in 100 mM phosphate buffer containing 25 mM citric acid at pH 5.0 and initiated by the addition of H_2O_2. The reaction mixture contained 2 nM CPO or CPO mutants, 2.5 mM H_2O_2, 1.7 mM ABTS substrate. The initial rate of the reaction was determined by measuring the increase in absorbance at 405 nm for the first 20 seconds.

2.2.8 Ligand binding study

Titration experiments were employed to determine the apparent dissociation constant (K_d) in the ligand binding. The reaction mixture contained 5 μM enzyme and appropriate concentrations of ligands in 25 mM phosphate buffer. The UV-Visible spectroscopy was carried out to record the spectrum at different concentrations and the K_d value was calculated by using the following formula: $K_d = [L] (1-v)/v$, where K_d is the apparent dissociation constant, [L] is the free ligand concentration and $(1-v)/v$ is the ratio of free enzyme to total enzyme concentration.

2.3 Resutls

2.3.1 UV-Visible spectroscopic properties of Wt CPO and the N74V mutant

One of the important characteristics for heme-containing proteins is that they show a Soret peak in UV-Vis spectra, which reveals useful information about the heme active center. Upon Asn 74 replacement with valine, at pH 5.9, 25℃, the Soret band shifts to the red compared to Wt CPO, and the α, β bands become partially resolved. The spectrum indicated that the N74V mutant was a hexacoordinate, low-spin ferric heme protein with a Soret maximum at 420 ± 1 nm (Fig 2.9). The spectrum of Wt CPO was different from the N74V mutant by showing the Soret peak at 398 ± 1 nanometers. The minor peaks of N74V mutants were located at 356, 540 and 560 nm, but those of Wt CPO were at 515, 545 and 650 nm (Fig 2.10). The results indicated that there might be one water molecule bound at the heme center of the N74V mutant, and therefore this binding property resulted in a low-spin heme at the catalytic center. The spectroscopic properties of the N74V mutant and the wild-type enzyme indicated that the active site of the mutant was structurally intact.
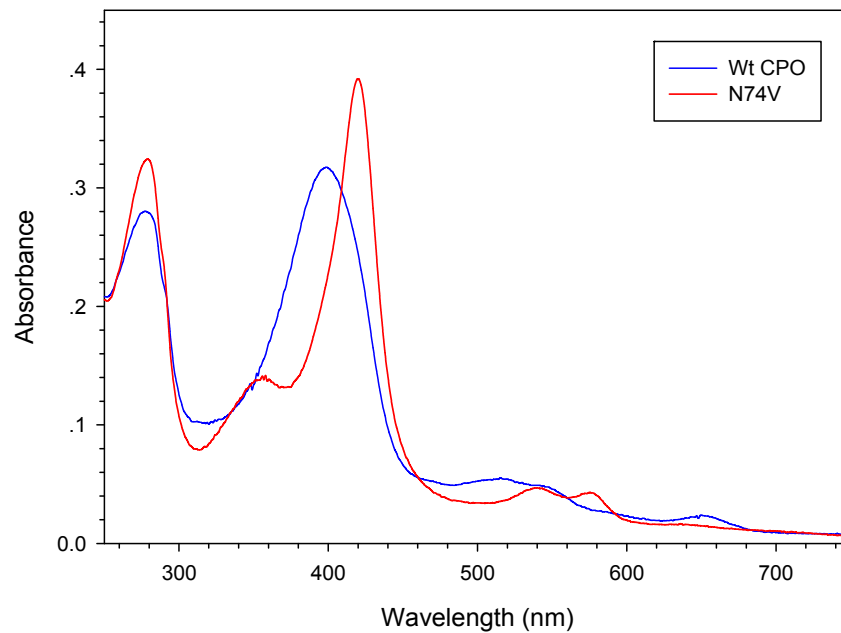
Fig 2.9 Absorption spectra of the purified Wt CPO and the N74V mutant in 25 mM potassium phosphate buffer at pH 5.9.
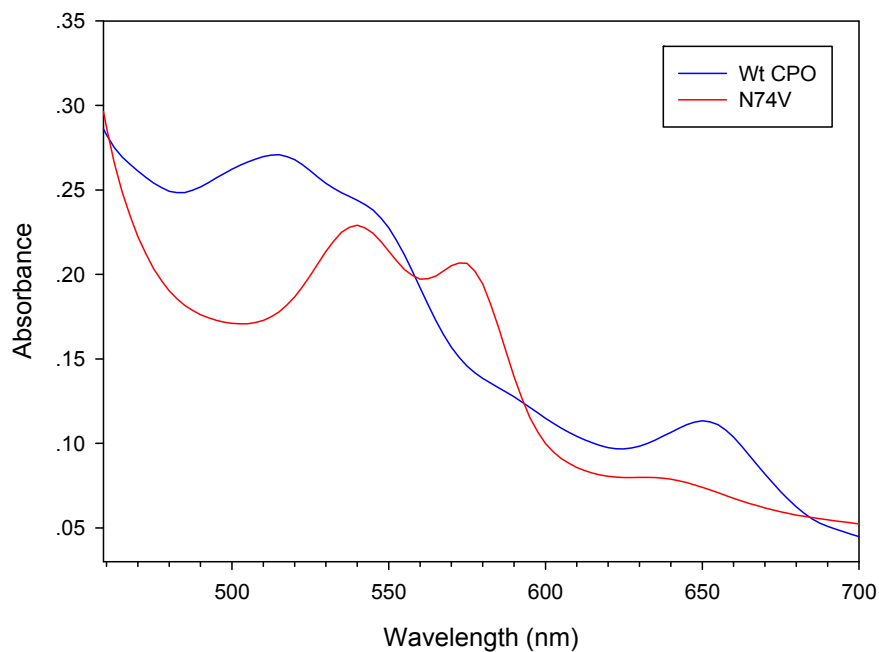
Fig 2.10 Detailed UV-Vis spectra of Wt CPO and the N74V mutant in 25 mM potassium phosphate buffer at pH 5.9.

2.3.2 Characterization of CO binding with the N74V mutant
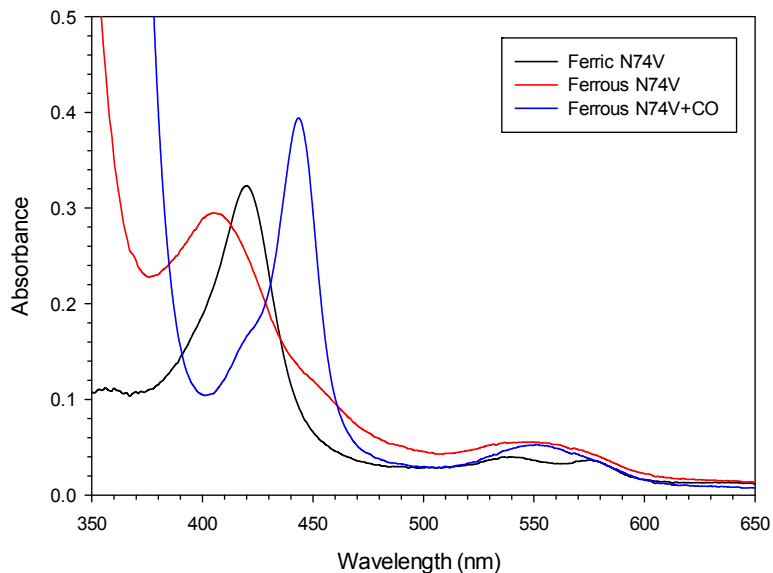
Fig 2.11 UV-Visible spectra of the ferrous-CO complex of the N74V mutant in 25 mM potassium phosphate buffer at pH=5.9.

The UV-Vis spectra for the ferrous-CO forms of the N74V mutant were obtained to examine the coordination structure of the heme iron. The binding of CO with hemoproteins is a typical assay for cytochrome P450 enzymes. As is widely known, CO complex of thiolate-ligated systems shows an absorption band at approximately 450 nm. However in histidine-ligated systems, the corresponding band is blue-shifted to about 420 nm. It is worth mentioning that the ferrous complexes of the N74V mutant displayed the Soret maxium initially at approximately 412 nm upon reduction by addition of sodium dithionite. The result could be an indication of changed electron density on the thiolate ligand in the reduced form of the CPO mutant. In Wt CPO, the formation of ferrous-CO state completely shifted the Soret peak from 400 nm to 445 nm. Compared with Wt CPO,

36

the major peak of the CO complex of N74V shifted slightly from 446 to 443 nm, indicating that the proximal ligand in N74V mutant was a cysteine residue (Fig 2.11).

2.3.3 CD spectroscopic study of the N74V mutant
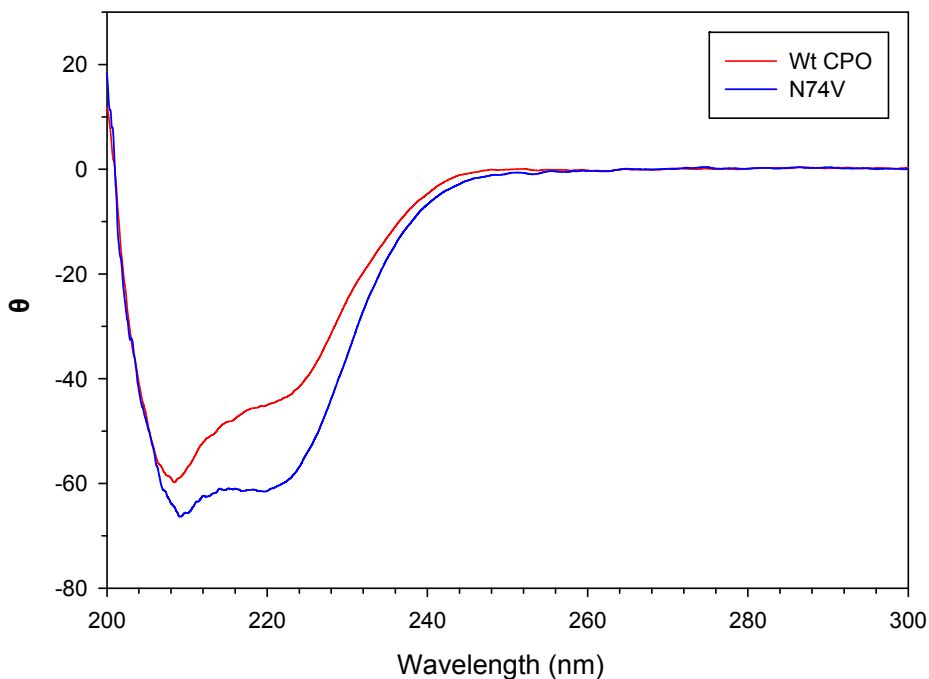
Fig 2.12 Far-UV CD spectra of Wt CPO and the N74V mutant. 0.5 μM enzyme was dissolved in 25 mM potassium phosphate buffer at pH 6.0. The experiments were recorded from 200 to 300 nm at room temperature. The path length was 1 cm.

The far-UV CD spectra of proteins demonstrated the composition of the secondary structure of polypeptide chains. Therefore, CD spectra were used to convey the information of secondary structure induced by mutation of the Asn 74 residue. The N74V mutant exhibited a slightly different CD spectrum compared with that of Wt CPO (Fig 2.12). Although the possibility that activities of mutant enzyme were affected by large structural changes was excluded, some conformational changes did exist. The secondary structural change of the N74V mutant may be attributed to the non-polar distal environment of the heme pocket induced by the valine residue.

2.3.4 Optimum pH values for Soret band shift
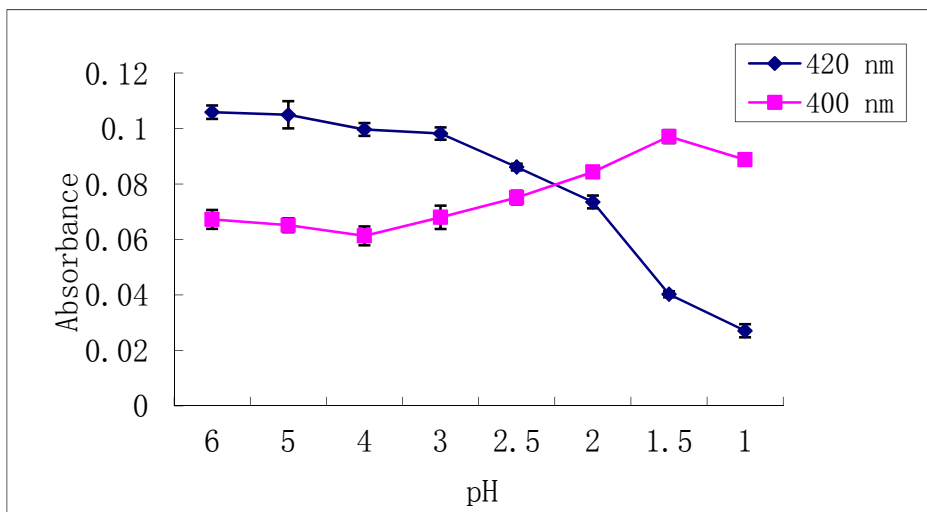
Fig 2.13 pH profiles for UV-Vis spectra at 400 and 420 nm in the N74V mutant.

The pH dependence of the UV-Vis spectrum of the N74V mutant suggested that an ionizable amino acid had become solvent accessible in the absence of asparagine. Since Asn to Val mutation partially broke the H-bonds in the network, it would affect the dissociation constant of the bound water molecule. To further elucidate the role of the N74 residue in the narrow channel, the pH optimum of the N74V mutant was examined. After comparing the position of the Soret band at different pH values, we found that the Soret band shifted from 420 nm to 400 nm at pH 3.0 (Fig 2.13). The result indicated that the N74V mutation provided enough space for a water molecule to bind at the heme center. At low pH, the heme bound water molecule becomes protonated and therefore dissociates from the heme active center.

2.3.5 pH profile for MCD assay

The chlorination ability of the N74V mutant was measured at various pH values ranging from pH 2.0 to pH 7.0 (Fig 2.14). For Wt CPO, the optimum pH for chlorination

activity was 2.75. However, the N74V mutant was most active at pH 3.5. The changing of the optimum pH is normally related to the polarity of the heme distal pocket, which affects the catalysis of substrates at the active center. Therefore, it was concluded that the mutation at the N74 residue changed the polarity of its local environment and the effect was relayed to the heme environment, although N74 was located at the end of narrow channel not immediately adjacent to the heme iron.
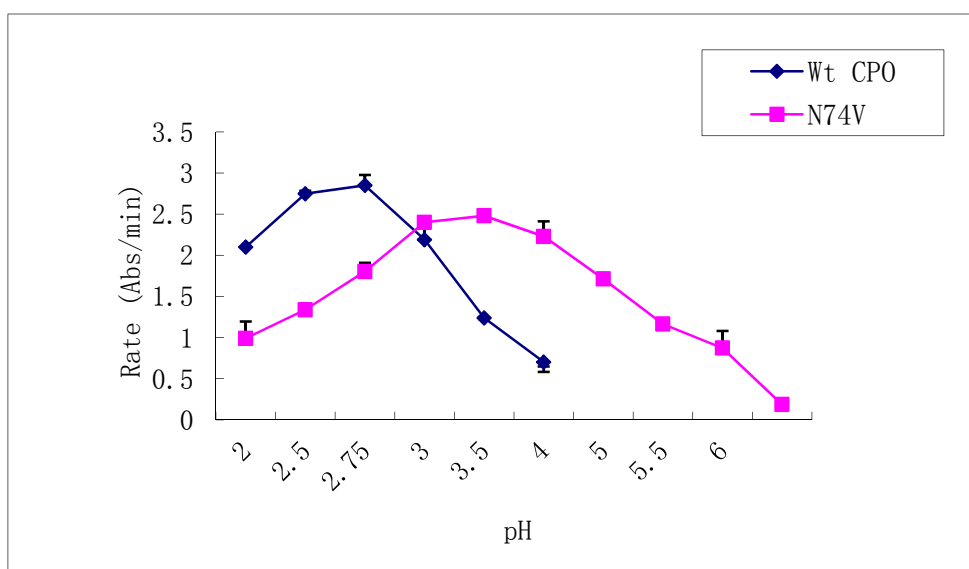
Fig 2.14 pH profiles for chlorination activity in the N74V mutant enzyme and Wt CPO.

2.3.6 Characterization of the N74V mutant activities

To evaluate the effect of mutation in the narrow channel on the catalytic property of CPO, the activities of the N74V mutant were measured with four different assays. As expected, the mutation from Asn to Val decreased chlorination and catalase activity rate compared with that of Wt CPO because of the decreasing polarity in the heme center (Fig 2.15). However, the N74V mutant showed much higher epoxidation activity attributable to the increased hydrophobicity induced by the mutation. Most epoxidation substrates are

non-polar such as styrene and hydrophobic envrionment enhances their interaction with the enzyme.
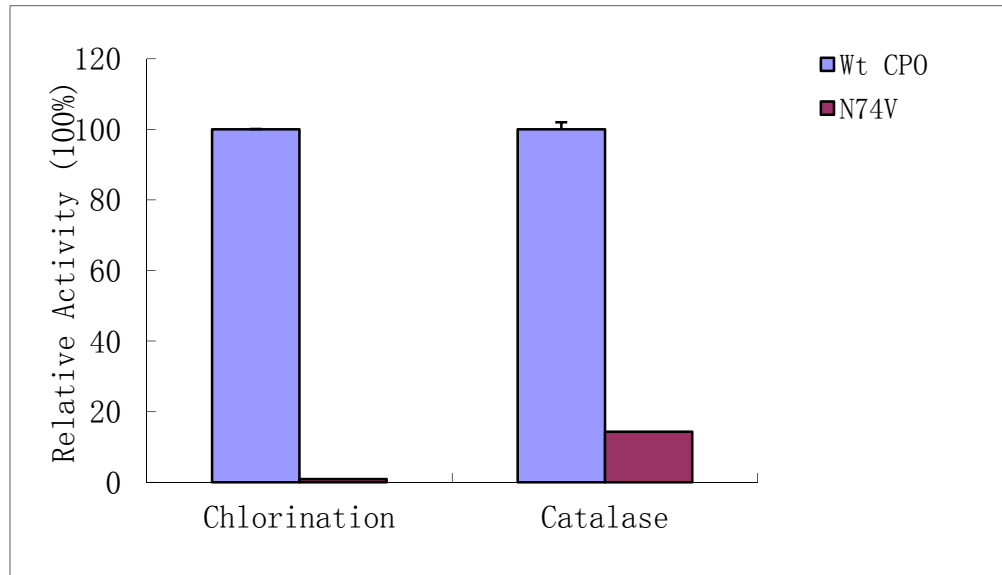
Fig 2.15 Relative activity of Wt CPO and the N74V mutant in chlorination, catalase, epoxidation and peroxidation assays.
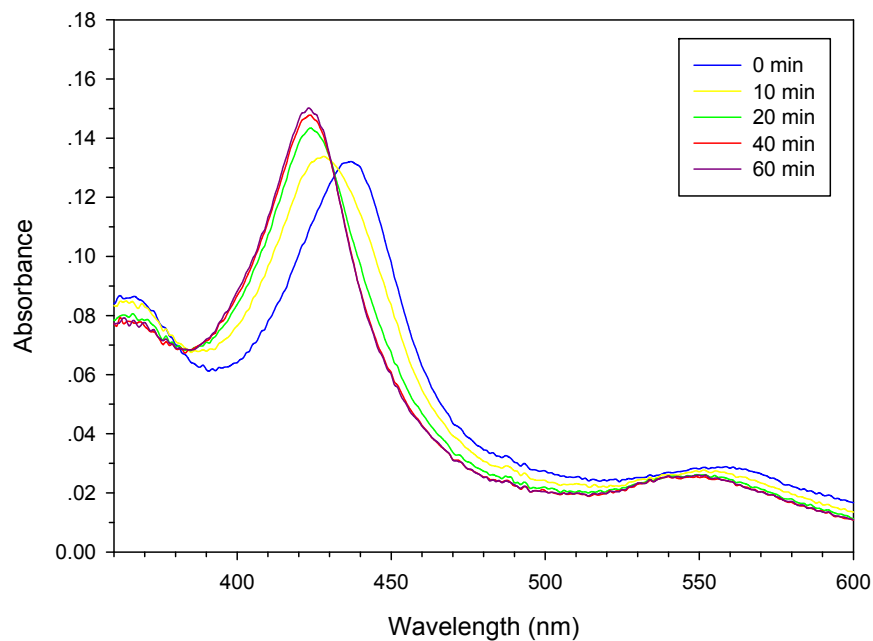
Fig 2.16 UV-Visible spectra of the cyanide complexes with the N74V mutant at different times in 25 mM potassium cyanide alkaline solution at pH=12.0.
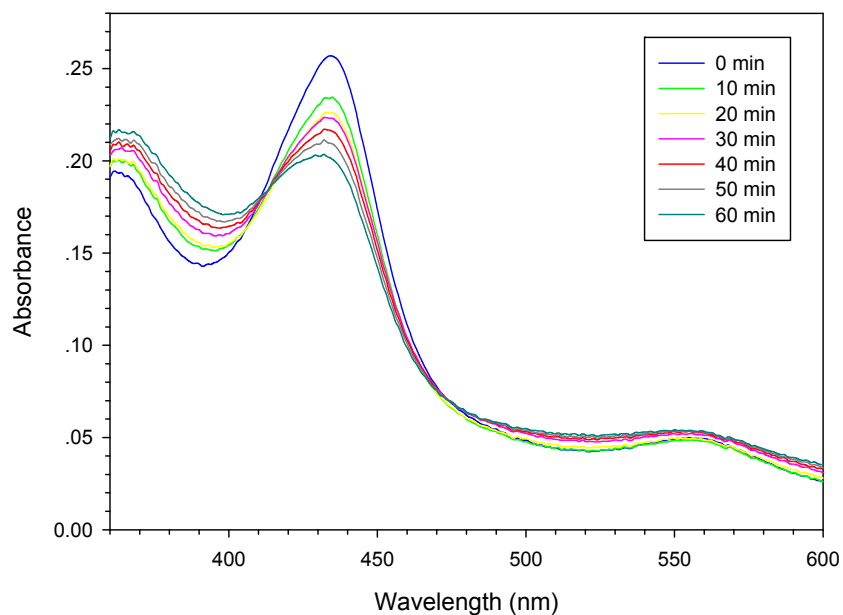
Fig 2.17 UV-Visible spectra of the cyanide complexes of the N74V mutant at different times in 25 mM potassium cyanide solution at pH=6.0.

2.3.7 Equilibrium titration of the N74V mutant with cyanide

The strong binding ligand cyanide was widely used to evaluate the affinity of the CPO mutant for the sixth axial ligand. Cyanide can convert high-spin iron to low-spin. Thereby, binding of cyanide to Wt CPO shifts the Soret peak from 400 nm to 439 nm. The spectral changes of N74V upon addition of cyanide are shown in Fig 2.16.

As mentioned above, the heme iron in ferric N74V mutant exhibited a low spin form without cyanide binding. When KCN bind to the heme iron in basic environment, the Soret peak of the complex was first shifted from 420 to 436 nm with a decrease in absorbance and then shifted back to 423 nm with increasing absorbance as time passes. The spectrum of KCN binding with the N74V mutant was quite different from those of Wt CPO, which did not exhibit any blueshift. To evaluate the effect of pH on cyanide binding to CPO mutant, the pH of the mixture was adjusted to 6.0. As shown in Fig 2.17, the cyanide bound form of CPO N74V mutant displayed a major peak at 436 nm. No change in peak position was observed as in the case of basic environment. However, remarkable decrease in absorbance at 436 nm was noticed at pH 6.0. In contrary, Wt CPO cyanide complex showed the Soret peak at 439 nm without further changes. It is, however, difficult to explain the unusual cyanide binding behavior displayed by Asn74 at this time. It was reported that lack of polarity in the heme pocket of *S. inaequivalvis* hemoglobin was considered to be a major factor in the cyanide complex stabilization (Boffi, Chiancone et al. 1997). These results indicated that the native Asn74 residue was critical to the Fe^{3+}-CN binding phenotype.

The study of the pH dependence upon addition of cyanide conveyed important information about cyanide coordinated heme iron state because cyanide could easily bind

to the Fe^{3+} heme in proteins. At pH 6.0, the spectra of N74V mutant cyanide complex indicated a typical hexacoordinate, low-spin ferric heme protein with the Soret peak at 436 nm. However, above pH 10.0, the Soret peak was blue shifted with maxium absorption at 423 nm. The reason for the observed spectral shifts is beyond our access with our current data available.

2.3.8 N74V KSCN binding
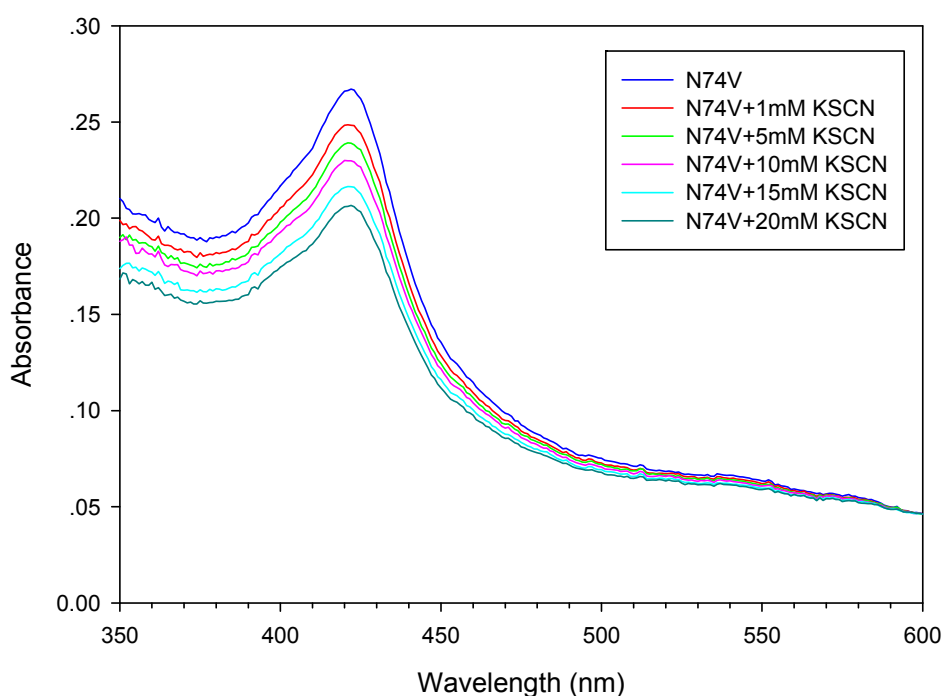
Fig 2.18 UV-Visible spectra of the thiocyanate complexes of the N74V mutant in 25 mM potassium phosphate buffer at pH 6.0 with 5 µM enzyme concentration. The ligand concentration was from 1 to 20 mM.

Potassium thiocyanate was also a widely used ligand for studying ligand binding properties of heme proteins. The UV-Vis spectra of the SCN complex of CPO N74V indicated that there was no Soret peak shift as shown in the cyanide complex (Fig 2.18). The maximum absorbance remained to 422 nm with the decreasing absorbance as the concentration of thiocyanate increased.

2.3.9 N74V halide binding study

Halide	pK_a	Soret peak	K_d^{app} (mM)		
			pH=2.0	pH=3.0	pH=4.0
Cl⁻	-2.2	418	801.8	957.1	878
Br⁻	-4.7	419.5	617.9	788.2	616
I⁻	-5.2	421	209.1	248.1	204.5

Table 2.1 Apparent K_d for halide binding of the N74V mutant.
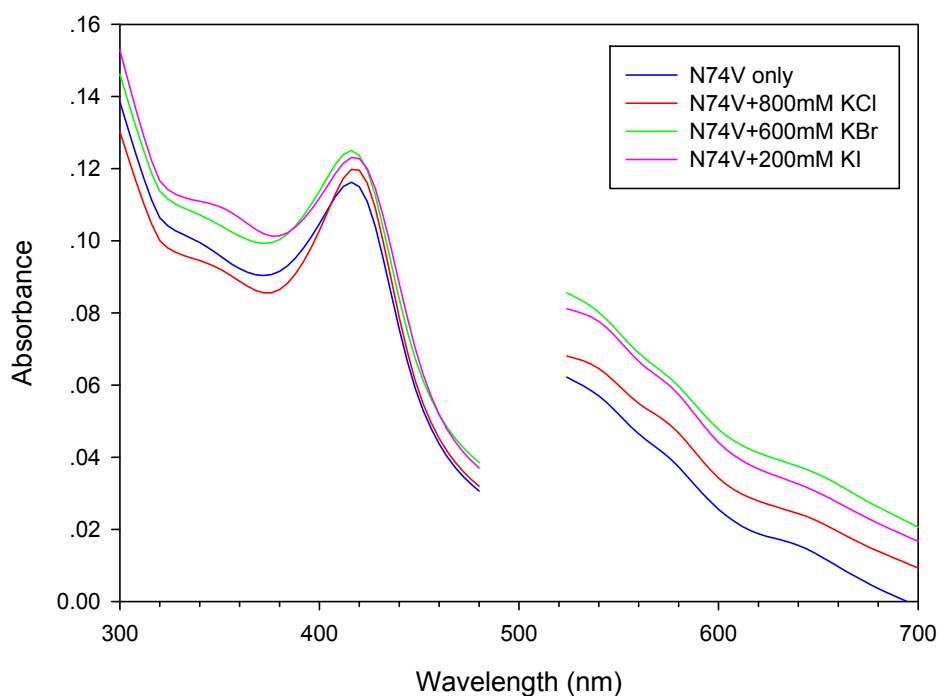
Fig 2.19 UV-Visible spectra of halide complexes of the N74V mutant in 25 mM potassium phosphate buffer at pH 6.0 with 5 μM enzyme concentration.

Chlorination activity was the most prominent feature for CPO (Libby 1982). It has been proposed that halide binding is related to CPO's halogenations activity as there were several halide binding sites in the narrow channel (add refecences). The halide binding study showed that K_d of iodide was the lowest and that of chloride was the highest. It is further noted that halide binding affinity toward CPO was not affected by pH values

(Table 2.1). However, the K_d of Br^- and Cl^- complexes of Wt CPO increased from 20 - 30 mM at pH 2.0 to 400 - 660 mM at pH 3.5 (Sono 1986). And the high concentrations of Br^- and Cl^- ions altered the spectrum of ferric Wt CPO by shifting the maxium absorbance from 399 to 422 nm (Sono 1986). The Soret peak of iodide bound complex was located at 421 nm, which was 3 nm different with that of the chloride compound. The close proximity of Asn74 to iodide binding site Ⅲ accounts for the observed effects after mutation of this residue to a more hydrophobic amino acid.

2.3.10 k_{cat} & K_M values in halogenation and epoxidation reactions

		K_M (µM)	k_{cat} (S^{-1})	k_{cat}/K_M (µM^{-1} S^{-1})
MCD	Wt CPO	4.7±1.2	0.24±0.02	5.0×10^{-2}
	N74V	1.1±0.16×10^2	0.23±0.01	2.0×10^{-3}
Styrene	Wt CPO	1.34±0.12×10^4	0.63±0.18	4.7×10^{-5}
	N74V	5.5±0.43×10^2	2.2±0.8	4.0×10^{-3}

Table 2.2 Kinetic parameters of MCD chlorination and styrene epoxidation reactions by Wt CPO and the N74V mutant.

Kinetic parameters for the Wt CPO and N74V mutant catalyzed halogenation and epoxidation reactions were examined with MCD and styrene as the respective substrates (Table 2.2). The N74V mutant has a higher K_m value in the halogenation reaction but much lower K_m in the epoxidation reaction compared to those of wild type chloroperoxidase. However, the turnover number of the N74V mutant is similar or higher than that of wild type chloroperoxidase. Therefore, the mutation did not or only little affected the catalytic efficiency of the enzyme, as proved by the comparable k_{cat}/K_m values between Wt CPO and CPO N74V.

2.4 Results of the N74Q mutant

2.4.1 UV-Visible spectroscopic properties of Wt CPO and the N74Q mutant
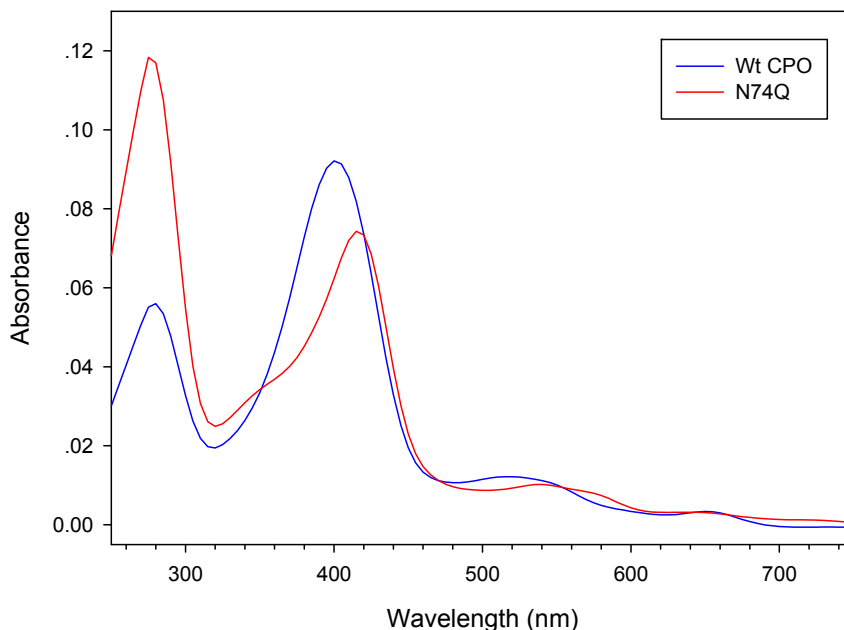
Fig 2.20 Absorption spectra of the purified Wt CPO and the N74Q mutant in 25 mM potassium phosphate buffer at pH 5.9.

Similar to the UV-Vis spectra of N74V enzyme, the N74Q mutant showed the characteristics of Soret maximum at around 420 nm (Fig 2.20). The minor peaks were located at 355, 541 and 560 nm (Fig 2.21). The peak at 355 nm serves as an indicator for the low spin heme at the reactive center. The spectral difference exhibited by N74Q mutant compared with that of Wt CPO was possibly due to the binding of a water molecule to the heme iron.

2.4.2 CD spectroscopic study of the N74Q mutant

To demonstrate the secondary structure of chloroperoxidase mutants, a far-UV CD spectrum of the N74Q mutant was obtained (Fig 2.22). The result showed that there was

no apparent difference in the spectra induced by the site directed mutagenesis. Even some

conformational changes exist, they must have been very localizedand undetectable.
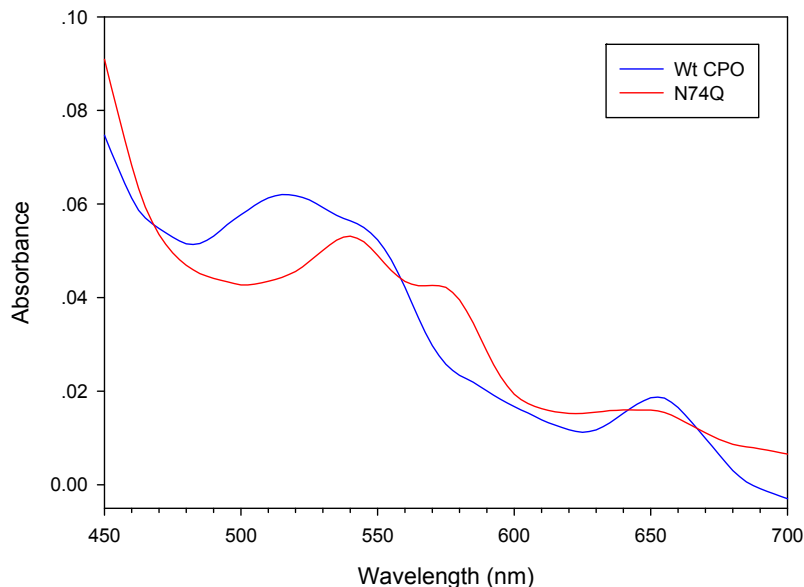
Fig 2.21 Detailed UV-Vis spectra of Wt CPO and the N74Q mutant in 25 mM potassium
phosphate buffer at pH 5.9.

2.4.3 Characterization of CO binding to the N74Q mutant

Ultraviolet-visible spectroscopy was carried out to examine the binding of the N74Q

mutant with carbon monoxide (CO). The CO complexes of thiolate-ligated heme

peroxidases give an absorption band at 450 nanometers. However, in the histidine-ligated

systems, that band is blue-shifted to 420 nanometers. As mentioned before, in Wt CPO,

the formation of the ferrous-CO state completely shifted the Soret peak from 400 nm to

445 nm (Fig 2.23). After reducing iron in the N74Q mutant from ferric to ferrous, the

major peak was partially shifted from 420 nm to 443 nm after CO is bound, indicating

that the proximal ligand in the N74Q mutant is identical to that in the Wt CPO.
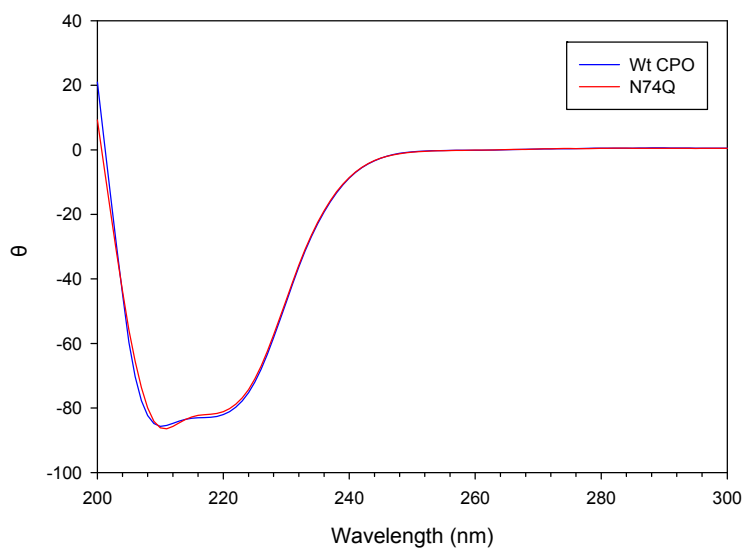
Fig 2.22 Far-UV CD spectra of Wt CPO and the N74Q mutant. 0.5 µM enzyme was dissolved in 25 mM potassium phosphate buffer at pH 6.0. The data were recorded from 200 to 300 nm at room temperature. The path length was 1 cm.
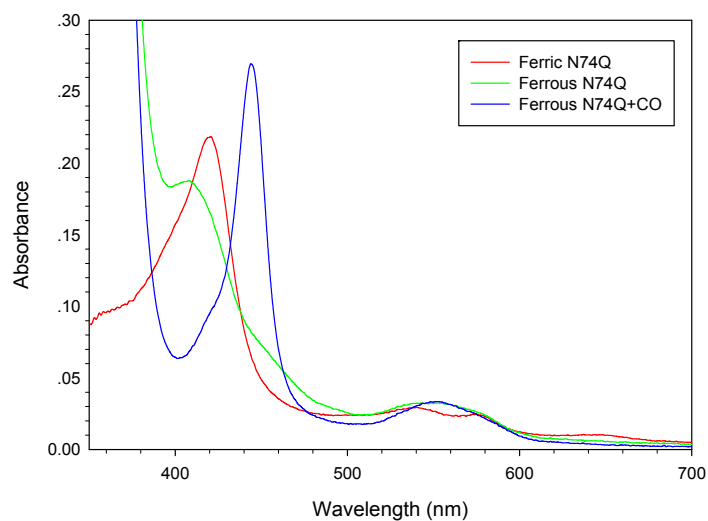
Fig 2.23 UV-Visible spectra of the ferrous-CO complex of the N74Q mutant in 25 mM potassium phosphate buffer at pH=5.9.

2.4.4 Equilibrium titration of N74Q with cyanide

Cyanide can convert the high-spin iron state to the low-spin form (Lambeir 1983). Therefore, this strong binding ligand was used to evaluate the affinity of CPO for

exogenous ligand. In wild type CPO, the Soret peak was shifted from 400 to 439 nm. However, the Soret peak of N74V mutant appeared at 423 nm with the decreasing absorbance as the concentration of KCN was increased (Fig 2.24). Therefore, the mutation from Asn to Gln changed the binding affinity of cyanide at the heme active center.
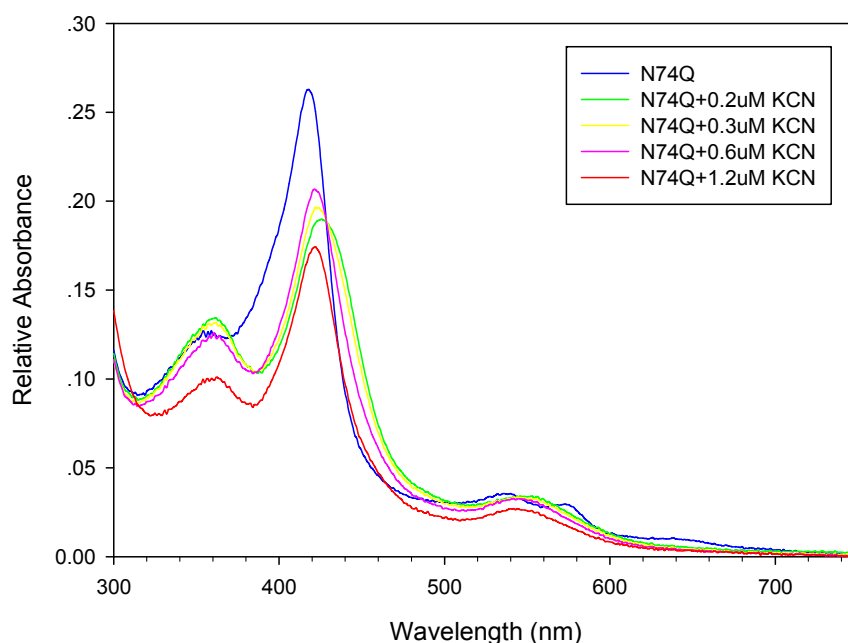
Fig 2.24 UV-Visible spectra of the cyanide complexes of the N74Q mutant with different substrate concentrations in 25 mM potassium cyanide solution at pH= 6.0.

2.4.5 MCD, ABTS and catalase assays performed with the N74Q mutant

Chlorination of monochlorodimedone (MCD) to dichlorodimedone (DCD) was used to measure the chlorination activity of the N74Q mutant (Fig 2.25). Results showed that the N74Q mutant lost almost all its chlorination ability compared to wild-type chloroperoxidase. Also, the N74Q mutant lost its catalase activity as a result of mutation
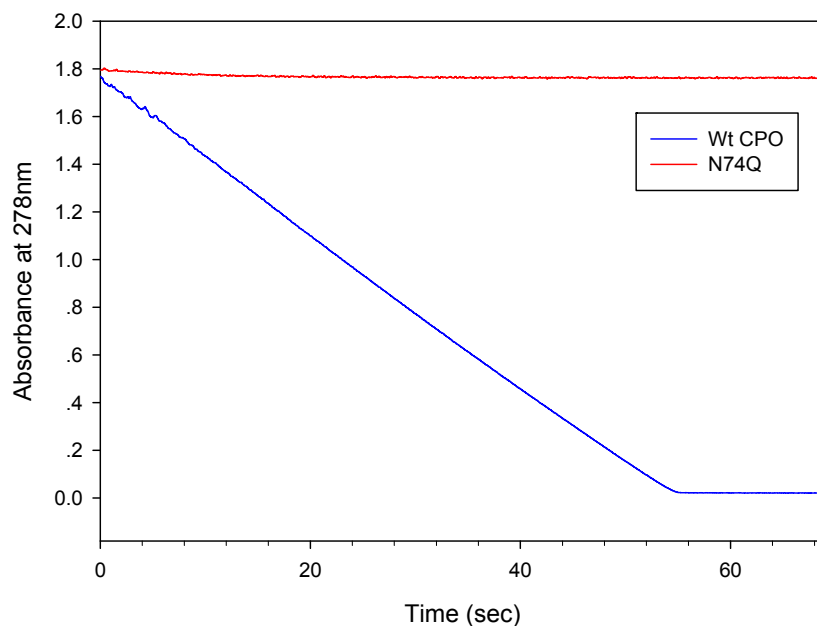
Fig 2.25 UV-Visible kinetic spectra of the N74Q mutant MCD assay in 100 mM phosphate buffer at pH 2.75. The reaction was initiated by the addition of hydrogen peroxide. The decreasing rate of absorbance at 278 nm was recorded.
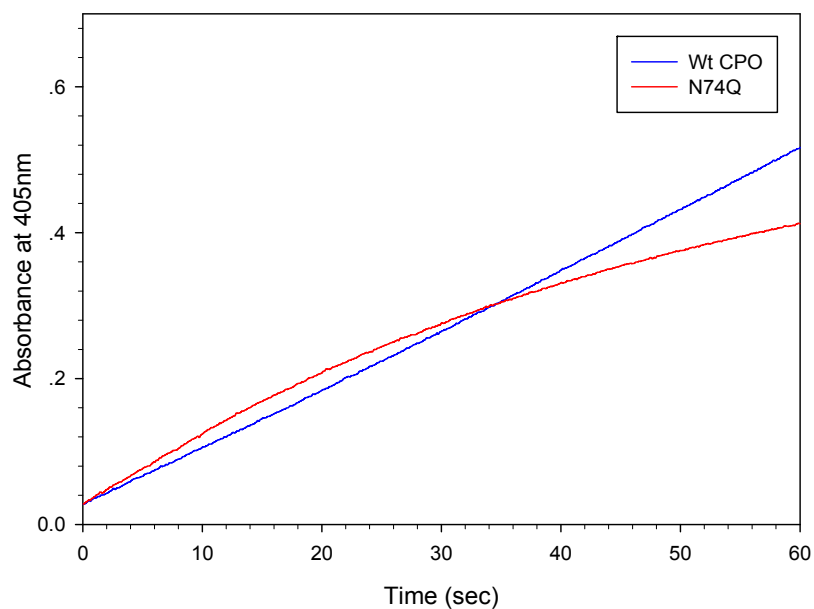
Fig 2.26 UV-Visible kinetic spectra of the N74Q mutant ABTS assay in 100 mM phosphate-citrate buffer at pH 5.0. The reaction was initiated by the addition of hydrogen peroxide. The increasing rate of absorbance at 405 nm was recorded.
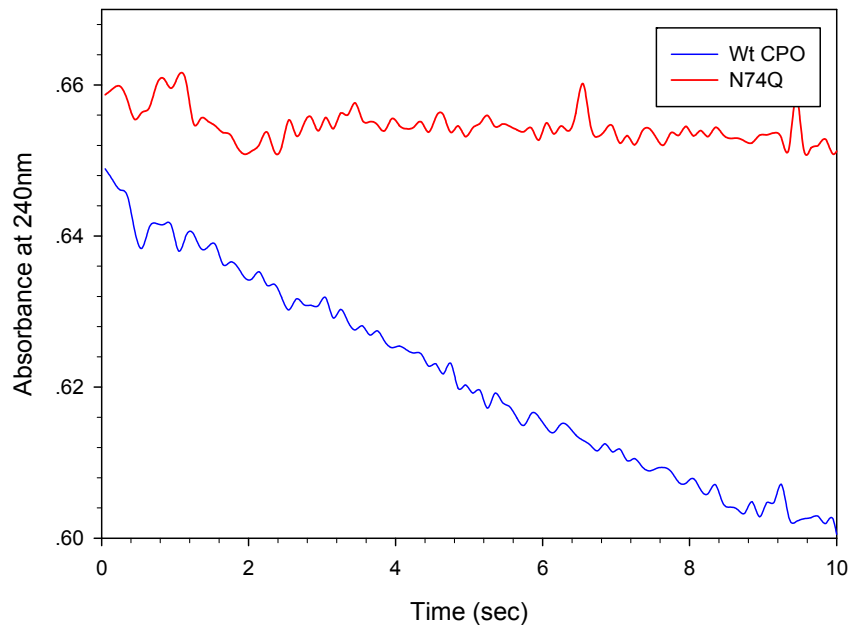
Fig 2.27 UV-Visible kinetic spectra of the N74Q mutant catalase assay in 50mM phosphate citrate buffer at pH 5.0. The reaction was initiated by the addition of the enzyme and monitored at 240 nm.

of the Asn 74 residue. However, in the ABTS assay, the N74Q mutant showed enhanced peroxidation ability compared with that of the wild-typre chloroperoxidase (Fig 2.26). These results may be caused by the difference of polarity in the distal heme pocket and the mechanisms of enzyme-catalyzed reactions.

2.5 Discussion

To verify the function of asparagine74, site-directed mutagenesis was used to replace Asn74 by either a valine or a glutamine. These substitutions were chosen because Val was similar in size tobut dramatically different in hydrophobicity from that of Asn, while Gln has a bigger size than Asn but comparable polarity with Asn. The characteristics of these mutants were quite different with those of Wt CPO.

The spectrum indicated that the N74V mutant was a hexacoordinate, low-spin ferric heme protein with a Soret maximum at 420 nm. The minor peaks of the N74V mutant were located at 356, 540 and 560 nm. After the heme iron of the N74V mutant was reduced from ferric to ferrous and bound to carbon monoxide, the major peak was partially shifted from 420 nm to 443 nm, which indicated that the proximal ligand in the N74V mutant was a cysteine residue. As expected, mutation from Asn to Val decreased the chlorination and catalase reactivity of the N74V mutant, but increased the epoxidation ability compared to wild-type chloroperoxidase. Catalase activity was the primary reason for the destruction of Wt CPO because of the generated reactive oxygen. In addition, epoxidation activity of the Asn74 mutant increased 4-fold compared with that of wild type chloroperoxidase. The results of activity assays could be explained by a non-polar environment of the distal heme pocket in the N74V mutant introduced by a Val residue.

Another important improvement induced by site-directed mutagenesis was the ability of the N74V mutant to catalyze the epoxidation of styrene and its derivatives with high enantioselectivity that were poor substrates for wild-type chloroperoxidase. Styrene and its derivatives are an important group of substrates with significate industrial applications (Hager, Lakner et al. 1998). The improvement in kinetic perfection introduced by the N74V mutation was reflected by the favorable changes in k_{cat} and k_{cat}/K_M values of these reactions. Therefore, Asn74 mutant is a promising candidate for industrial applications due to its relaxed substrate specificity.

Interestingly, the N74Q mutant showed similar properties compared to the N74V mutant in the halogenation, peroxidation, and catalatic reactions. Since there were no significant structural changes in the N74Q mutant as indicated by the CD spectroscopic

study, my research on the N74Q mutant could help better understand the mechanisms of CPO-catalyzed enantioselective reactions and fine-tune the catalytic properties of chloroperoxidase.

The Asn74 residue may also play a critical role in orienting ligands in the narrow channel as reflected in the halide binding behavior. Cyanide binding to the Asn74 mutant was investigated as a function of pH using spectroscopic, equilibrium, and kinetic methods. The Asn74 mutant has a higher K_M value in the halogenation reaction, much lower K_M in the epoxidation reaction than those of Wt CPO and similar or higher turnover numbers compared to those of wild type chloroperoxidase.

It is very interesting that a single mutation outside the catalytic center could result in such significant changes in the catalytic profile. Although Asn74 was originally proposed to form hydrogen bonds with many polar substrates to orient them to the heme catalytic center, it could also interact with some nonpolar substrates in the epoxidation of styrene and its derivatives.

The N74 mutants are very interesting targets to study thiolate-ligated hemoproteins, as they provide greater enzymatic activities and several clues on how CPO orients its substrates to the catalytic center. Since they have a greater resemblance to P450cam in its UV-Vis spectrum, the N74 mutants are also better models for understanding the long standing and difficult question of P450 mechanism than chloroperoxidase. Therefore, my study provides the fundamental principle for understanding the structural and functional role of the substrate access channel in thiolate-ligated hemoproteins. It demonstrates the feasibility of engineering novel enzymes with tailor-made activities that are effective in biocatalysis, bioremediation and other biotechnological applications.

CHAPTER III

CHIRAL STUDY OF CPO MUTANTS

3.1 Background

3.1.1 High performance liquid chromatography (HPLC)

High performance liquid chromatography (HPLC) was first invented in the late 1960s by using high pressure to detect and separate different compounds (Horváth 1967). With the expansion in the use of computers and detectors, HPLC quickly became an indispensable technique for the separation of chemical or chiral compounds in different industrial fields in the 1980s (Hung 1988). Recently, various types of columns have been developed on the basis of different principles of interactions between the samples and the stationary phase to separate certain types of compounds, such as ion-exchange, adsorption, and chiral columns. In the biochemistry and analytical chemistry field, HPLC was also a widely used technique to separate different components in a mixture (Snyder 2009).

Two types of phases are used in the liquid chromatographic technique: one is the stationary phase and the other is the mobile phase. The stationary phase is positioned in a certain type of columns and the mobile phase is driven by a high pressure pump with an injected sample to flow through the column to separate the chiral products. The separated components are then monitored by a detection unit when they are eluted from the column (Fig 3.1). Nowadays, ultraviolet, mass-spectrometry, fluorescence, electrochemical, refractive index, and conductivity based detectors are the commercially available measuring devices. Among them, the ultraviolet (UV) detector is the most widely used

one because of the adequate response to most analyzed chemicals. The operating wavelength for the UV detector is from 190 to 700 nanometers.
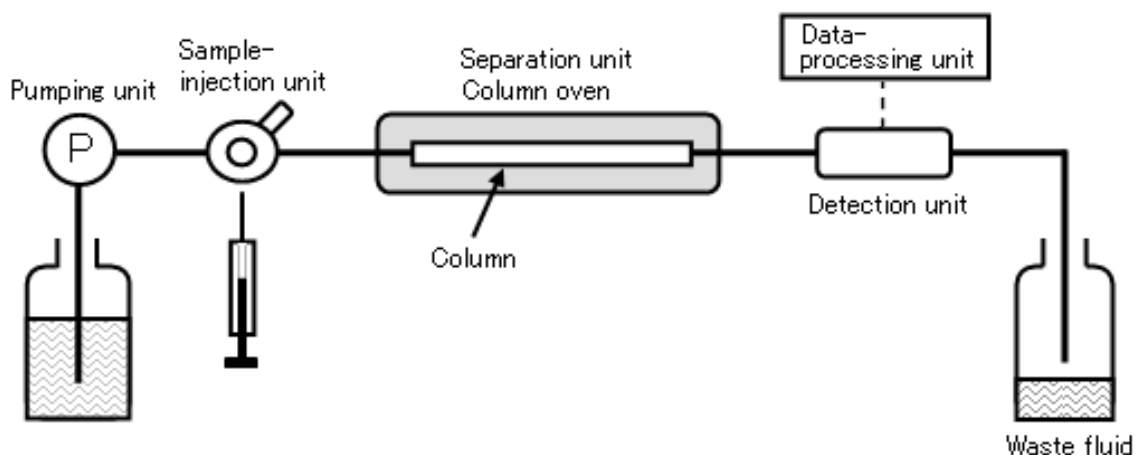
Fig 3.1 Diagram of the chromatographic process in an HPLC unit.

Chiral separation of the enantiomers is quite important in the chiral synthesis, biochemistry, pharmacology and medicine field, because the pharmacological and toxicological behaviors of the enantiomers can be significantly different (Schmid 2001). Efficient and accurate separation of enantiomers is one problem in the development of enantioselective drugs with chiral centers (Eichelbaum 2007). In recent years, HPLC has been rapidly developed in the chiral application field, which can provide rapid, sensitive and efficient sample anaylsis and separation.

3.1.2 Whelk-O 1 chiral stationary phase

The versatile and robust Whelk-O 1 column is chosen as the chiral stationary phase (CSP) to separate the enantiomers of reaction mixtures because of the nonpolar properties of products (Zhao 2009). The chiral stationary phase of the column (Fig 3.2), is a typical brush-type compound using 1-(3, 5-dinitrobenzamido)-1, 2, 3, 4- tetrahydrophenanthrene

as the binding material. It is reported that CSP can be linked to silica via a hydrocarbon tether and a siloxane bond (Mikes 1976). The basic principle of the Whelk-O 1 column to separate the enantiomers could be concluded as a "three point rules", which summarizes three direct interactions between the enantiomers and the chiral selector. Among these interaction sites, at least one is stereoselectively dependent and contributed to the effienciency of chiral separation. Typically hydrogen bonding, π-π or dipole interactions and inclusion complexation are involved in the interactions. In the Whelk-O 1 column, an extraordinary degree of the π-electron acceptor signal is observed from the 3, 5-dinitrobenzamide π-system because of the two electron-withdrawing nitro groups. Furthermore, the hydrogen donor of the amide group is often involved in the hydrogen bonding network.
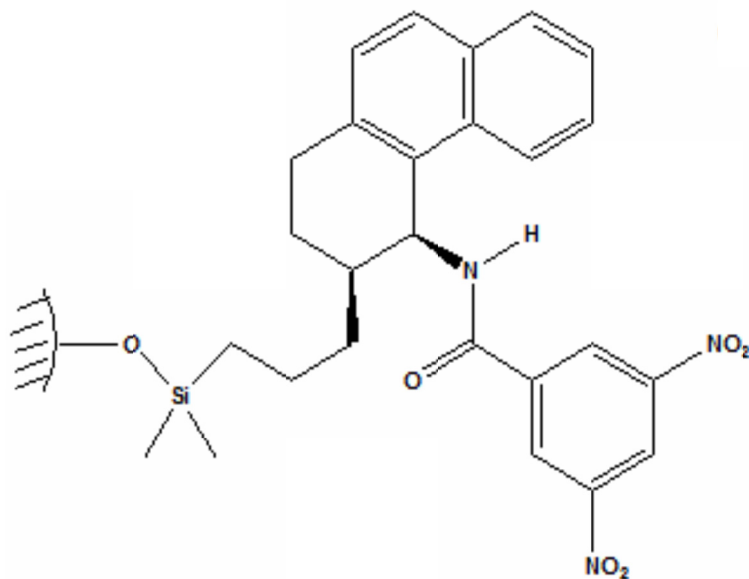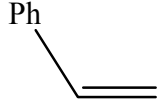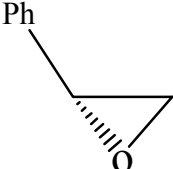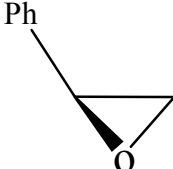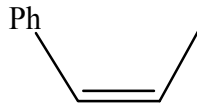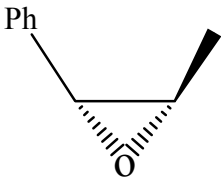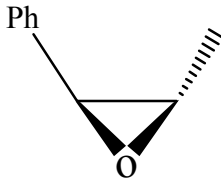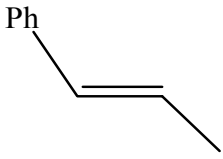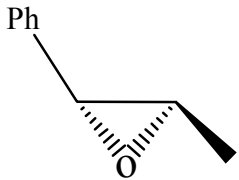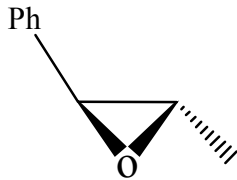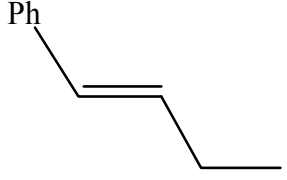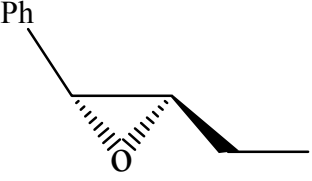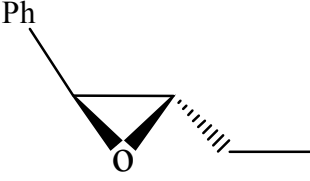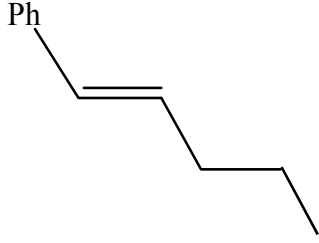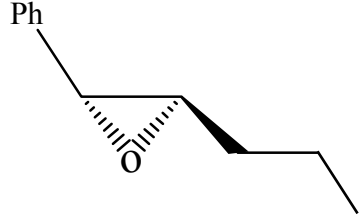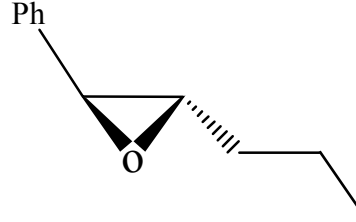
Fig 3.2 Chemical structure of Whelk-O 1.

Table 3.1 Structures of styrene oxide and its derivatives.

Substrate	Epoxidation products	
	(R)-isomer	(S)-isomer

Styrene

Cis-β-methylstyrene[a]

Trans-β-methylstyrene[b]

Trans-β-ethylstyrene[c]

Trans-β-ethylstyrene[d]

[a] (1*R*, 2*S*)-*cis*-β-methylstyrene and (1*S*, 2*R*)-*cis*-β-methylstyrene.
[b] (1*R*, 2*R*)-*trans*-β-methylstyrene and (1*S*, 2*S*)-*trans*-β-methylstyrene.
[c] (1*R*, 2*R*)- *trans*-β-ethylstyrene and (1*S*, 2*S*)-*trans*-β-ethylstyrene.
[d] (1*R*, 2*R*)- *trans*-β-propylstyrene and (1*S*, 2*S*)-*trans*-β-propylstyrene.

The Whelk-O 1 column is more widely applied than other chiral stationary phases on the basis of the covalent bonding to support materials and the tolerance of CSP to many organic solvents. In my research, epoxidation products of styrene and its derivatives were successfully separated with this column. The (*R*)- and (*S*)-styrene oxide and their derivatives from tepoxidation reactions catalyzed by Wt CPO and the CPO mutants were summarized in Table 3.1.

3.1.3 Function of histidine 105

In the distal pocket of CPO, even though the environment around the heme is polar like other peroxidases, a glutamic acid instead of a histidine is employed to cleave the peroxide bond during the formation of compound I (Yi, Conesa et al. 2003). In the distal heme pocket of CPO, glutamic acid 183 is the residue closest to the heme iron and involved in CPO reactions as a catalytic acid-base. Histidine 105 is about 3.5 Å away from the heme propionate and responsible for formation of a hydrogen bond with Glu183 (Sundaramoorthy, Terner et al. 1995; Yi, Conesa et al. 2003). When the substrates bind at the heme center, the side chain of Glu183 is locked because it forms hydrogen bond to a water molecule and a histidine residue. Therefore, Glu183, His105 and Asp106 interact together as a proton relay shuttle to facilitate the cleavage of hydrogen peroxidase (Wang 2003). Acturally the X-ray result of native chloroperoxidase discovered a proton shuttle among Glu183, His105, and Asp106 (Sundaramoorthy 1995), which confirmed the hypothesis mentioned above.

Even though His105 is not directly involved in the reaction of chloroperoxidase, it may play an important role in the orientation of the glutamine 183 residue. During the catalysis, His105 forms a hydrogen bond network between Glu183 and a water molecule

or hydrogen peroxide (Wang, Tachikawa et al. 2003). Hydrogen bond network could facilitate the cleavage of peroxide oxygen-oxygen bond. Therefore, the replacement of histidine to a nonpolar alanine may destabilize/desrrupt the hydrogen bond network, giving more freedom for Glu183, and thus lower CPO's catalytic activities. The change of binding properties may increase the enantioselectivity of certain reactions catalyzed by CPO mutants.

3.1.4 Aim of the study

Histidine 105 (H105) was replaced by a nonpolar amino acid alanine using site-directed mutagenesis to study the chlorination and catalase activity of the H105A mutant because of decreased polarity in the distal heme environment and breakage of the hydrogen bond with glutamic acid 183 (E183). Also, enantioselective studies of the epoxidation of bulky styrene derivatives can obtain strong evidence for the proposed histidine/cysteine ligand switch in chloroperoxidase, providing experimental support for the structure of the 420-nm absorption maximum in a number of carbon monoxide complexes of heme-thiolate proteins.
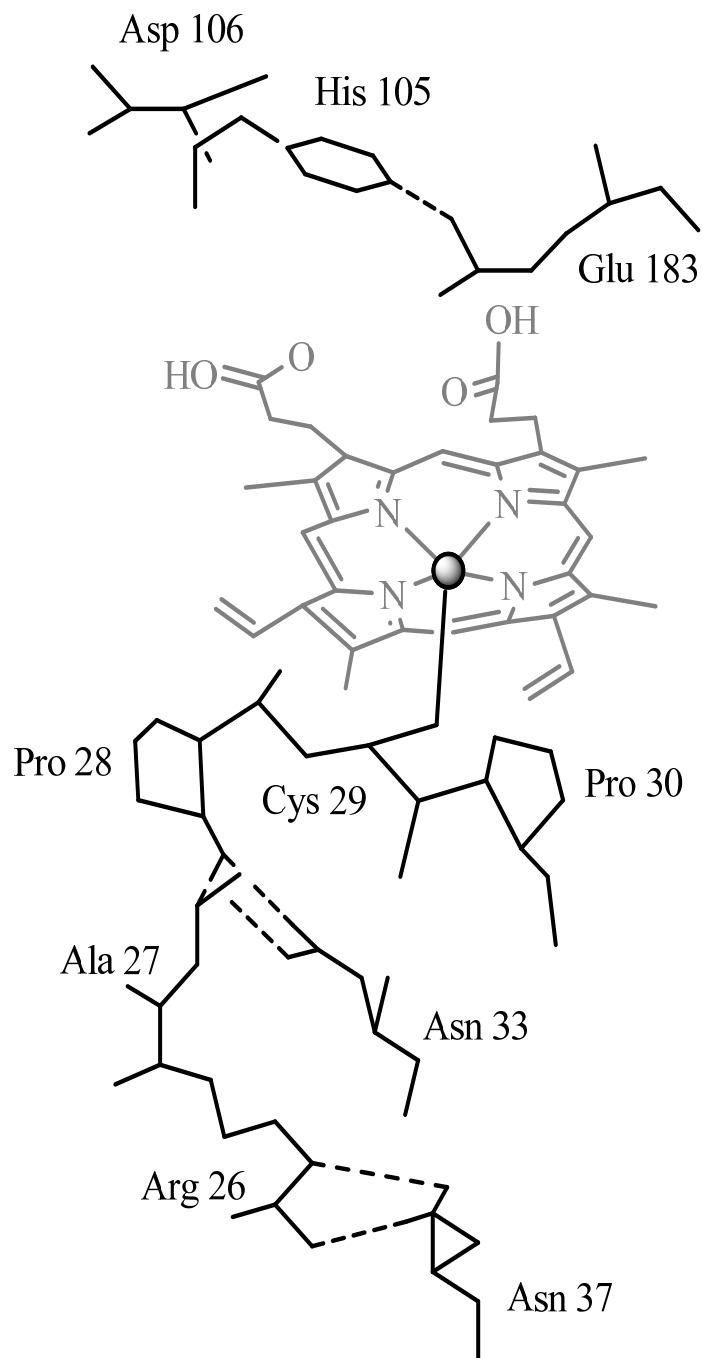
Fig 3.3 Active site structure of chloroperoxidase. Proximal and distal ligand residues are indicated in bold. Heme coordination to the proximal ligand is indicated by a grey solid line. Hydrogen bonds are represented by dashed lines (PDB: 1CPO).
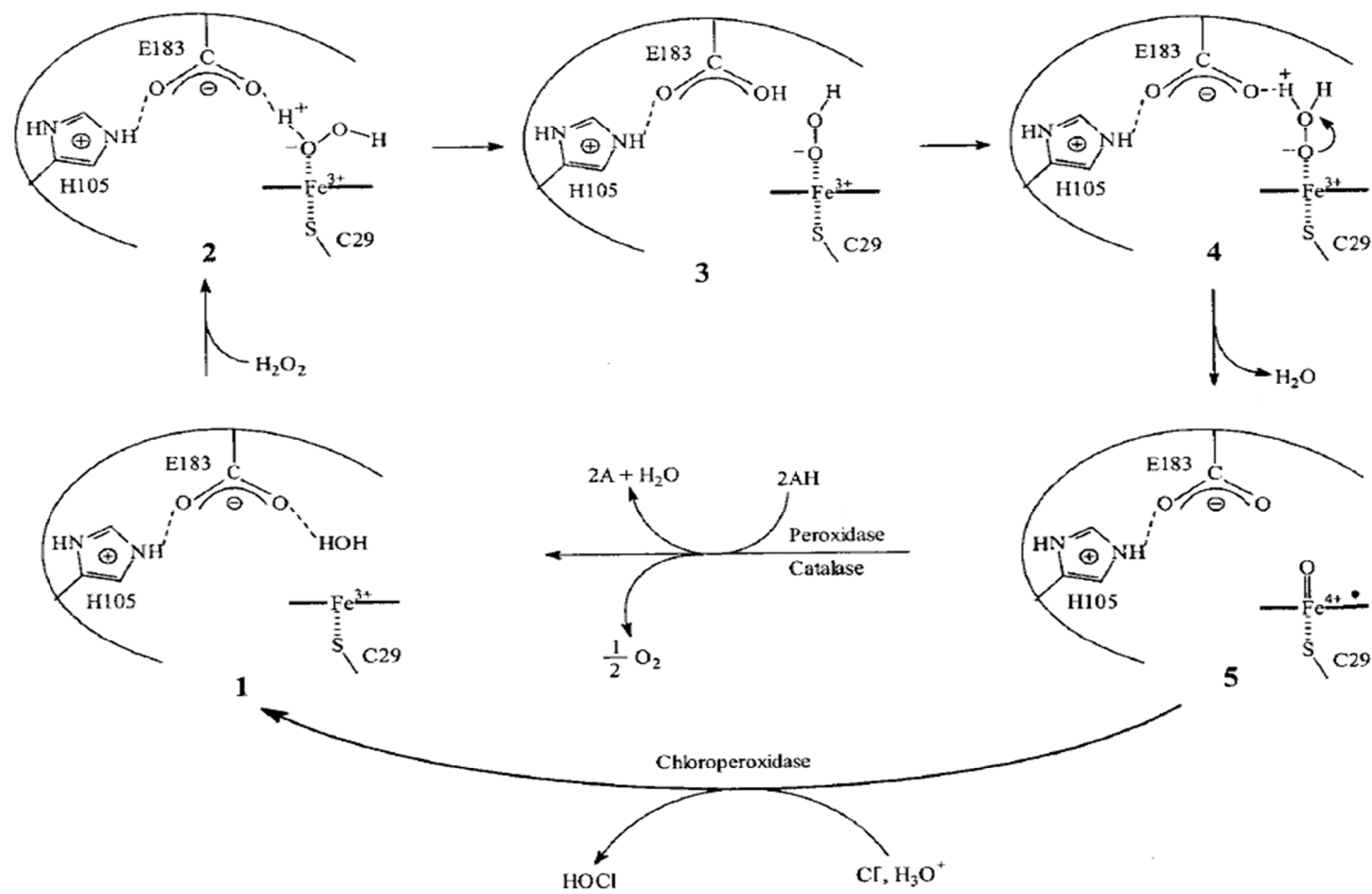
Fig 3.4 Proposed mechanism that His 105 facilitates the cleavage of the peroxide O–O bond.

3.2 Materials and Methods

3.2.1 Materials

Marine fungi *Caldariomyces fumago* and filamentous fungi *Aspergillus niger* (MGG029) were purchased from American Type Culture Collection (ATCC) (Manassas, VA). Gene expression vector pCPO3.I-Amds and co-transformation plasmid pAB4.1 with a selection marker (GenBank accession no. AJ300448) were kindly provided by Dr. Punt (TNO Nutrition and Food Research Institute, Netherlands). Restriction enzymes were purchased from New England Biolabs (Beverly, MA). Ultra-*Pfu* DNA polymerase with relatively high fidelity was obtained from Stratagene (San Diego, CA). Purified oligonucleotide primers were obtained from MWG-Biotech (Ebersberg, Germany). The QuickChange site-directed mutagenesis kit was purchased from Stratagene (La Jolla, CA). De-ionized water for all the experiments were prepared freshly by Milli-Q Biocel (Millipore, Billerica, MA). The JASCO J-720 spectropolarimeter was used to record far UV-CD spectra from 190 to 250 nm. Ultraviolet-Visible absorption was monitored by using a VARIAN Cary 300 spectrophotometer.

Styrene, α-methylstyrene, *trans*-β-methylstyrene, *trans*-β-ethylstyrene, *trans*-β-propylstyrene were purchased from Sigma-Aldrich (St. Louis, MO). A Waters 1525 instrument equipped with a photodiode array UV-detector (Waters, Milford, MA) was used to carry out all HPLC experiments. All instrumental parameters and data analysis were set up by using Waters Empower 2 software (Waters, Milford, MA). WhelkO-1 column (250 mm x 4.6 mm, Regis Technologies, Morton Grove, IL) was used to separate the enantiomers in the reaction mixture.

3.2.2 H105A mutant gene construction

Protocols of H105A site-directed mutagenesis were from Stratagene Quikchange Kit and PCR amplification. Expression vector pCPO3.I-AmdS with the complete set of *cpo* gene encoded was used as the template. The plasmid was designed to use the *A. niger* glucoamylase as the promoter and *A. nidulans trpC* as the terminator. A selection marker *AmdS* gene was inserted into the *NotI* restriction enzyme digestion site.

Encoded primers for the H105A mutant were 5' ccc cac gct ttc gag GCC gac cac tcc ttc tcc 3'. The PCR reactions were carried out by using the following steps: initial denaturation at 94 ºC for 1 min followed by 34 cycles at 94 ºC for 30 secs (denaturation) and 68 ºC for 6–9 mins (annealing and extension). The desired mutation was confirmed by DNA sequencing and the expression vector pCPO3.I-AmdS containing the H105A mutation was named as pCPO-H105A-AmdS. The high fidelity Ultra-*pfu* DNA polymerase was employed in the reactions.

3.2.3 Mutant DNA sequencing and restriction endonuclease digestion

Results of the H105A single mutation were identified by DNA sequencing and construction of a restriction enzyme digestion map. The mutant DNA was extracted from the transformed *E. coli* strain under the instruction of QIAGEN DNA extraction mini kit (QIAGEN, CA). The plasmid DNA of the H105A mutant was further examined by BsiHKAI restriction endonuclease. The restriction endonuclease cleaved the mutant *cpo* gene at the specific location shown below, which did not exist in the original plasmid containing the gene for wild-type chloroperoxidase. The results were examined by SDS-PAGE gel electrophoresis. The primers (5'-cgc gga tcc atg ttc tcc aag gtc c -3' & 5'- ccg gaa ttc aag gtt gcg ggc-3') were used to amplify the CPO coding region.

3.2.4 Mutant gene transformation into *A. niger*

Filamentous fungi MGG029/ATCC62590 strain were inoculated in 125 mL of minimal media with 10 mM uridine and 0.1 mg/mL carbonicilin, and cultured for several days at 30 degrees Celsius. Mycelia from the fungi were disrupted by using a homogenizer at the full speed for 20 secs for 3 times and then transferred to 2 L of minimal medium. The cultures were incubated for 20 hours at 250 rpm and 30 degrees Celsius. Mycelia were filtered through a sterile myracloth and resuspended in 1.7 Osm (0.27 M $CaCl_2$, 0.6 M NaCl). Protoplasts were then treated with 7.5 mg/mL lysing enzyme (Interspex, Sigma L-1412) for 4 hours at 150 rpm and 37 degrees Celsius. Digested protoplasts were resuspended and incubated on ice for 20 minutes. After centrifugation (3500 rpm, 15 minutes, 0 ºC), samples were washed twice with STC 1700 (1.2 M sorbitol, 10 mM Tris-HCl at pH 7.5, 50 mM $CaCl_2$, 35 mM NaCl), and the protoplasts were resuspended in STC1700 and mixed with 10 μg pCPO3.I-Amds mutant plasmid and 1 μg pAB4.1 co-transformation plasmid and then incubated at 25 ºC for 25 minutes. In three steps, 60% PEG4000 in 10 mM Tris-HCl at pH 7.5 and 50 mM $CaCl_2$ were carefully mixed with the treated protoplast mixture and diluted by addition of 5~10 mL of STC1700 to spread on 1.2 M sorbitol selective agar medium plates.

3.2.5 Expression of the H105A mutant protein

Filamentous fungi were cultured in *A. niger* minimal growth medium containing 50 g/L maltose, 10 g/L glucose, 5 g/L casamino acid, 6 g/L $NaNO_3$, 0.5 g/L KCl, 0.8 g/L KH_2PO_4, 1 g/L K_2HPO_4, 0.25 g/L $MgSO_4$, 0.1 mM heme precursor and 100 mg/L carbenicillin. After culturing in a rotary shaker at 250 rpm and 25 ºC for 24 hours, the fungi continued to grow at 22 ºC for an additional 6 days. Chlorination activity of the

culturing medium was examined daily for the yield of mutant protein using the MCD assay.
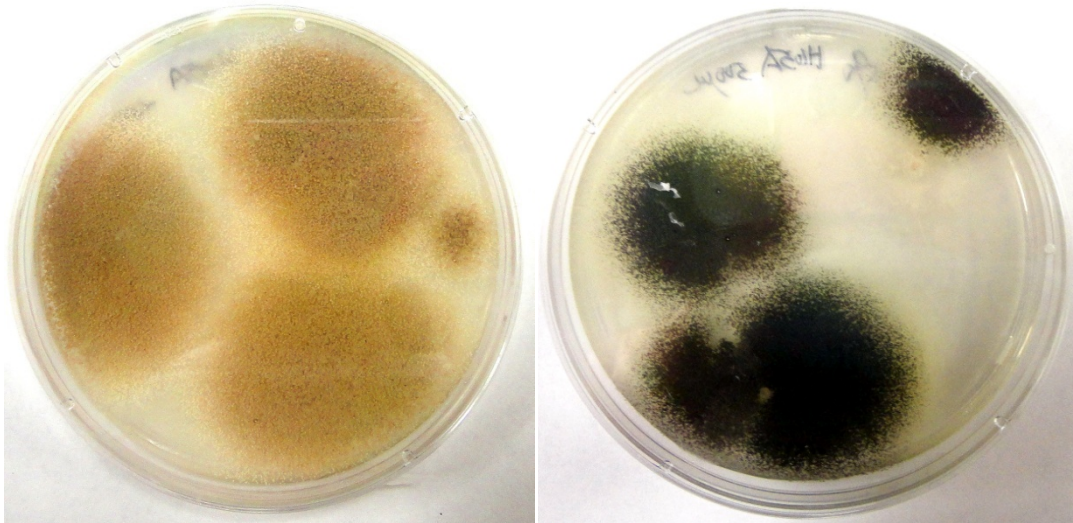
Fig 3.5 Single mutant H105A transformed into MGG029 (left) and ATCC62590 (right), grown on 1.2 M sorbitol selective agar plates.

3.2.6 Purification of the mutant protein

Collection of culturing medium was carried out by filtering through the miracloth and 0.8 μm membrane to remove the fungi and mycelium. After that, a high output ultrafiltration cell with 30 kDa cut off membrane was used to condense the large volume of crude medium. About 100 mL samples were collected and dialyzed in 4 L buffer containing 25 mM potassium phosphate at pH 5.9 for 24 hrs with at least one buffer exchange. For protein purification, DEAE sepharose fast flow column (Amersham, 2.6 × 20 cm) and Sephadex G-75 column (Amersham, 2.6 × 100 cm) were applied. Ion exchange chromatography was used to separate the desired protein from others by ionic strength gradient difference (0-0.5 M NaCl) in 25 mM potassium phosphate buffer at pH

5.9. All the experiments were carried out at 4 °C to keep the mutant protein stable. Reinheitzahl (Rz) value was employed to examine the purity of enzymes and practions of Rz > 0.8 were collected and condensed by using Centriprep-YM30 (Amincon) for further kinetic study.

3.2.7 Protein kinetic activity assay

Chlorination capability of CPO was measured by the transformation of monochlorodimedone (MCD) to dichlorodimedone (DCD). The reaction system contained 20 mM KCl, 0.17 mM MCD, certain amounts of the enzyme in 100 mM phosphate buffer at pH 2.75 and the reaction was initiated by the addition of hydrogen peroxide. The decreasing rate of absorbance at 278 nm was recorded.

Epoxidation reaction was carried out in 100 mM sodium acetate buffer at pH 4.5, containing 0.2 mM p-nitrostyrene as the substrates and suitable aliquots of enzymes. The decrease in absorbance at 312 nm as a function of time was monitored.

Catalase activity of CPO was measured by the rate of decreasing absorbance of H_2O_2 in 50 mM phosphate citrate buffer at pH 5.0. The reaction was initiated by the addition of the enzyme and monitored at 240 nanometers.

In the peroxidation activity assay, 2, 2'-azino-bis-3-ethy-benzthiazoline-6-sulfonic acid (ABTS) was used the electron donor. The reaction mixture was in 100 mM phosphate-citrate buffer at pH 5.0 and initiated by the addition of hydrogen peroxide. The increase of absorbance at 405 nm was recorded.

3.2.8 Epoxidation of styrene and its derivatives catalyzed by H105A

Styrene and its derivatives (α-methylstyrene, cis-β-methylstyrene, $trans$-β-methylstyrene, $trans$-β-ethylstyrene, and $trans$-β-propylstyrene) were used to study the

enantioselectivity of Wt CPO, H105A and N74Q mutants in the epoxidation assay. The reaction mixture was composed of 100 µl of tert-butyl hydroperoxide and 70 µL of styrene or other styrene derivatives. The reaction was triggered by the addition of 25 µL reaction mixture into 750 µL 100 mM citrate buffer at pH 5.5. About 2 mg of Wt CPO or mutants was added to reaction mixture. After incubated in the shaker at 150 rpm and room temperature for 3 hrs, the reaction products were extracted three times using 300 µL isooctane (Sigma-Aldrich, St. Louis, MO).

3.2.9 Chiral separation of CPO epoxidation products by HPLC

A Whelk-O 1 column was used as the stationary phase to separate the chiral products of the expoxidation reactions catalyzed by Wt CPO, H105A and N74Q mutants. The mobile phase was hexane mixed with 0.2% to 2% ethanol. The flow rate was 1.0 mL/min at 4 ºC or room temperature. The injection volume of each sample was set to 20 µL. The UV-Visible absorption wavelength for the chiral products was ranged from 208.6 to 218.6 nm. Retention time and peak intensity were not optiminzed at some cases to get the better separation results of the enantiomers.

3.2.10 Data analysis

Parameters used to analyze the CPO and its mutants catalyzed epoxidation products were shown as follows:

$$\text{Retention factor: } k' = (t_R - t_0)/ t_0$$

where t_R was the retention time and t_0 was the void time;

$$\text{Separation factor: } \alpha = k_2' / k_1'$$

where k_1' and k_2' represented the retention factors of two eluted enantiomers;

$$\text{Resolution factor: } R_s = 2(t_{R2} - t_{R1})/ (W_1 + W_2)$$

where t_{R1} and t_{R2} standed for the retention times of two eluted enantiomers and W_1 and W_2 were related individual peak widths.

$$ee= \% \text{ (major isomer) - } \% \text{ (minor isomer)}$$

3.3 Results

3.3.1 UV-Visible spectroscopic properties of Wt CPO and the H105A mutant

An important characteristic of heme-containing proteins is that they show a Soret peak in UV-Vis spectra, which can reveal useful information about the heme active center. The spectrum indicated that the H105A mutant was a hexacoordinate, low-spin ferric heme protein with a Soret maximum at 418 ± 1 nm (Fig 3.6). The spectrum of Wt CPO was different from that of the H105A mutant by showing the Soret peak at 398 ± 1 nanometers. The minor peaks of the H105A mutant were located at 345, 540 and 580 nm, but those of Wt CPO were at 515, 545 and 650 nm, respectively. Results indicated that there was one water molecule bound to the heme iron in the H105A mutant, and therefore gave a low-spin heme at the catalytic center.

3.3.2 UV-Vis spectroscopy of Wt CPO, rCPO and H105A with CO at different pH

The properties of Wt CPO, recombinant CPO (rCPO) and the H105A mutant in their ferric or ferrous forms and their carbon monoxide (CO) complexes were examined using UV-vis spectroscopy. The CO binding method is a typical assay for cytochrome P450 enzymes. As is widely known, the CO complexes of thiolate-ligated hemoperoxidases show a characteristic absorption band at around 450 nanometers. However in the histidine-ligated systems, the Soret band is blue-shifted to 420 nanometers. In Wt CPO, the formation of ferrous-CO state completely shifted the Soret peak from 400 nm to 445 nm at pH 5.9. But at different pH, the patterns of spectra were quit different for Wt CPO,

rCPO and the H105A mutant (Fig 3.7-Fig 3.15). By replacement of the distal histidine by alanine, the peak of the CO complex at 425 nm did not disappear, which indicated that there was partial histidine/cysteine ligand switch in the distal and proximal heme pockets.
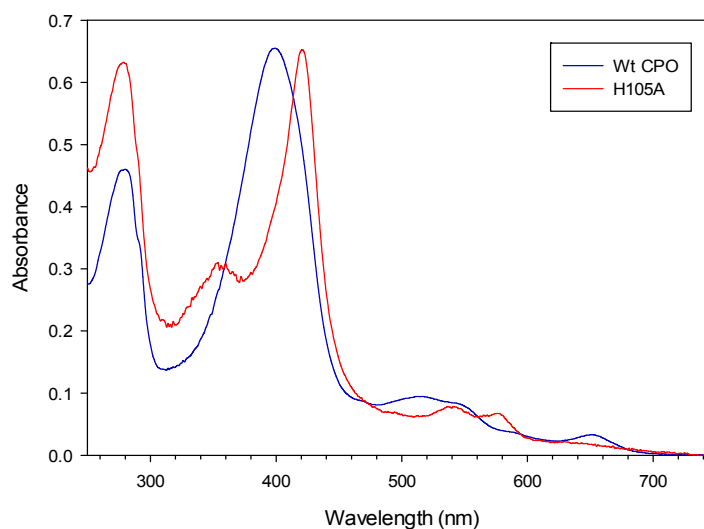
Fig 3.6 Absorption spectra of the purified Wt CPO and H105A mutant in 25 mM potassium phosphate buffer at pH 5.9.
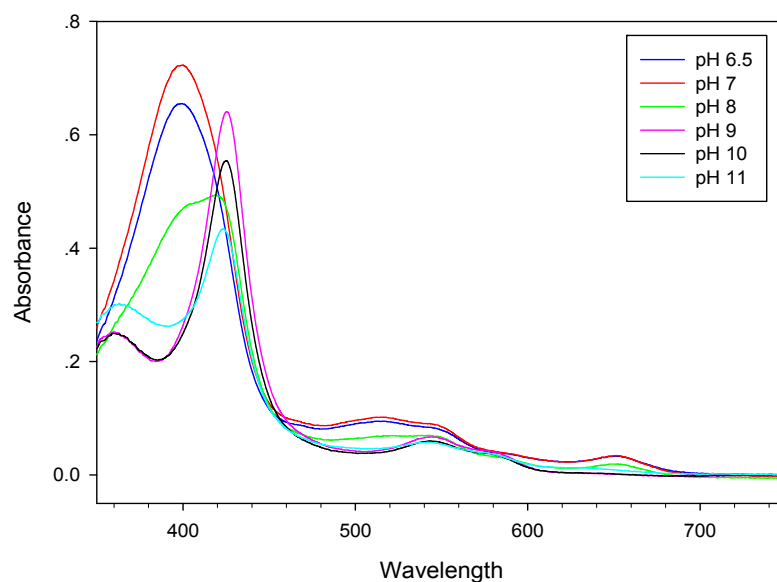
Fig 3.7 UV-Visible spectra of the ferric Wt CPO in 25 mM potassium phosphate buffer at different pH values of 6.5, 7, 8, 9, 10, and 11.
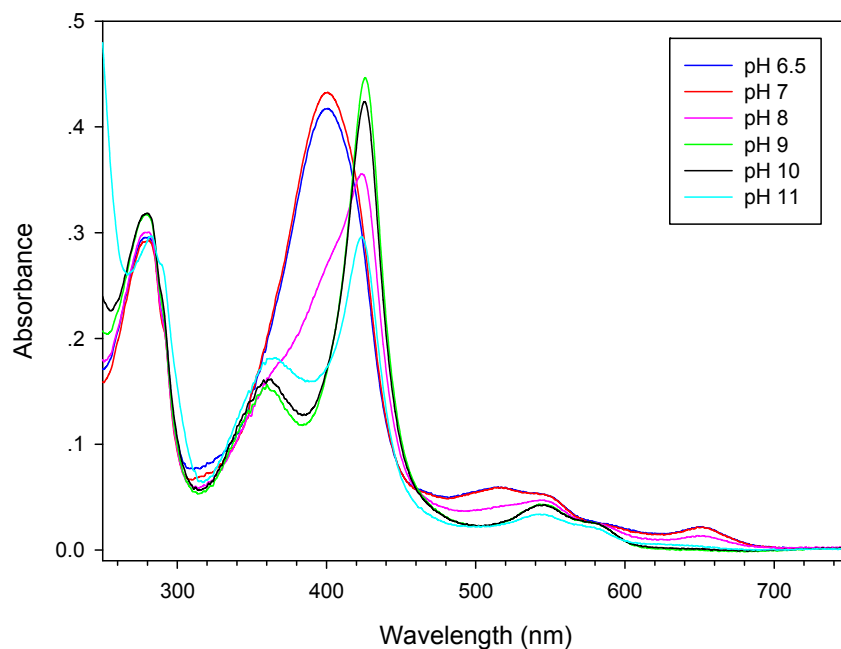
Fig 3.8 UV-Visible spectra of the ferric recombinant CPO in 25 mM potassium phosphate buffer at different pH values of 6.5, 7, 8, 9, 10, and 11.
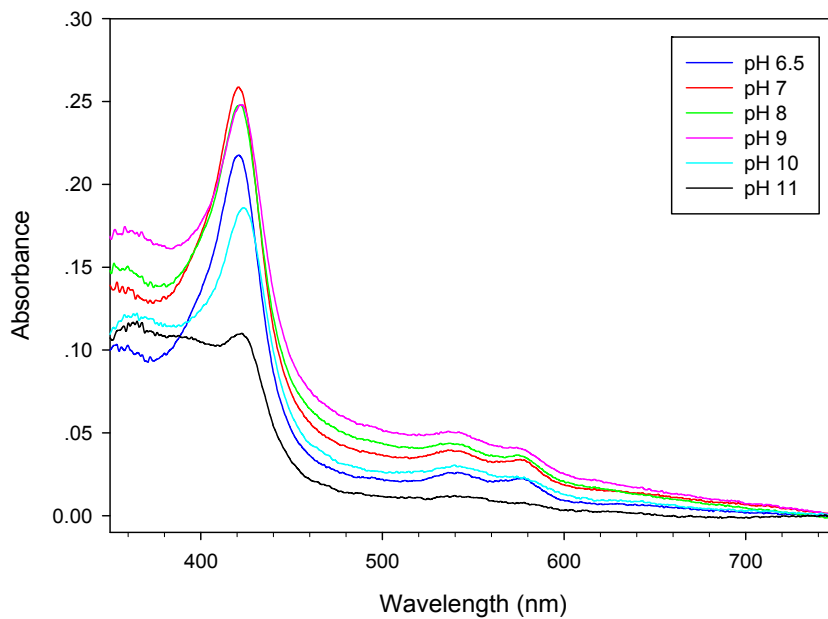
Fig 3.9 UV-Visible spectra of the ferric H105A in 25 mM potassium phosphate buffer at different pH values of 6.5, 7, 8, 9, 10, and 11.
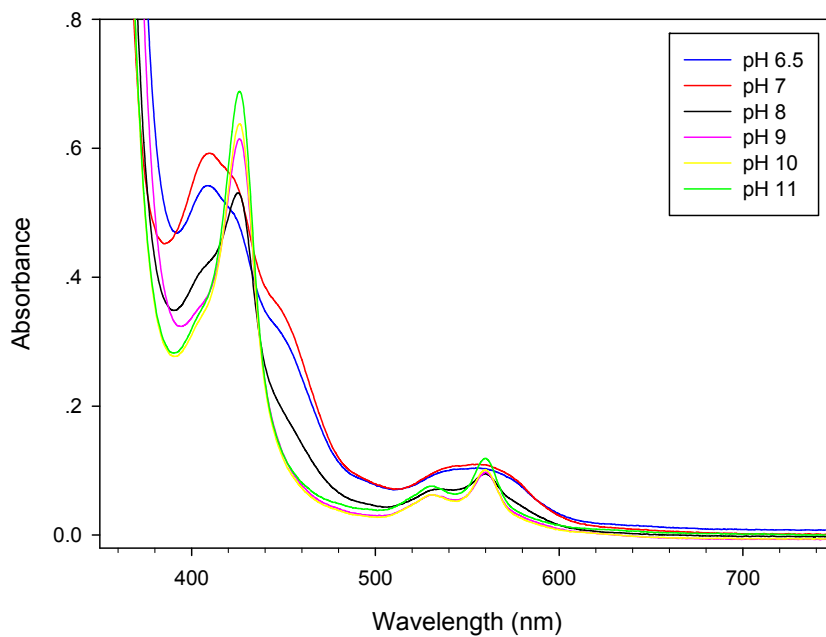
Fig 3.10 UV-Visible spectra of the ferrous Wt CPO in 25 mM potassium phosphate buffer at different pH values of 6.5, 7, 8, 9, 10, and 11.
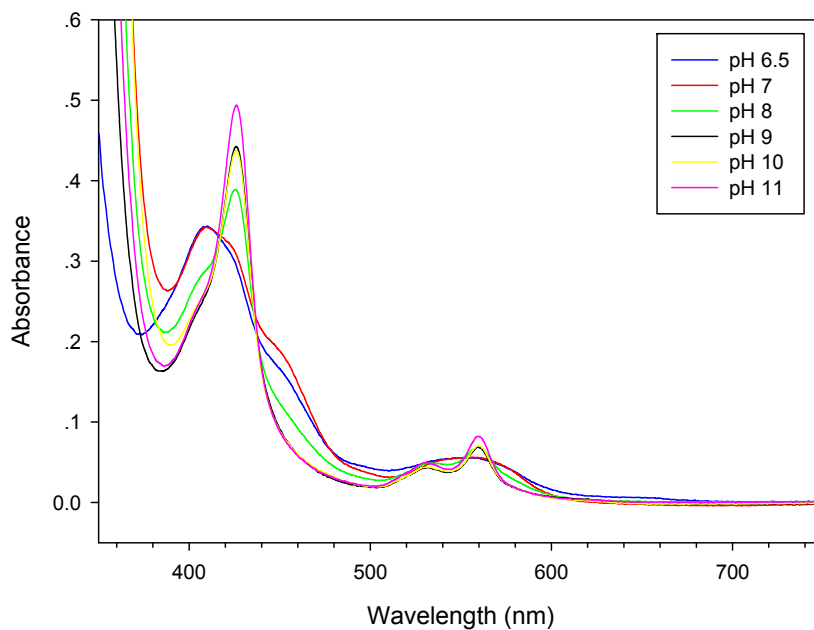
Fig 3.11 UV-Visible spectra of the ferrous recombinant CPO in 25 mM potassium phosphate buffer at different pH values of 6.5, 7, 8, 9, 10, and 11.
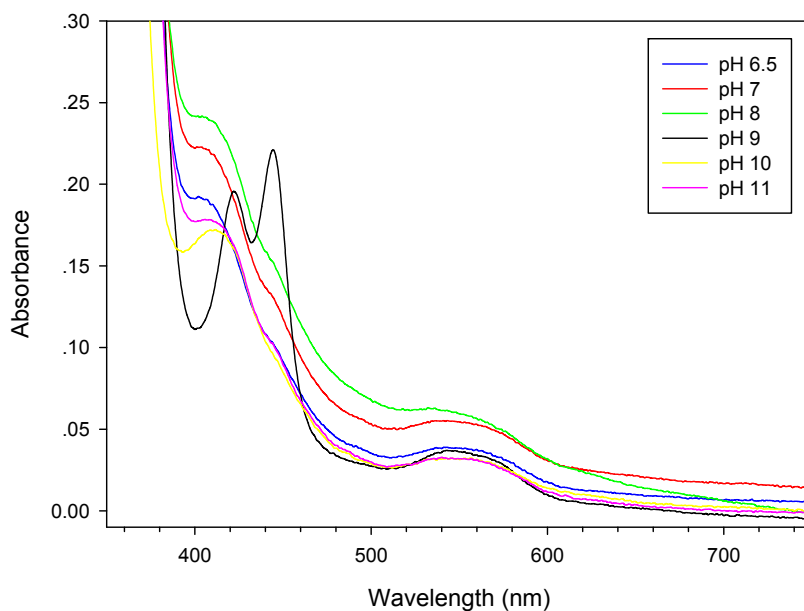
Fig 3.12 UV-Visible spectra of the ferrous H105A in 25 mM potassium phosphate buffer at different pH values of 6.5, 7, 8, 9, 10, and 11.
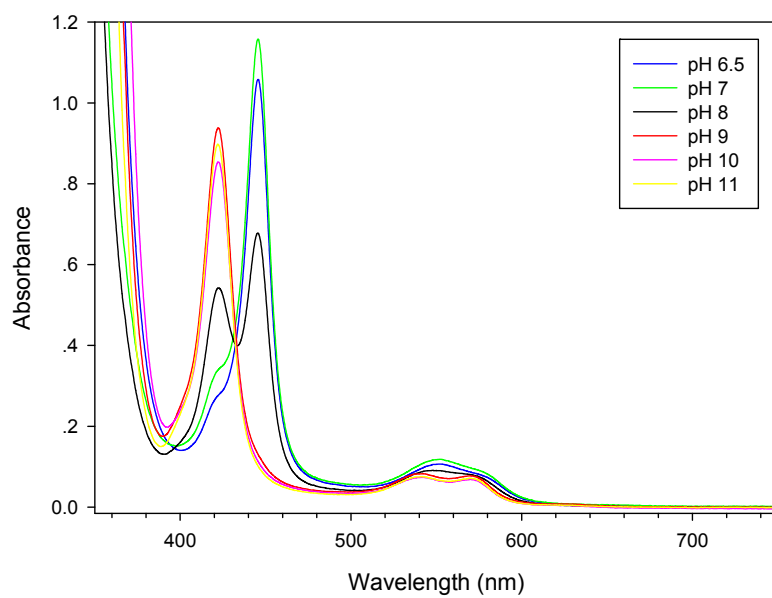
Fig 3.13 UV-Visible spectra of the ferrous Wt CPO and CO complex in 25 mM potassium phosphate buffer at different pH values of 6.5, 7, 8, 9, 10, and 11.
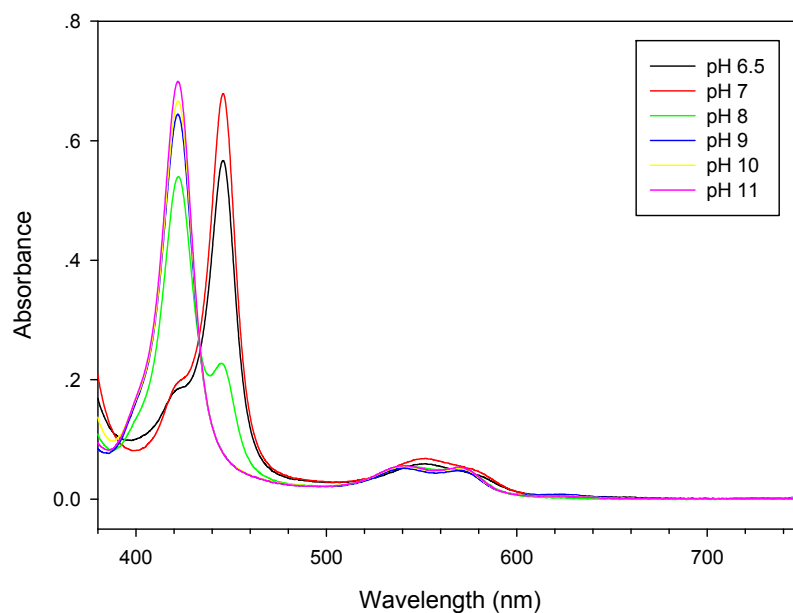
Fig 3.14 UV-Visible spectra of the ferrous recombinant CPO and CO complex in 25 mM potassium phosphate buffer at different pH values of 6.5, 7, 8, 9, 10, and 11.
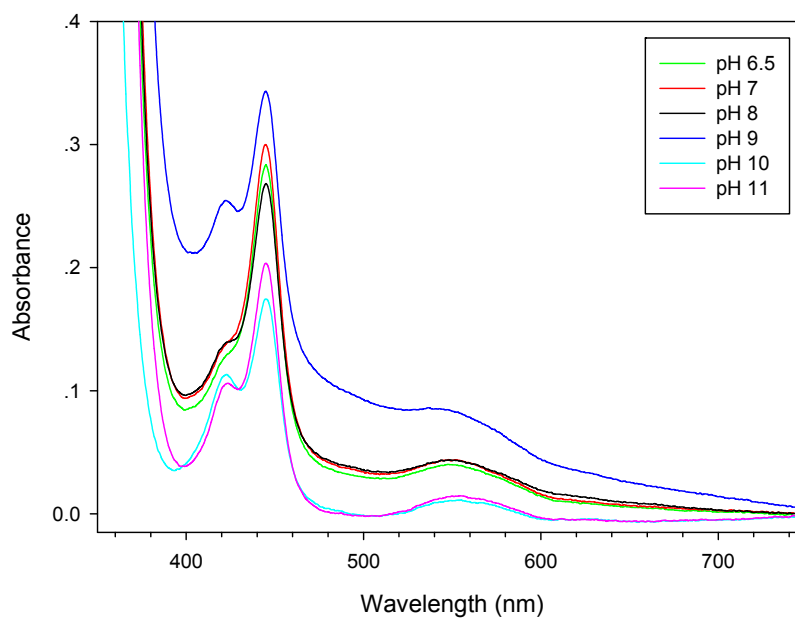
Fig 3.15 UV-Visible spectra of the ferrous H105A and CO complex in 25 mM potassium phosphate buffer at different pH values of 6.5, 7, 8, 9, 10, and 11.

3.3.3 Epoxidation of styrene catalyzed by Wt CPO and the H105A mutant

Products of the styrene epoxidation catalyzed by Wt CPO and the H105A mutant were separated and identified by HPLC (Fig 3.16 and 3.17). The resolution factor R_s, calculated for Wt CPO, was 1.07 and for the H105A mutant was 1.01. The retention factors k_1' and k_2' for Wt CPO were 1.90 and 2.90, and for the H105A mutant they were 1.97 and 2.95, respectively. The separation factor α for Wt CPO was 1.53 and for H105A mutant was 1.50. It was reported that the elution order of the similar enantiomers by the Whelk-O 1 column was (*R*)-enantiomers before (*S*)-enantiomers. The dominant product for Wt CPO was (*R*)-styrene oxide, which had a shorter retention time than (*S*)-styrene oxide and the enantiomeric excess (*ee*) value was 43.64%. However, the H105A mutant catalyzed reaction yielded only 0.06% of the *ee* value.

Fig 3.16 Enantioselective separation of styrene oxide formed in catalysis by Wt CPO on Whelk-O 1 column at the room temperature using n-hexane/ethanol (99.9/0.1, v/v) as the mobile phase. The monitoring wavelength was 215.7 nm.

Fig 3.17 Enantioselective separation of styrene oxide formed in catalysis by the H105A mutant on Whelk-O 1 column at the room temperature using *n*-hexane/ethanol (99.9/0.1, v/v) as the mobile phase. The monitoring wavelength was 215.7 nm.

3.3.4 Epoxidation of *cis*-β-methylstyrene catalyzed by Wt CPO and H105A

The epoxidation products of *cis*-β-methylstyrene catalyzed by Wt CPO and the H105A mutant were separated and studied by HPLC (Fig 3.18 and 3.19). Wt CPO-catalyzed epoxidation of *cis*-β-methylstyrene had only one product, which was the (1S, 2R)-enantiomer. However, the H105A-catalyzed reaction generated the byproduct. The resolution factor R_s calculated for the H105A mutant was 0.739. The retention factors k_1' and k_2' for the H105A mutant were 6.90 and 7.95, respectively. The separation factor α for the H105A mutant was 1.15. The enantiomeric excess (*ee*) value of the H105A mutant was 13.52%, which indicated that this mutation caused partial loss of enantioselectivity for *cis*-β-methylstyrene.

Fig 3.18 Enantioselective separation of *cis*-β-methylstyrene oxide formed in catalysis by Wt CPO on Whelk-O 1 column at 4 ºC using pure hexane as the mobile phase. The monitoring wavelength was 215.7 nm.

Fig 3.19 Enantioselective separation of *cis*-β-methylstyrene oxide formed in catalysis by the H105A mutant on Whelk-O 1 column at 4 ºC using pure hexane as the mobile phase. The monitoring wavelength was 215.7 nm.

3.3.5 Epoxidation of *trans*-β-methylstyrene catalyzed by Wt CPO and H105A

The epoxidation products of *trans*-β-methylstyrene catalyzed by Wt CPO and the H105A mutant were separated and identified by HPLC after comparing the retention times of the products with the pure standards (Fig 3.20 and 3.21). The elution order of epoxidation products for this reaction was that the (1*R*, 2*R*)-enantiomer preceded the (1*S*, 2*S*)-enantiomer. The resolution factor R_s calculated for Wt CPO was 3.19 and for the H105A mutant was 2.40. The retention factors k_1' and k_2' for Wt CPO were 2.02 and 4.31, and for the H105A mutant they were 2.02 and 4.36, respectively. The separation factor α for Wt CPO was 2.13 and for the H105A mutant was 2.16.

Fig 3.20 Enantioselective separation of *trans*-β-methylstyrene oxide formed in catalysis by Wt CPO on Whelk-O 1 column at the room temperature using *n*-hexane/ethanol (99.9/0.1, v/v) as the mobile phase. The monitoring wavelength was 215.7 nm.

The *ee* value for Wt CPO was 0.08%. However, the H105A mutant catalyzed reaction gave 48.04% *ee*. So the mutation of H105 amino acid allowed the better positioning of *trans*-β-methylstyrene at the heme center and increased the enantioselectivity for this substrate.

Fig 3.21 Enantioselective separation of *trans*-β-methylstyrene oxide formed in catalysis by the H105A mutant on Whelk-O 1 column at the room temperature using *n*-hexane/ethanol (99.9/0.1, v/v) as the mobile phase. The monitoring wavelength was 215.7 nm.

3.3.6 Epoxidation of *trans*-β-ethylstyrene catalyzed by Wt CPO and H105A

The enantioseparation of *trans*-β-ethylstyrene oxide catalyzed by Wt CPO and the H105A mutant were studied (Fig 3.22 and 3.23). The elution order of the epoxidation products for this reaction was that the (*R*)-enantiomer preceded the (*S*)-enantiomer. The resolution factor R_s, calculated for Wt CPO, was 2.88 and for the H105A mutant was 2.57. The retention factors k_1' and k_2' for Wt CPO were 2.31 and 5.01, and for the
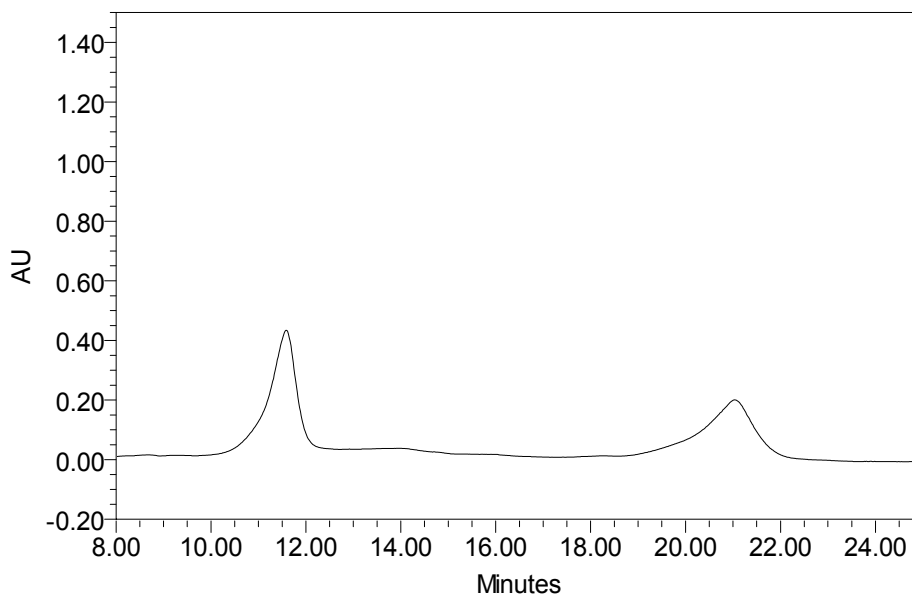
Fig 3.22 Enantioselective separation of *trans*-β-ethylstyrene oxide formed in catalysis by Wt CPO on Whelk-O 1 column at 4 ºC using *n*-hexane/ethanol (99.9/0.1, v/v) as the mobile phase. The monitoring wavelength was 218.0 nm.
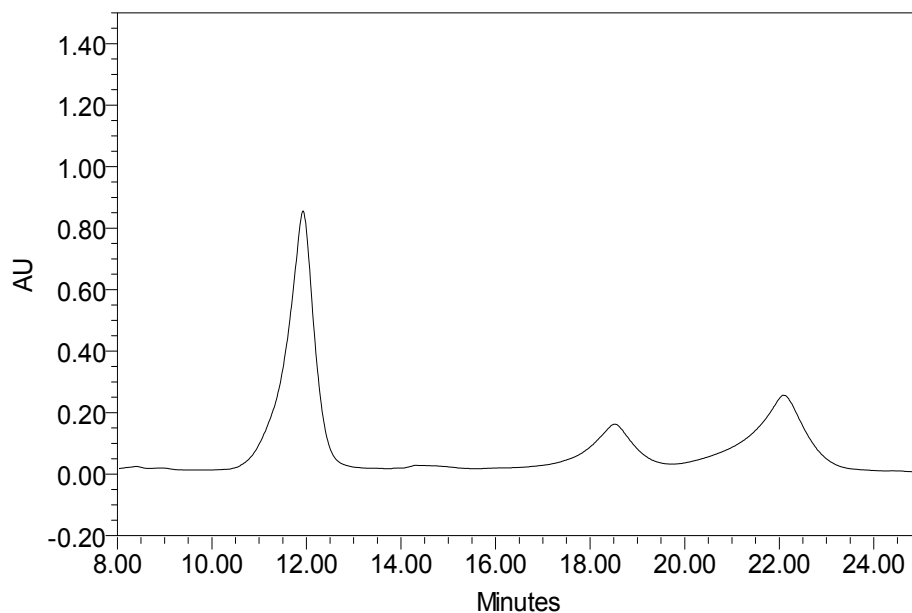
Fig 3.23 Enantioselective separation of *trans*-β-ethylstyrene oxide formed in catalysis by H105A on Whelk-O 1 column at 4 ºC using *n*-hexane/ethanol (99.9/0.1, v/v) as the mobile phase. The monitoring wavelength was 218.0 nm.

H105A mutant they were 2.41 and 5.31, respectively. The separation factor α for Wt CPO was 2.17 and for the H105A mutant was 2.20. The *ee* value for Wt CPO was 13.02%. However, the H105A mutant catalyzed reaction gave 33.56% *ee*. Therefore, similar to the result of *trans*-β-ethylstyrene epoxidation, the H105A mutant allowed the *trans*-β-ethylstyrene to orient at the heme center and increased the enantioselectivity for this substrate compared to wild-type chloroperoxidase.

3.3.7 Epoxidation of *trans*-β-propylstyrene catalyzed by Wt CPO and H105A

The enantioseparation of *trans*-β-propylstyrene oxide by Wt CPO and the H105A mutant were studied (Fig 3.24 and 3.25). The elution order of epoxidation products for this reaction was that the (*R*)-enantiomer preceded the (*S*)-enantiomer. The resolution factor R_s calculated for Wt CPO was 3.76 and for the H105A mutant was 3.34. The retention factors k_1' and k_2' for Wt CPO were 4.60 and 8.20, and for the H105A mutant they were 4.52 and 8.23, respectively. The separation factor α for Wt CPO was 1.79 and for the H105A mutant was 1.82. The *ee* value for Wt CPO was 5.66%. However, the H105A mutant catalyzed reaction gave 44.14% of the *ee* value. The result of the enantioselective epoxidation was amazing because it indicated that the H105A mutant allowed *trans*-β-propylstyrene, which was a bulky substrate, to position at the heme center to facilitate the epoxidation reactions and showed increased enantioselectivity compared to wild-type chloroperoxidase. Among several CPO mutants, the H105A mutant was the only one to catalyze the bulky styrene derivatives with good yield and great enantioselectivity. Therefore, the H105A mutant has a significant potential for industrial applications.
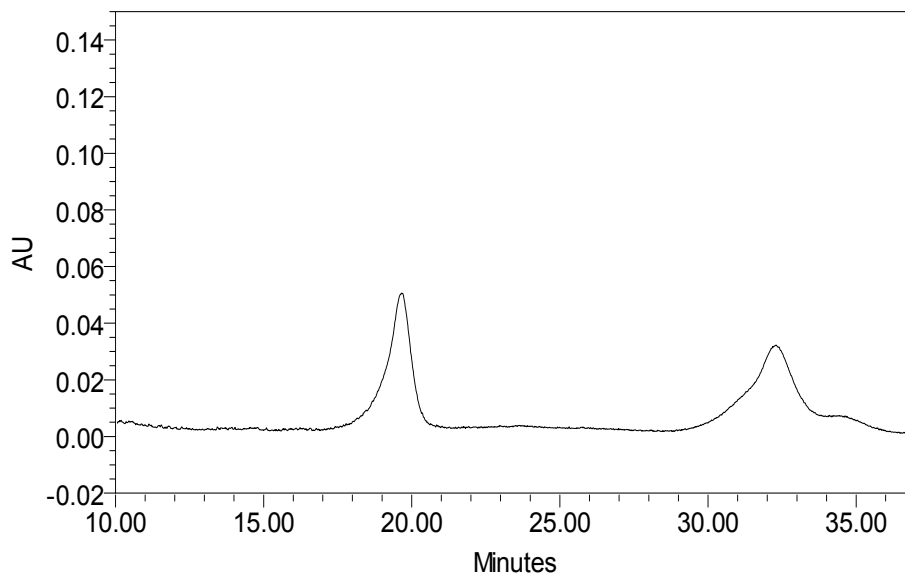
Fig 3.24 Enantioselective separation of *trans*-β-propylstyrene oxide formed in catalysis by Wt CPO on Whelk-O 1 column at the room temperature using pure hexane as the mobile phase. The monitoring wavelength was 218.0nm.
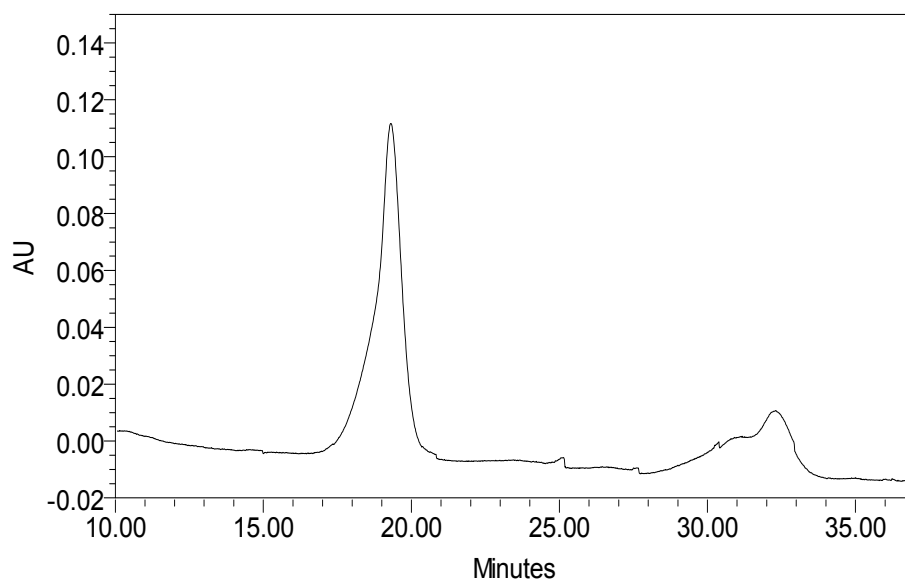
Fig 3.25 Enantioselective separation of *trans*-β-propylstyrene oxide formed in catalysis by H105A on Whelk-O 1 column at the room temperature using pure hexane as the mobile phase. The monitoring wavelength was 218.0nm.

3.3.8 Epoxidation of styrene catalyzed by Wt CPO and the N74Q mutant

The epoxidation products of styrene catalyzed by Wt CPO and the N74Q mutant were separated and identified using HPLC after comparing the retention times of the products with the pure standards (Fig 3.26 and 3.27). The resolution factor R_s calculated for Wt CPO was 1.64 and for the N74Q mutant was 1.67. The retention factors k_1' and k_2' for Wt CPO were 3.29 and 4.43, and for the N74Q mutant they were 3.29 and 4.40, respectively. The separation factor α for Wt CPO was 1.35 and for the N74Q mutant was 1.33. The *ee* value for Wt CPO was 49.74%. The N74Q mutant catalyzed reaction gave 1.94% of the *ee* value, which was quite different from the wild-type chloroperoxidase. Therefore, the mutation of the N74 amino acid changed the enantioselectivity for styrene substrates.

3.3.9 Epoxidation of *cis*-β-methylstyrene by Wt CPO and the N74Q mutant

The epoxidation products of *cis*-β-methylstyrene catalyzed by Wt CPO and the N74Q mutant were separated and studied by HPLC (Fig 3.28 and 3.29). Wild- type chloroperoxidase-catalyzed epoxidation of *cis*-β-methylstyrene had only one product, which was (1S, 2R)-enantiomer. However, the N74Q mutant catalyzed reaction gave the unspecified byproduct. The resolution factor R_s calculated for the N74Q mutant was 0.614. The retention factors k_1' and k_2' for the N74Q mutant were 6.12 and 7.12, respectively. The separation factor α for the N74Q mutant was 1.16. The *ee* value of the N74Q mutant was 14.12%, which indicated that this mutation caused partial loss of the enantioselectivity for *cis*-β-methylstyrene.
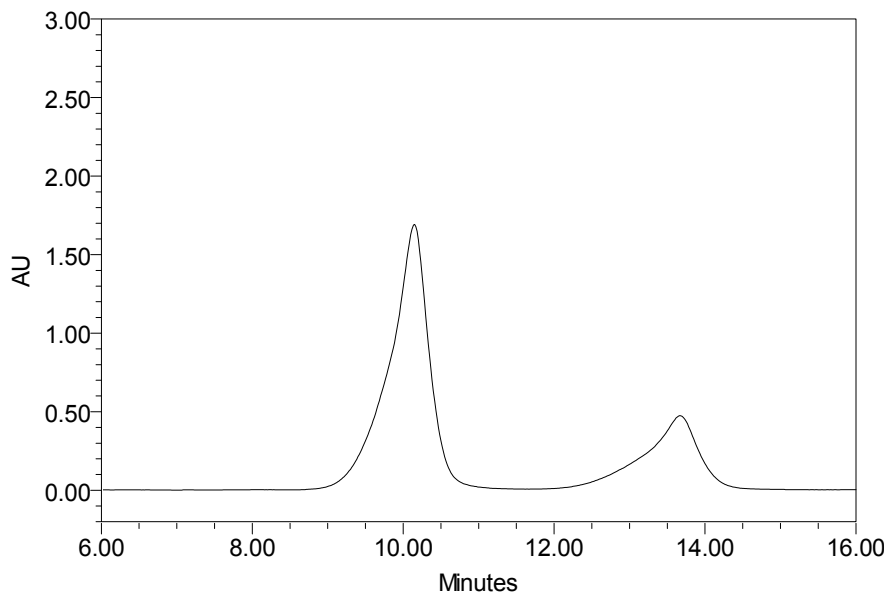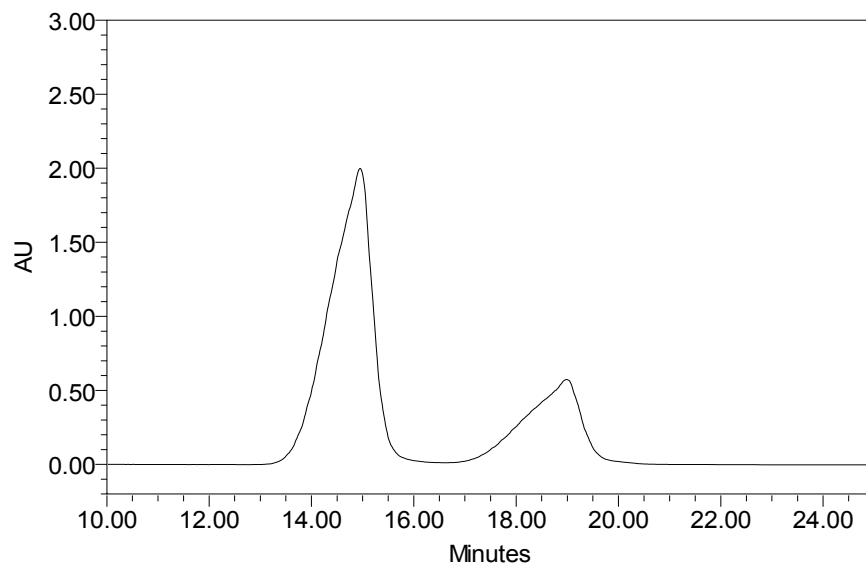
Fig 3.26 Enantioselective separation of styrene oxide formed in catalysis by Wt CPO on Whelk-O 1 column at the room temperature using n-hexane/ethanol (99.8/0.2, v/v) as the mobile phase. The monitoring wavelength was 215.7 nm.
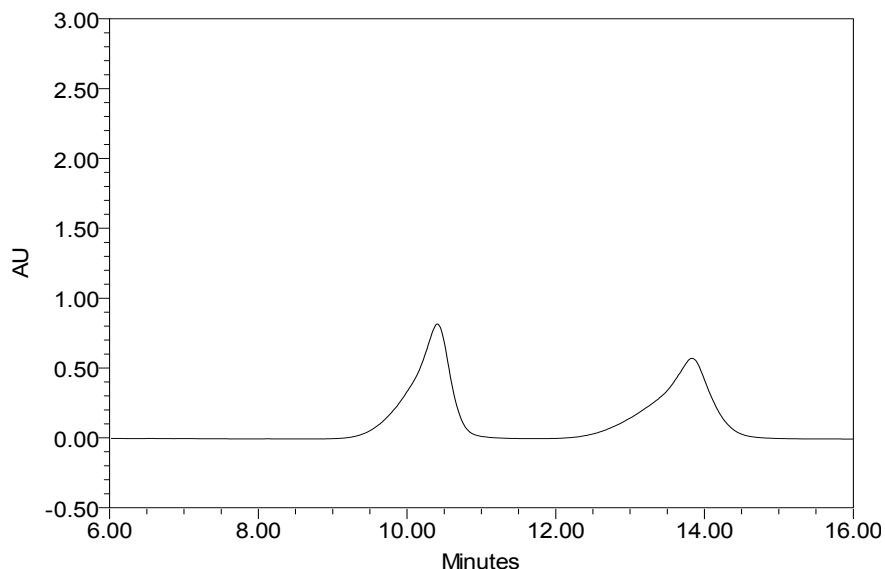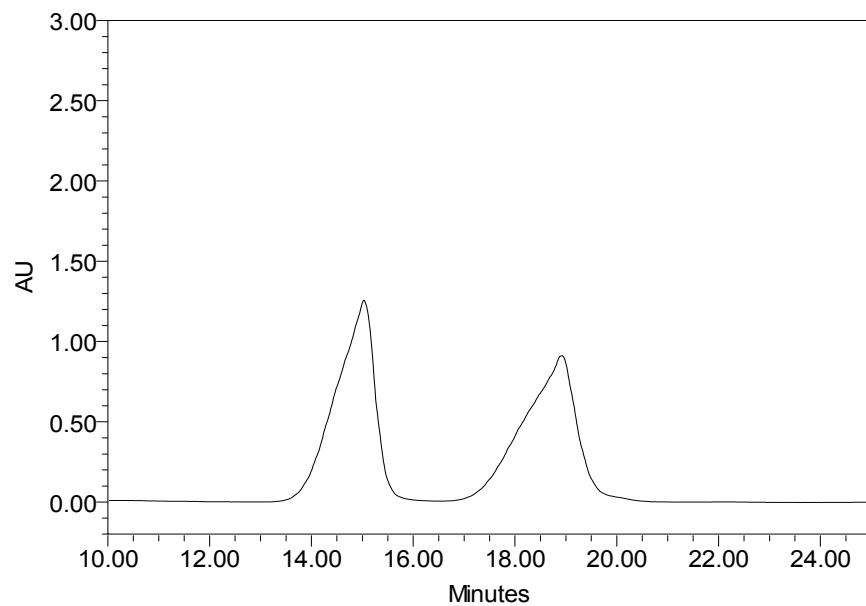

Fig 3.27 Enantioselective separation of styrene oxide formed in catalysis by the N74Q mutant on Whelk-O 1 column at the room temperature using *n*-hexane/ethanol (99.8/0.2, v/v) as the mobile phase. The monitoring wavelength was 215.7 nm.
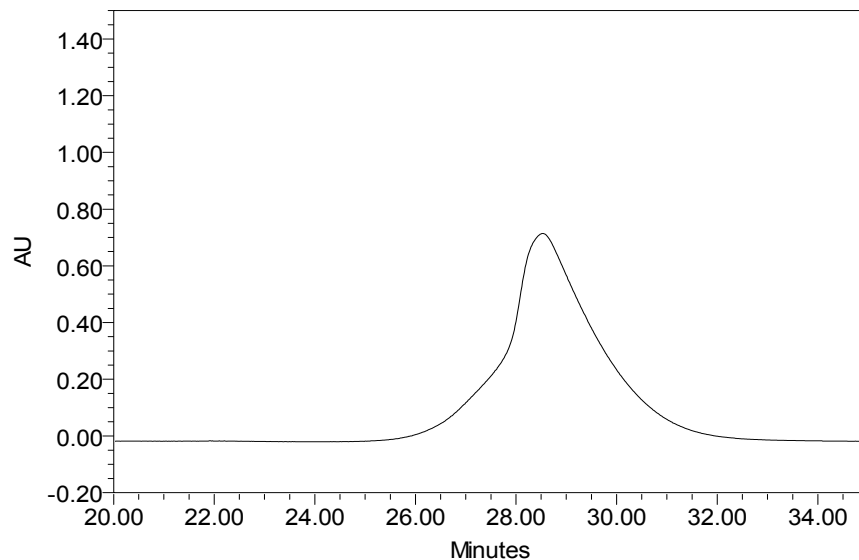
Fig 3.28 Enantioselective separation of *cis*-β-methylstyrene oxide formed in catalysis by Wt CPO on Whelk-O 1 column at 4 ºC using pure hexane as the mobile phase. The monitoring wavelength was 215.7 nm.
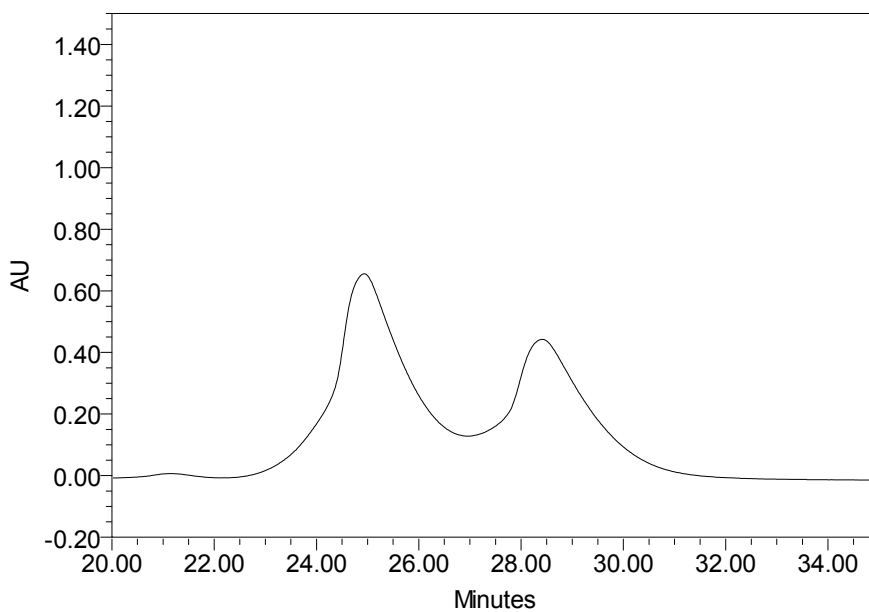
Fig 3.29 Enantioselective separation of *cis*-β-methylstyrene oxide formed in catalysis by the N74Q mutant on Whelk-O 1 column at 4 ℃ using pure hexane as the mobile phase. The monitoring wavelength was 215.7 nm.

84

3.3.10 Epoxidation of *trans*-β-methylstyrene by Wt CPO and the N74Q mutant

The epoxidation products of *trans*-β-methylstyrene by Wt CPO and the N74Q mutant were separated and identified using HPLC by comparing the retention times of the products with the pure standards (Fig 3.30 and 3.31). The elution order of epoxidation products for this reaction was that the (1*R*, 2*R*)-enantiomer preceded the (1*S*, 2*S*)-enantiomer. The resolution factor R_s calculated for Wt CPO was 3.76 and for the N74Q mutant was 3.95. The retention factors k_1' and k_2' for the products of Wt CPO-catalyzed epoxidation were 3.32 and 5.86, and for the N74Q mutant they were 3.34 and 5.87, respectively. The separation factor α for Wt CPO was 1.76 and for the N74Q mutant was 1.75. The *ee* value for Wt CPO was 2.1%. However, the N74Q mutant catalyzed reaction gave 58.1% *ee*.
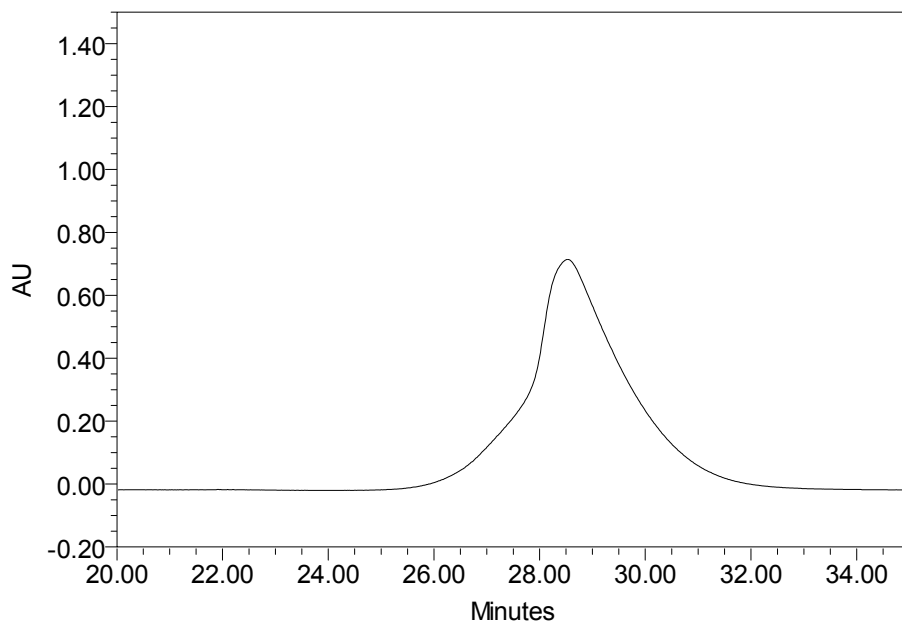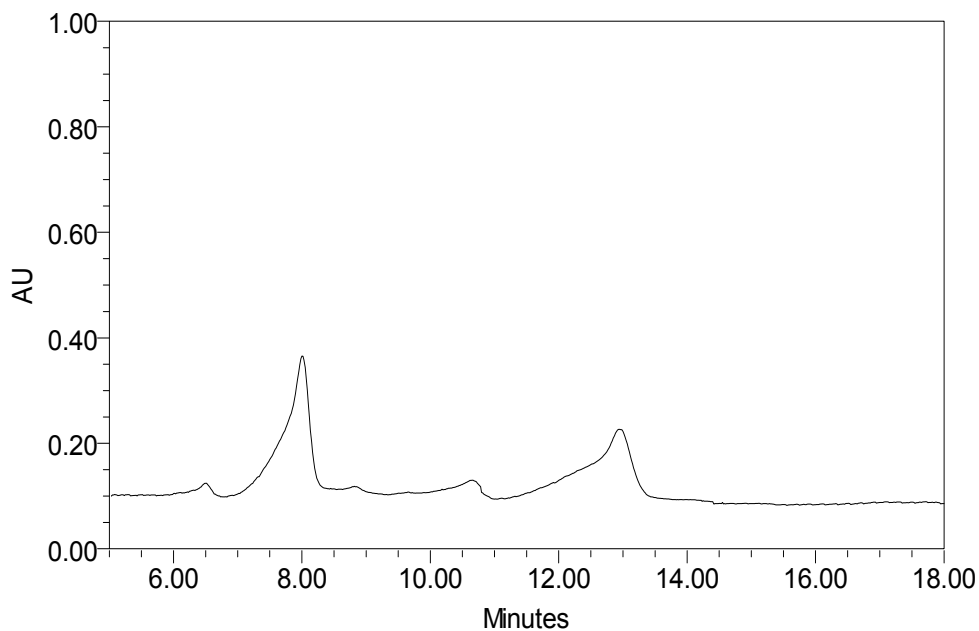

Fig 3.30 Enantioselective separation of *trans*-β-methylstyrene oxide formed in catalysis by Wt CPO on Whelk-O 1 column at the room temperature using *n*-hexane/ethanol (99.8/0.2, v/v) as the mobile phase. The monitoring wavelength was 215.7 nm.
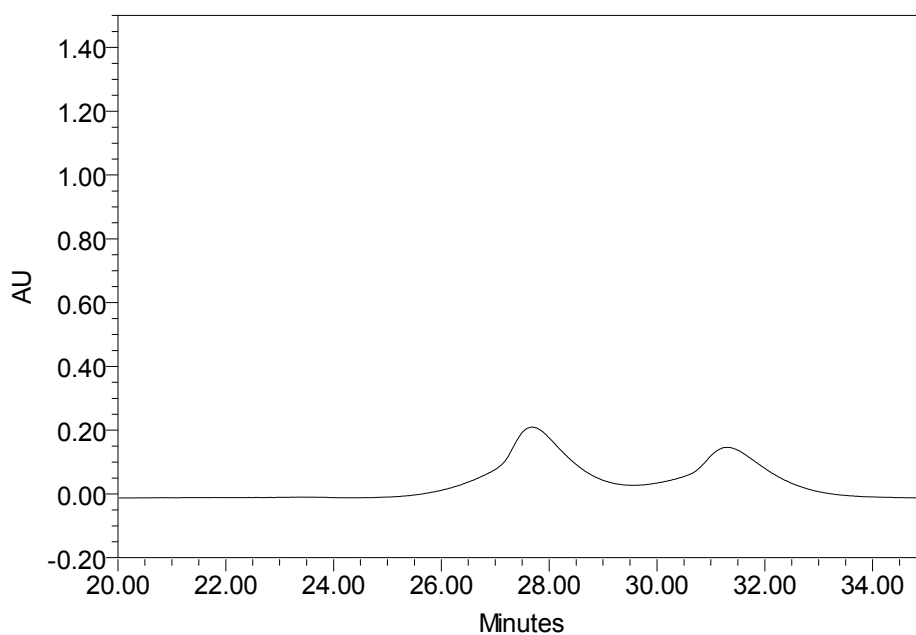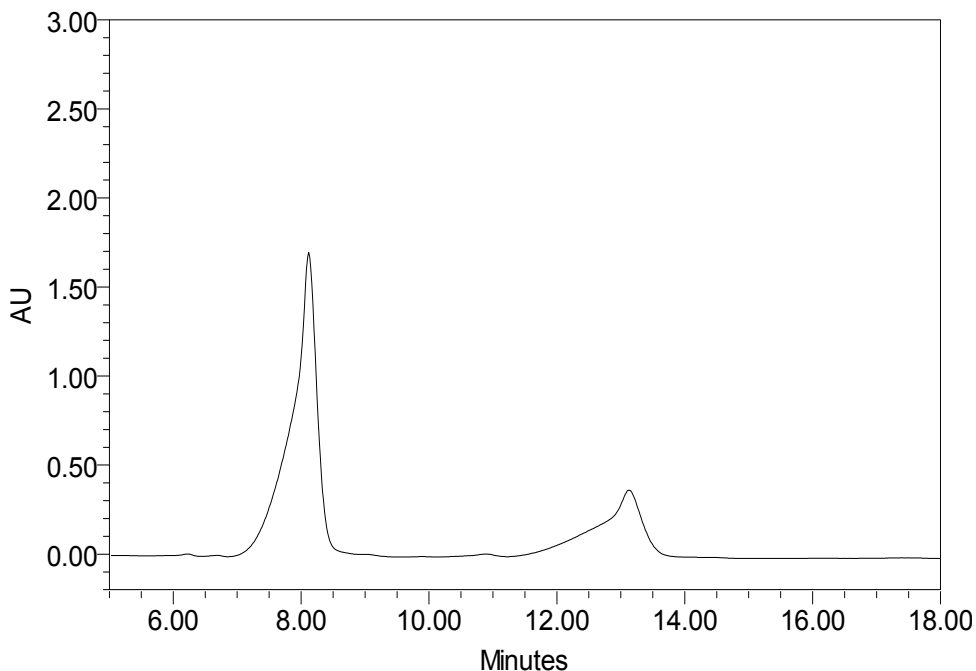
Fig 3.31 Enantioselective separation of *trans*-β-methylstyrene oxide formed in catalysis by the N74Q mutant on Whelk-O 1 column at the room temperature using *n*-hexane/ethanol (99.8/0.2, v/v) as the mobile phase. The monitoring wavelength was 215.7 nm.

3.3.11 Epoxidation of *trans*-β-ethylstyrene by Wt CPO and the N74Q mutant

The enantioseparation of *trans*-β-ethylstyrene oxide by Wt CPO and the N74Q mutant were studied (Fig 3.32 and 3.33). The elution order of epoxidation products for this reaction was that the (*R*)-enantiomer preceded the (*S*)-enantiomer. The resolution factor R_s calculated for Wt CPO was 3.62 and for the N74Q mutant was 3.93. The retention factors k_1' and k_2' for Wt CPO were 4.08 and 8.80, and for the N74Q mutant they were 4.29 and 9.42, respectively. The separation factor α for Wt CPO was 2.16 and for the N74Q mutant was 2.19. The *ee* value for Wt CPO was 14.34%.

86
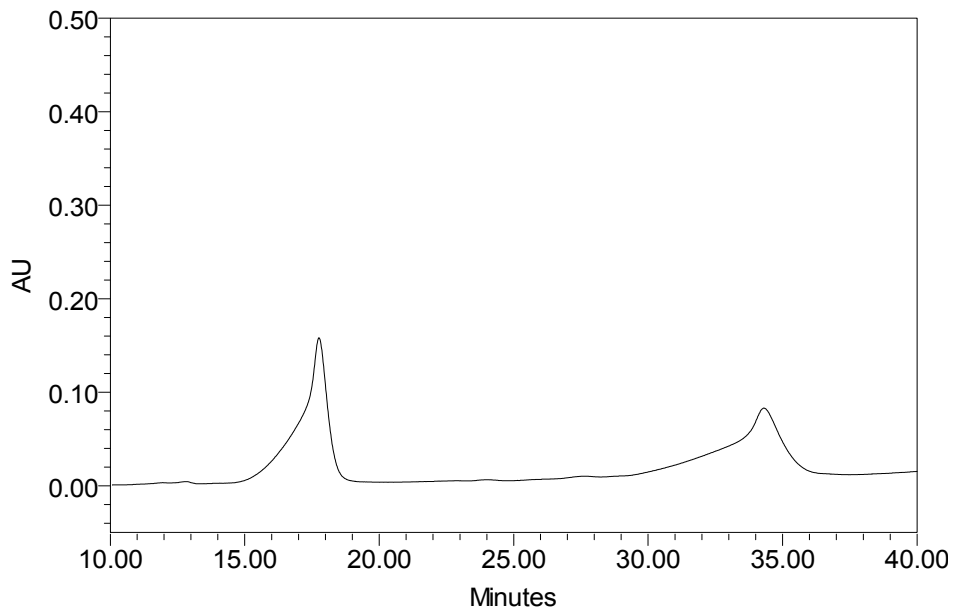
Fig 3.32 Enantioselective separation of *trans*-β-ethylstyrene oxide formed in catalysis by Wt CPO on Whelk-O 1 column at 4 ℃ using *n*-hexane/ethanol (99.95/0.05, v/v) as the mobile phase. The monitoring wavelength was 218.0 nm.
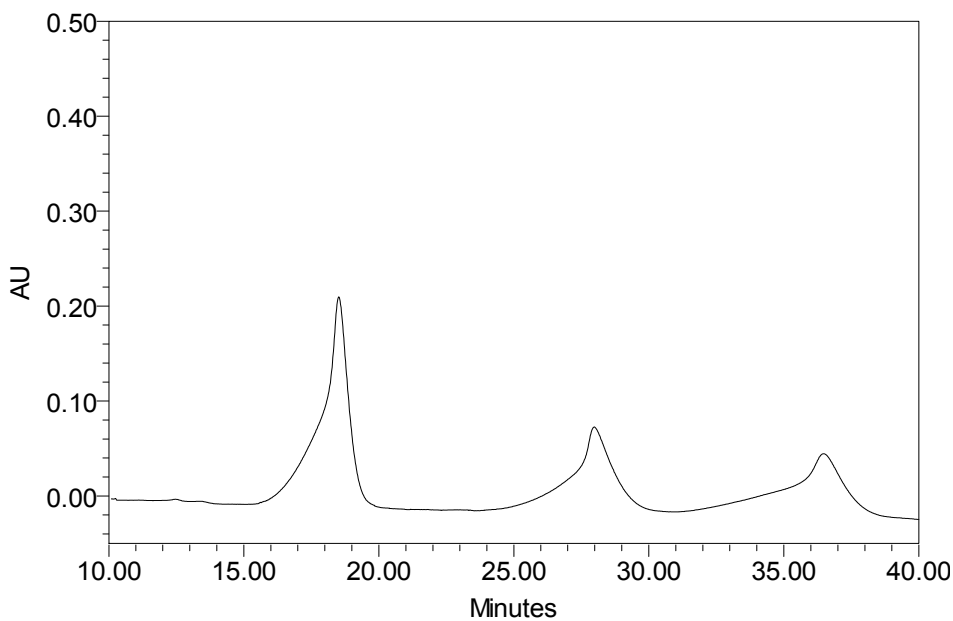
Fig 3.33 Enantioselective separation of *trans*-β-ethylstyrene oxide formed in catalysis by N74Q on Whelk-O 1 column at 4 ℃ using *n*-hexane/ethanol (99.95/0.05, v/v) as the mobile phase. The monitoring wavelength was 218.0 nm.
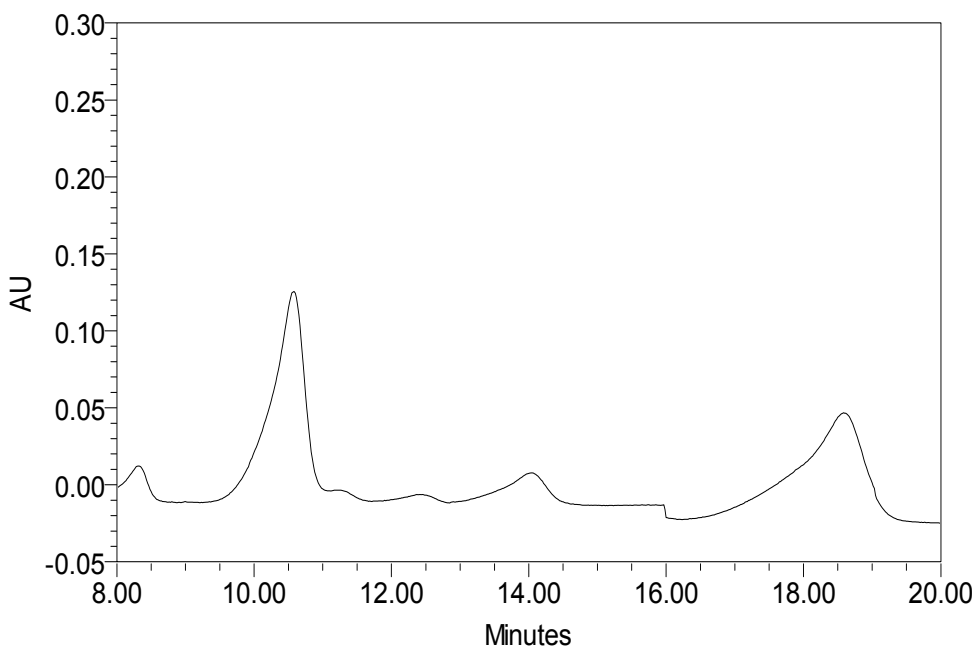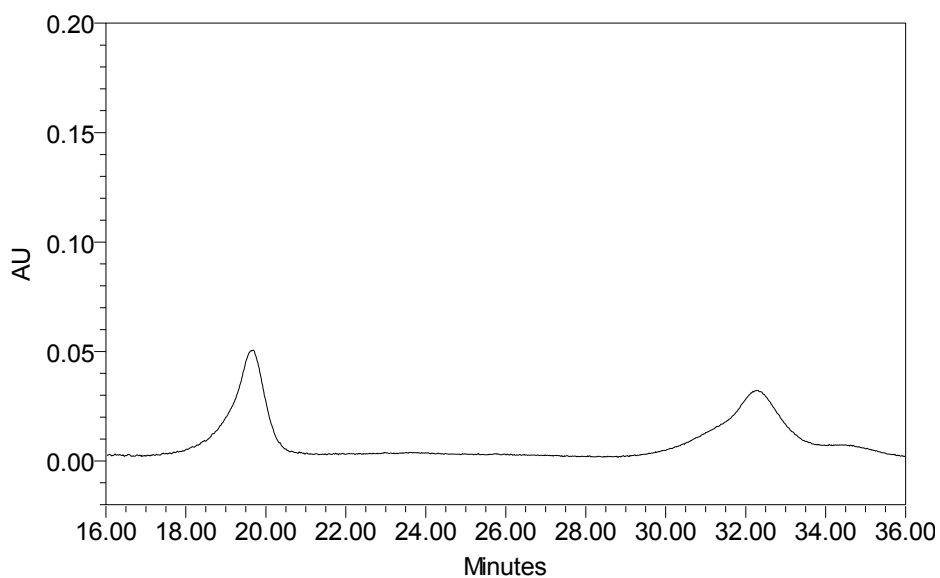
Fig 3.34 Enantioselective separation of *trans*-β-propylstyrene oxide formed in catalysis by Wt CPO on Whelk-O 1 column at the room temperature using pure hexane as the mobile phase. The monitoring wavelength was 218.0nm.
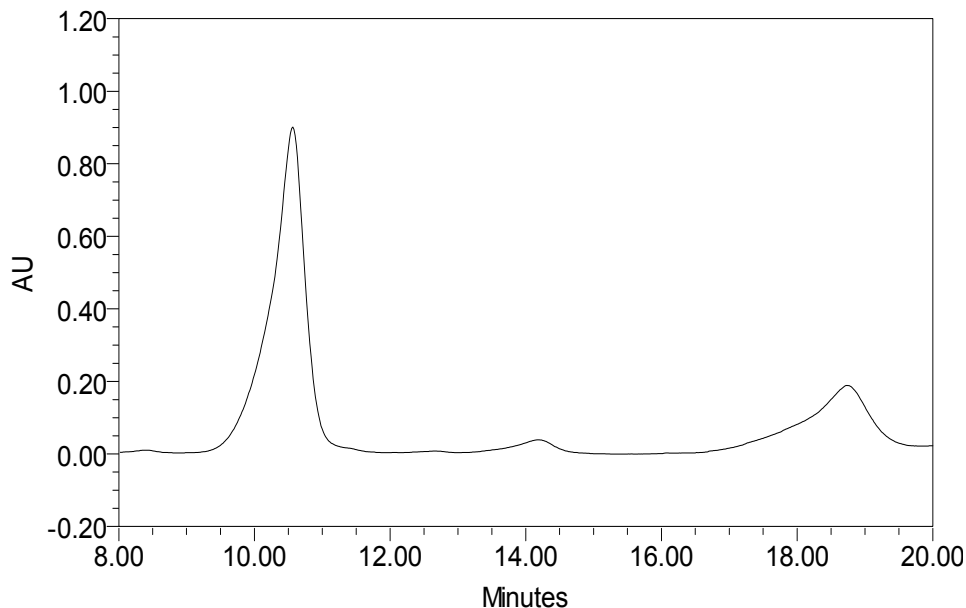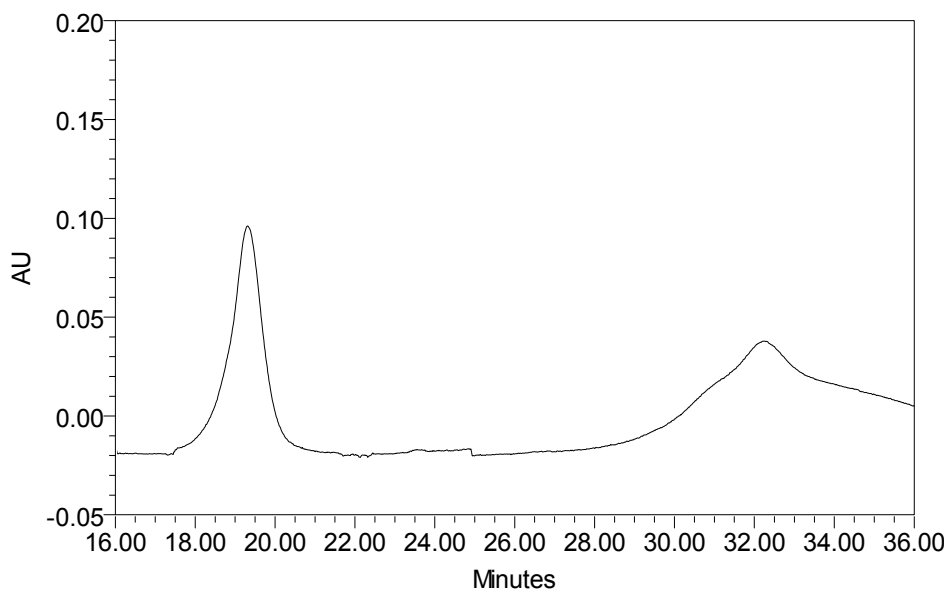

Fig 3.35 Enantioselective separation of *trans*-β-propylstyrene oxide formed in catalysis by N74Q on Whelk-O 1 column at the room temperature using pure hexane as the mobile phase. The monitoring wavelength was 218nm.

However, the N74Q mutant catalyzed reaction gave 41.52% as the *ee* value. Therefore, similar to the result of *trans*-β-ethylstyrene epoxidation, the N74Q mutant allowed *trans*-β-ethylstyrene to position at the heme center and enhanced the enantioselectivity for this substrate compared to that of the wild-type chloroperoxidase.

3.3.12 Epoxidation of *trans*-β-propylstyrene catalyzed by Wt CPO and N74Q

The enantioseparation of *trans*-β-propylstyrene oxide by Wt CPO and the N74Q mutant were carried out to study the expoxidation of long-side-chain styrene derivatives by the N74Q mutant (Fig 3.34 and 3.35). The elution order of epoxidation products for this reaction was that the (*R*)-enantiomer preceded the (*S*)-enantiomer. The resolution factor R_s calculated for Wt CPO was 3.76 and for the N74Q mutant was 2.75. The retention factors $k_1'$ and k_2' for Wt CPO were 4.60 and 8.20, and for the N74Q mutant they were 4.52 and 8.20, respectively. The separation factor α for Wt CPO was 1.79 and for the N74Q mutant was 1.82. The *ee* value for Wt CPO was 5.66%. However, the N74Q mutant catalyzed reaction gave 12.12% *ee*. The epoxidation result indicated that the N74Q mutant had similar enantioselectivity for bulky substrates compared to wild-type chloroperoxidase.

3.4 Discussion

In the hemoprotein family, CPO and cytochrome P450 share many similar properties, such as using cysteine as the proximal ligand (Ortiz de Montellano, 1995; Sundaramoorthy et al., 1995). It has been reported that titration of CPO to pH values greater than 7.0 can induce a rapid transition to form a stable but inactive protein (Hollenberg & Hager, 1973). The alkaline form of ferric CPO can result in a red shift in the Soret absorbance from 400 to 420 nm, and is usually named C420. Even the Soret

absorption band of the ferrous CPO-CO complex can be shifted from 446 to 420 nm, which is similar with inactivated cytochrome P420 (Hollenberg & Hager, 1973; Imai & Soto, 1967; Yu & Gunsalus, 1974). Some results indicate that the coordination sphere of C420 may be analogous to P420 (Martinis et al., 1996).

Ferric CPO is very stable at a lower pH, but when the solution becomes basic, it can readily convert to a stable but inactive alkaline form. It has been reported that the pK_a for the alkaline transition is 7.5, which is also confirmed by my reasearch. The convertion of the ferric CPO in the alkaline condition may be caused by the interaction of an ionizable residue with the heme iron. The transition from CPO to C420 may suggest the partial breakage of proximal thiolate ligation and a mixture of coordination structures. In the CPO structure, His 105 is hydrogen-bonded to Glu 183 in the heme distal pocket and may be responsible for this transition.

In my study, site-directed mutagenesis of His 105 residue was carried out and characteristics of the H105A mutant were explored. When the distal histidine was replaced, the spectrum of H105A in the C420 form was quite different compared to those of Wt CPO and recombinant chloroperoxidase. The ferrous Wt CPO and rCPO were high-spin, thiolate-ligated heme proteins. When they were converted to C420, low-spin state forms were generated and this process was indicative of the binding of the additional ligand to the heme iron to form a six coordinated compound. However, the result showed that the ferrous C420 form of Wt CPO or rCPO partially lost the thiolate ligand in the proximal site because the ferrous low-spin, thiolate-ligated heme complexes would generate the Soret peak at approximately 445 nm (Dawson et al., 1983) compared to the 425-nm Soret band exhibited by ferrous C420. The difference in the spectra

indicated that there was partial imidazole ligation in the ferrous C420. The spectra of the ferrous H105A mutant, which exhibited the decreasing Soret peaks at 445 nm instead of 425 nm, confirmed this conclusion because there was no histidine in the distal site to carry out the partial ligand switch. Histidine 105 can form hydrogen bonds with nearby amino acids, therefore this residue is very important to protein stability.

Ferrous C420 can readily bind small exogenous ligands, such as carbon monoxide (Hollenberg 1973). The Soret abosrbance of CPO-CO complex at 445 nm is typical for ferrous, low-spin, thiolate-ligated heme complexes. The alkaline specta of the ferrous CPO-CO complex were blue shifted to 420 nm, which indicated that ferrous-CO C420 was not thiolate-ligated. There was no shift in the H105A mutant complex, which further confirmed the histidine and cysteine switching hypothesis. Actually a mixed population of thiolate-bound and imidazole-bound coordination structures may explain these results, as found in P420 (Wells et al., 1992; Martinis et al., 1996). The transition to C420 can cause distal and proximal switch at the heme center. The presence of a histidine in the sixth axial site may cause a spin state transition and prevent the binding of other substrates.

To explore the enantioselectivity of the H105A mutant, styrene, *cis*-β-methylstyrene, *trans*-β-methylstyrene, *trans*-β-ethylstyrene and *trans*-β-propylstyrene were selected to react with Wt CPO and its mutants. The Wt CPO was very effective in catalyzing the epoxidation of styrene and *cis*-β-methylstyrene with high yield and *ee* values. However, the epoxidation of *trans*-β-methylstyrene, *trans*-β-ethylstyrene and *trans*-β-propylstyrene exhibited low yield and *ee* values, especially when the substrates had long side chains. These results can be explained by the restricted channel and structure of the CPO heme

pocket. Therefore, the good yield and *ee* values for epoxidation of styrene and *cis*-β-methylstyrene were a result of their proper fit in the heme pocket. Bulky substrates with long side chains were not easy to enter and properly orient at the active center. The H105A and N74Q mutants were not good at catalyzing styrene and *cis*-β-methylstyrene, However, their catalyzed epoxidation of *trans*-β-methylstyrene and *trans*-β-ethylstyrene showed a dramatic increase in both yield and enantioselectivity. Amazingly, the H105A mutant can catalyze the bulky substrate *trans*-β-propylstyrene with more than 50% *ee*.

As mentioned in the introduction part, His105 is located in the distal pocket and can form a hydrogen bond with Glu183. When this amino acid was replaced by a small and nonpolar alanine, it would open more space above the heme center and allow more bulky substrates to access the heme pocket and therefore get catalyzed by the enzyme. These results gave H105A mutant a great potential for the industrial applications of CPO to catalyze some specific bulky styrene derivatives.

CHAPTER IV

EXPRESSION, PURIFICATION AND NMR STUDIES OF DEUTERATED CPO

4.1 Introduction

4.1.1 Background

Many chemical and spectroscopic techniques are now available for structural characterization of hemoproteins (Finzel 1984; Frew 1984; Banci 1992; Boddupalli 1992; Hasemann 1995; Kuhnel 2006). Among them, NMR spectroscopy is a most powerful method for high-resolution structural characterization of metalloenzymes (Wang 2003). However, making complete heme proton assignments for CPO has been difficult and the proper assignment is important because the heme is the catalytic unit, which determines the diversity of enzyme's functions. Only about half of the heme protons have been correctly assigned, and this fact has compromised all NMR attempts to unambiguously study the active site solution chemistry of this enzyme (Wang, Tachikawa et al. 2003). For example, incorrect heme proton assignments can lead to incorrect assignments of heme pocket amino acid protons and questionable conclusions about active site chemistry. So the first step in the present effort is to achieve unambiguous and complete heme proton assignments, which will subsequently lead to hyperfine resonance assignments of amino acids at the heme active center. The complete assignment of heme protons will provide the necessary foundation for expanding solution studies of active site dynamics.

4.1.2 Aim of the study

There are several objectives for this project. One of my goals is to determine if any deuterated forms of CPO can be produced in the marine fungus *C. fumago* because the fungi expression system has never been studied to secrete deuterated hemoproteins. I also

want to determine whether, if successfully expressed and purified, these enzymes would be stable and their chemical properties varied from those of the corresponding wild-type chloroperoxidase. A prime motivation for producing these deuterated enzymes is to obtain more or a complete set of unambiguous heme proton resonance assignments using the low-spin, CN-ligated forms. Another purpose of this research is to assign the protons of important amino acids in the distal and proximal region of heme active center.

To make complete heme proton assignments, special [dCPO(heme)] was produced using 90% of deuterated growth medium with excess heme precursors and [dCPO(Phe)] was grown in the same highly deuterated medium that had been supplemented with excess natural phenylalanine. NMR spectroscopy was performed for high-resolution structural characterization of [dCPO(heme)] and [dCPO(Phe)] to achieve unambiguous and complete heme proton assignments, which also allowed important amino acids close to the heme active center to be assesed.

4.2 Materials and Methods

4.2.1 Materials

My sample of *Caldariomyces fumago* was purchased from American Type Culture Collection (ATCC, Manassas, VA). De-ionized water for all the experiments was prepared freshly by Milli-Q Biocel (Millipore, Billerica, MA). Deuterium oxide was purchased from Cambridge Isotope Laboratories (Andover, MA). Besides, all chemicals and reagents were purchased from either Sigma-Aldrich, St. Louis, MO or Fisher Scientific, Pittsburg, PA.

4.2.2 Expression of deuterated CPO in *C. fumago*

The *C. fumago* cells from ATCC were grown on the Potato Dextrose Agar (PDA) plates for a week at 25 degrees Celsius. The clones from the plates were transferred into 50 mL of fructose peptone salts (FPS) culturing media with 100 mg/L antibiotic carbenicillin. The Omni TH115 homogenizer was used to separate the mycelium for 30 secs with 10 secs interval. After culturing at 250 rpm and 21.5 °C for 7 days, the mycelium was homogenized again and centrifuged at 3000 rpm for 10 minutes. The fungi were then exported to the deuterated medium and were grown in different solutions prepared with 25%, 50% and 70% of D_2O to produce deuterated CPO (dCPO). Deuterated CPO, supplemented with excess native heme precursor [dCPO(heme)] and phenylalanine (at natural hydrogen isotope abundance) [dCPO(Phe)], were grown in 1 L baffled culture flasks containing 90% of deuterated oxide for additional 4 weeks at 21.5 degrees Celsius. The yield of dCPO was examined daily by the MCD assay until the reaction rate reached the maxium level. Then the culturing medium was collected via filtering through Mirocloth and ready for purification steps.

4.2.3 Purification of dCPO

Acetone precipitation, ion exchange and gel filtration chromatography were used to purify the deuterated protein after the collection of the crude media. The supernatant of culturing medium was precipitated in 25% of acetone to exclude the pigment and sugar, followed by the second 75% of acetone precipitation to collect the deuterated protein. About 100 mL of samples were collected by dissolving the precipitate into 50 mM potassium phosphate buffer at pH 5.9 and dialyzed for 24 hrs with at least one buffer exchange. For protein purification, DEAE Sepharose fast flow column (Amersham, 2.6 ×

20 cm) and Sephadex G-75 column (Amersham, 2.6 × 100 cm) were applied. Ion exchange chromatography was used to separate the desired protein from others by ionic strength gradient difference (0-0.5 M NaCl) in 50 mM potassium phosphate buffer at pH 5.9. All these experiments were carried out at 4 ºC to keep the mutant protein stable. Reinheitzahl (Rz) value was employed to examine the purity of enzymes and those of which higher than 0.9 was collected and condensed by using Centriprep-YM30 (Amincon) for further kinetic study. The yield of dCPO was 20 mg/L with Rz value 1.2 for 70%. The total yield of 90% dCPO (heme) was 10 mg/L with Rz value 0.9. The yield of purified 90% dCPO (Phe) was 10 mg/L with Rz value 1.1.

4.2.4 Sample preparation for NMR study

Protein samples for proton NMR experiments were concentrated to 0.5 mM by using Millipore Centricon YM30 filter in 95% of H_2O, 5% of D_2O or D_2O buffer solutions containing 50 mM potassium phosphate at pH 5.9. Samples were prepared by isotope exchange for at least five times. The cyanide adducts of the protein were prepared by the addition of excess cyanide from a freshly made 1 M stock solution in 99.9% of D_2O buffer.

4.2.5 NMR Spectroscopy

The NMR experiments were conducted with a Bruker Avance 600 spectrometer (Ultrashield) at the proton frequency of 600-MHz at room temperature. Observed proton chemical shifts were referred to the residual HDO peak at 4.76 ppm at 25 °C to match the previous NMR studies. The 1D proton NMR spectra of the high-spin ferric deuterated enzyme was studied at 125 kHz spectral width, 16k data points and 15 per sec repetition rate. To receive the better results on the basis of the property of high-spin heme, about

20k to 60k scans were collected. To prepare the low-spin cyanide complex, about 10 mM freshly made KCN was added into the high-spin protein sample. The proton NMR experiment of the low-spin ferric deuterated enzyme was carried out at 62.5 kHz spectral width, 4k data points and 0.2 per sec repetition rate. For the fast relaxing broad proton signals, 125 kHz spectral width, 2k data points and 10 ms repetition rate was also employed.

The relaxation time (T_1) of the hyperfine shifted protein in the deuterated samples was determined by investigating the inversion-recovery pulse sequence. Normally a 90° pulse of 7.54 μs with 3.2 per sec repetition rate was used. T_1 value was calculated from the null point (τ) by using the equation $T_1 = \tau/\ln 2$.

The NOESY and COSY two dimentional NMR spectra of deuterated CPO cyanide complex were collected at 600-MHz spectrometer 25 degrees Celsius. A single 90° pulse was used to get the maximum of the bandwidth. In the F1 dimension, 256 experiments with 400 scans were recorded. In the F2 dimension, 80 ppm spectral width, 5 per sec repetition rate, 10 ms mixing time, 2000 experiments with 4k data points was collected. The parameters of COSY experiments were very similar to NOESY.

4.3 Results

4.3.1 Gel electrophoresis of 70% dCPO

Gel electrophoresis was a widely used method to estimate the molecular weight of the polypeptides and proteins. Wild-type CPO contained about 2000 non-exchangeable protons, which could be replaced by the deuterium atoms in the deuterated form of chloroperoxidase. Wild-type CPO was a heavily glycosylated enzyme with 18% of sugar content and contained two isomers, which showed two close bands in gel electrophoresis

(Fig 4.1). The deuterated CPO had much less glycosylation and isomerization compared to Wt CPO on the basis of the infertile culturing enviroment. Therefore the SDS-PAGE result showed that the molecular weight of 70% deuterated CPO was very similar to that of Wt CPO and there was essentially no weak band for the isomers.
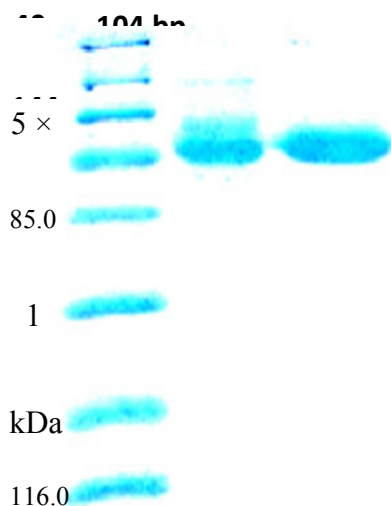
Fig 4.1 The 15% SDS-PAGE result for Wt CPO and dCPO. Lane 1 was the protein marker. Lane 2 was purified Wt CPO protein sample. Lane 3 was purified 70% of dCPO sample.

4.3.2 UV-Visible spectra of 70% dCPO and CO binding complex

The UV-Visible Soret absorption spectra of the heme proteins could convey significant information about the structure and the coordination state of the active sites (Nakajima 1985). The equilibrium absorption spectra of the ferric species of the deuterated CPO were measured in 50 mM phosphate buffer at pH 5.9 (Fig 4.2). The Wt CPO had strong Soret absorption bands in the 398 nm spectral region that arised from π-π^* electronic transitions. The minor peaks of Wt CPO were located at 515, 539, and 650 nm. Compared to that, the major peak of dCPO, shown in red, was shifted to 406 nm, and its minor peaks were also shifted to 515, 540 and 650 nm. These minor shifts may be

caused by replacement of H with D at the backbone of the enzyme. On the basis of the little shift of the Soret peak, it was concluded that deuteration did not cause large effects at the active center.
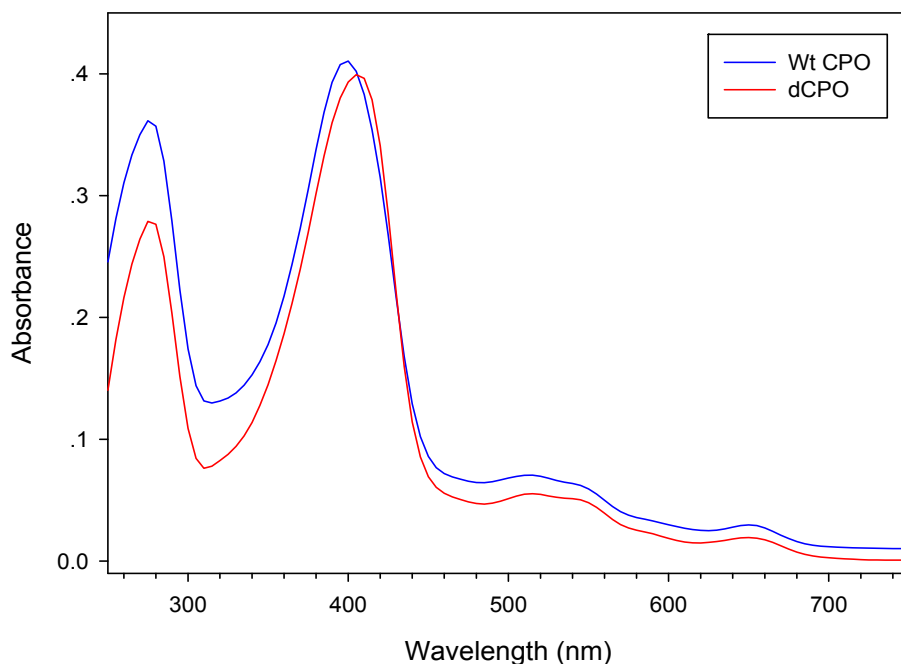
Fig 4.2 Absorption spectra of the purified Wt CPO and dCPO in 50 mM potassium phosphate buffer at pH 5.9.

4.3.3 UV-Vis spectroscopic study of dCPO-CO binding complex

The binding of dCPO with CO was also detected using UV-Vis spectroscopy. The carbon monoxide binding method was a classic assay for cytochrome P450s (Lewis 1996; Auclair 2001). The CO adducts of thiolate-ligated system showed a well-known absorption band near 450 nm, while for the histidine-ligated systems, that band was blue-shifted to 420 nm. In Wt CPO, the formation of the ferrous-CO state completely shifted the major peak from 398 to 445 nm. After reducing the central iron of dCPO from ferric

to CO bound ferrous form, the major peak was partially shifted from 404 nm to 442 nm, which indicated that the proximal ligand in the deuterated CPO was a cysteine (Fig 4.3).
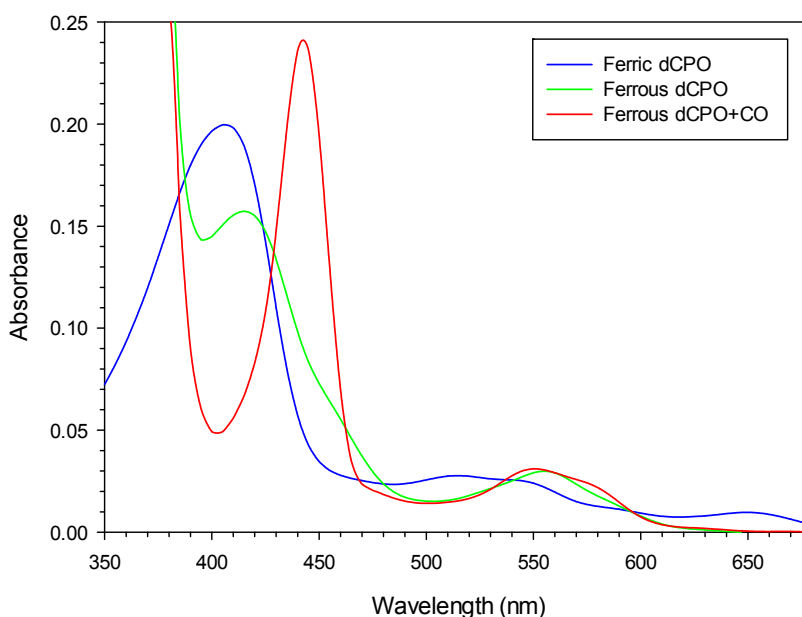
Fig 4.3 UV-Visible spectra of the ferrous-CO complex of Wt CPO and dCPO in 50 mM potassium phosphate buffer at pH=5.9.

4.3.4 Cyanide binding properties of 70% dCPO

The strong binding ligand cyanide was widely used to evaluate the affinity of CPO for a sixth axial ligand. The UV-Vis spectra of the binding complex were obtained. Cyanide had the ability to convert the high-spin iron state to the low-spin form, therefore the binding of cyanide to CPO resulted in the shift of the Soret peak. In Wt CPO, the Soret peak was shifted from 398 to 439 nanometers. Compared with that, the spectral change in 70% dCPO, which occurred upon addition of cyanide, was that the Soret peak was also shifted to 439 nanometers. The spectra of the cyanide binding complexes confirmed that the environment of the heme active center did not change during the deuteration.
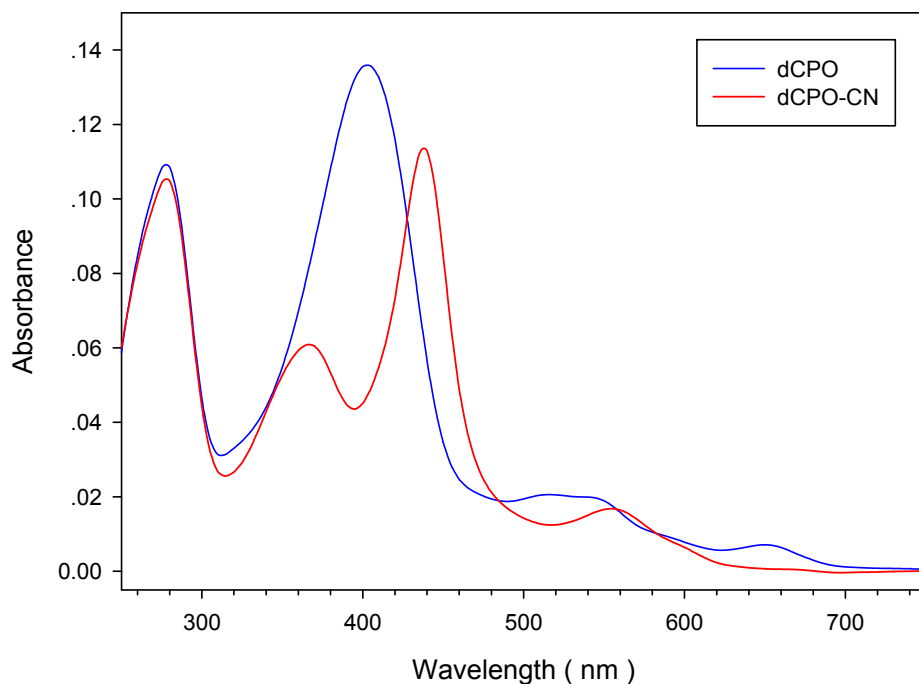
Fig 4.4 UV-Visible spectra of the cyanide complexes with dCPO in 50 mM potassium cyanide alkaline solution.

4.3.5 ^{1}H NMR spectra of 70% dCPO and Wt CPO cyanide complex

The proton NMR experiment of the native ferric high-spin dCPO was carried out using 600-MHz NMR spectrometer. Because of the high-spin nature of dCPO, considerably broad resonances were observed in the NMR spectra that provided only limited information about the structural properties of the enzyme. Therefore I focused on the NMR spectral properties of the cyanide-bound, ferric low-spin derivative of deuterated chloroperoxidase. The cyanide-bound deuterated CPO could provide much more information about the electronic, magnetic, and molecular structural properties of the heme pocket as compared to the native, high-spin resting forms.
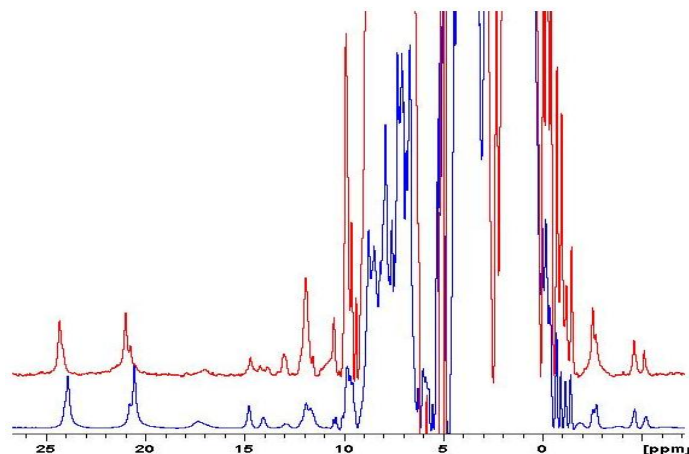
Fig 4.5 600-MHz ^{1}H NMR spectra of the low-spin cyanide complexes of 70% dCPO (lower trace) and Wt CPO (top trace) in 95% H_2O. The spectrum was collected at 298 K in 50 mM phosphate buffer at pH 5.9.

The spectral features of the dCPO-CN complex displayed a high degree of similarity to that of the Wt CPO-CN complex. The two intense signals with the integrated intensities of three protons each in the downfield region were typical of heme methyl groups. They have been assigned to the two heme methyls (8- and 3-CH$_3$). Other resonances with intensities of one proton each in the downfield region represented protons from other heme substitutes and those from amino acid residues in the proximal and distal heme pocket (Wang, Tachikawa et al. 2003). The dCPO-CN complex gave a much weaker intensity of proton signals on ^{1}H NMR spectra than that of the native CPO-CN complex. In Fig 4.5, two spectra were plotted at vertical expansions so that the tallest resonances of heme methyl groups have the identical heights. The similarity in these spectra emphasized that the essentially identical nature of the heme active site and reinforced the concept of structurally and functionally intact active site for the deuterated enzymes.

4.3.6 ^{2}H NMR spectra of 70% dCPO-CN complex

66.2
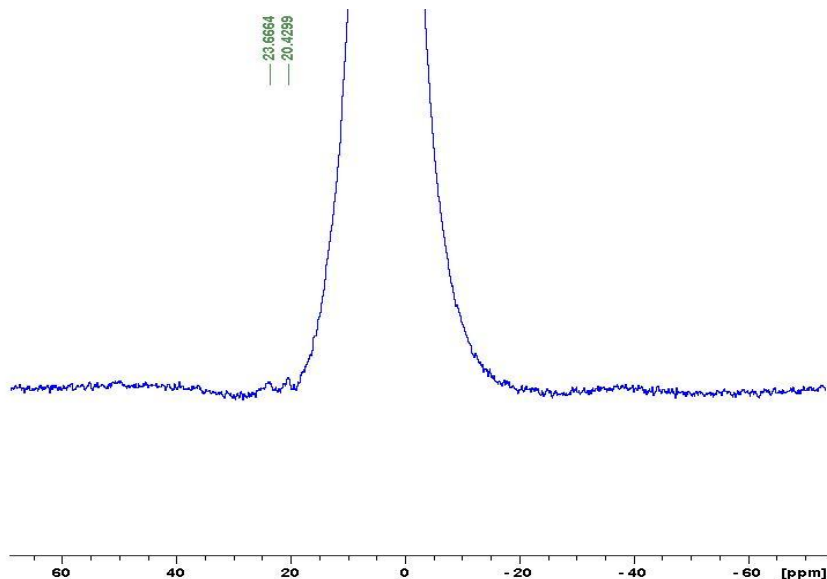
Fig 4.6 600-MHz ^{2}H NMR spectra of the low-spin cyanide complexes of 70% dCPO in 95% H_2O. The spectrum is collected at 298 K in 50 mM phosphate buffer at pH 5.9.

Deuterium NMR has a range of chemical shift similar to proton NMR but with poor resolution. It can be used to verify the effectiveness of deuteration. In Fig 4.6, we could find the two weak peaks at 23.6 ppm and 20.4 ppm, which had been assigned to 8-CH$_3$ and 3-CH$_3$ on the heme, respectively. The increased peak intensity indicated the successful replacement of the backbone protons by deuterium atoms.

4.3.7 ^{1}H NOESY spectra of 70% dCPO-CN

The NOESY spectrum of dCPO-CN collected in the D_2O buffer with a mixing time of 35 ms was shown in Fig 4.7. The peaks in the marked area were identical and confirmed with the NOESY spectra of nCPO-CN. However, there were half of peaks missing from the dCPO-CN spectra, compared to those of nCPO-CN. It was reasonable

because most protons on the backbone of the polypeptide chains had been replaced by deuterium atoms. Therefore, the signals became weak, even invisible in the deuterated spectra.
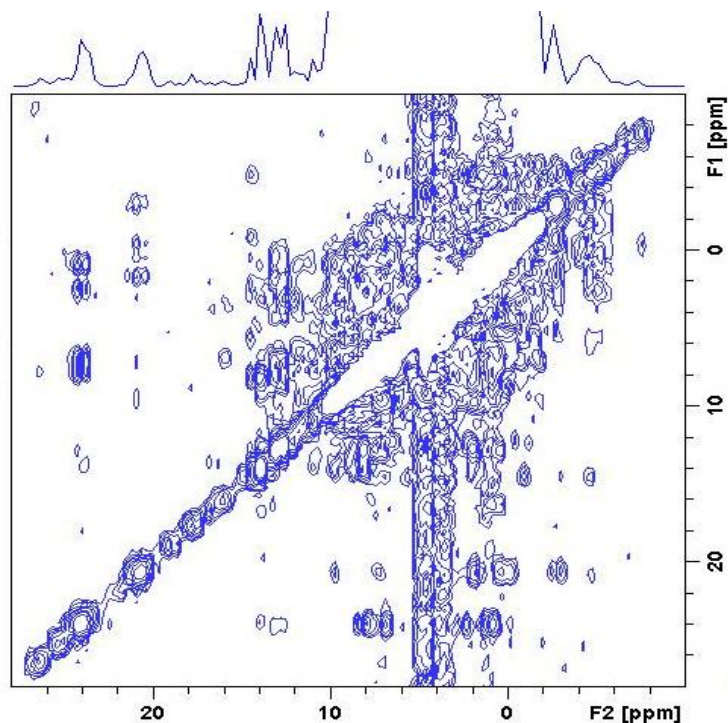
Fig 4.7 600-MHz ^{1}H NOESY spectrum of 0.5 mM 70% dCPO-CN in 95% H_2O taken with a mixing time of 35 ms.

The deuterated forms of CPO could be produced in marine fungus *C. fumago* with reasonable yield and deuteration did not significantly alter CPO's reactivity or ^{1}H NMR spectral pattern. Relatively high deuteration has been achieved by examining the ^{2}H and NOESY NMR spectra. As an example of potential NMR uses, dCPO containing selected amino acid with natural hydrogen isotope abundance could be used to achieve complete stereospecific ^{1}H resonance assignments for hyperfine-shifted protons of the heme or amino acids close to the heme center.

4.3.8 ^{1}H NMR spectra of 90% dCPO (heme)-CN and nCPO-CN
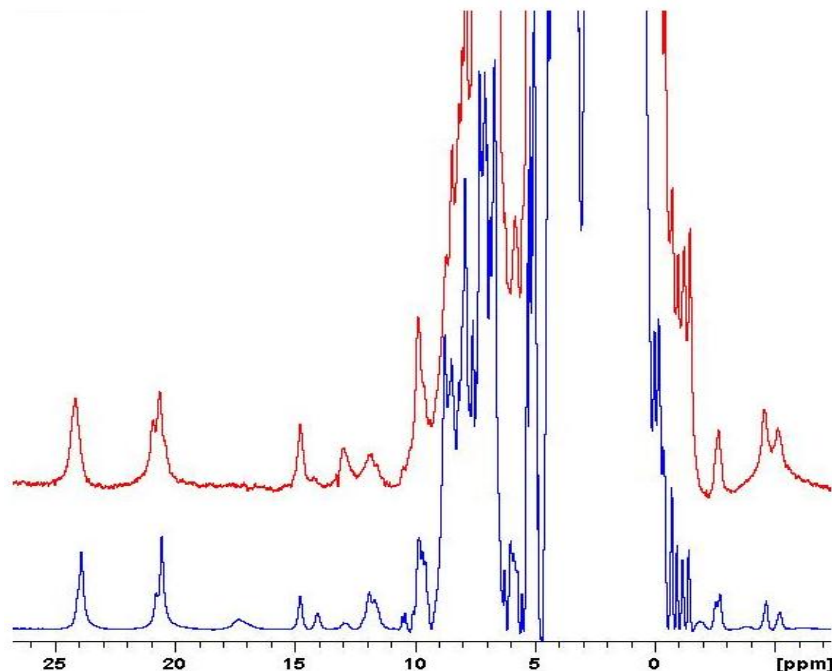
Fig 4.8 600-MHz ^{1}H NMR spectra of the low-spin cyanide complexes of 90% dCPO (heme) (top trace) and nCPO (lower trace) in D_2O. The spectra were collected at 298 K in 50 mM phosphate buffer at pH 5.9.

Comparison of ^{1}H NMR spectra of dCPO-CN and dCPO(heme)-CN complex was shown in Fig 4.8. The results were plotted so that in each spectrum the protein resonance of methyl group had the same intensity. Prominently reduced intensity at 14.1 ppm in dCPO(heme)-CN was the resonance previously assigned to the proton of 7-Hα. The missing resonance at 17.4 ppm had not been assigned yet, but it was definitely not from the heme. Since the T_1 value of this resonance was only 6 ms, it may be assigned to the proton of a certain amino acid, which was in close distance to the heme iron.

4.3.9 NOE connectivity between several resonances

The assignment of the hyperfine shifted signals for the dCPO(heme)-CN complex was examined through one dimensional NOE measurement. In Fig 4.9, the NOE
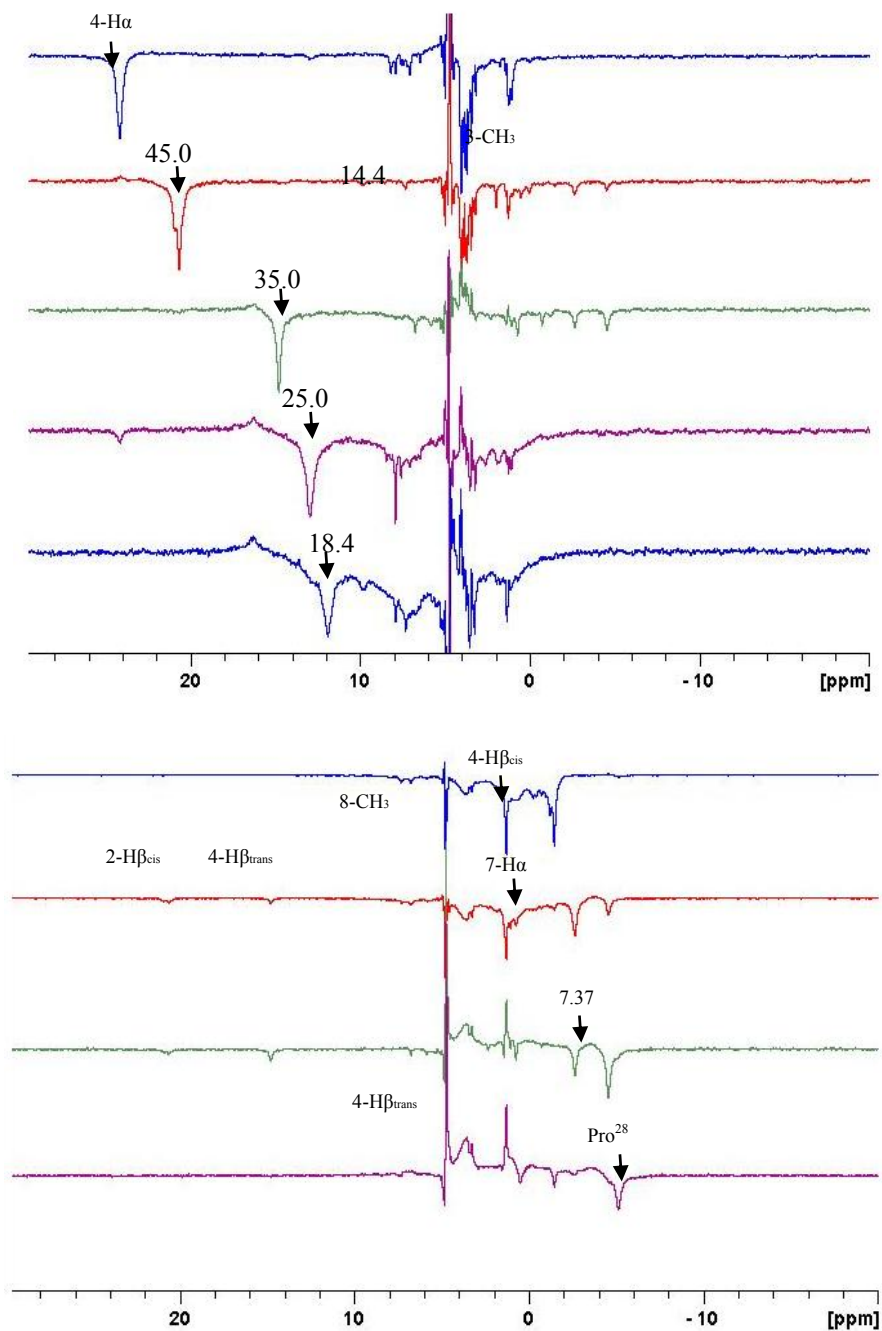
Fig 4.9 600-MHz ^{1}H NMR saturation transfer difference spectra of 90% dCPO (heme)-CN generated by subtracting the reference spectrum. Arrows indicate position of pulses.

connectivities proved the validity of the previous NOE assignment (Wang, Tachikawa et al. 2003). The heme methyl resonance at 24.0 ppm showed the weak NOEs to the peak at 11.6 ppm. The other set of the heme methyl signals at 20.4 ppm produced an extremely weak NOE to the resonance at 7.37 ppm and the weak NOEs to signals at -2.7 ppm and -4.4 ppm. The last two signals were assigned to 4-Hβ_{trans} and 4-Hβ_{cis}, respectively. However, resonances of 3-CH$_3$, 4-Hβ_{trans} and 4-Hβ_{cis} showed the weak NOEs to the peak at 7.37 ppm, which had not been assigned before.

4.3.10 Assignment of the proton with the shift at 17.4 ppm

As mentioned before, the peak with the chemical shift of 17.4 ppm had not been assigned yet. On the basis of the results of the ^{1}H NMR spectra, we could conclude that this resonance was definitely not from the heme protons. Since the T_1 value of this resonance was only 6 ms, it may be assigned to the proton of certain amino acid, which was very close to the heme iron. Fig 4.10 showed all the amino acids in the distance of 5 Å to the heme iron.

Even though the 10-0 ppm region in the 1D ^{1}H spectrum of the nCPO-CN complex seemed overlapped, resolution of deuterated sample was much higher by using heme at the natural isotope abandance, which could lead to the unambiguous connectivities and assignments. The NOE results of the deuterated sample gave more information in the diamagnetic region compared to those of the native CPO-CN complex. Since resonances of 3-CH$_3$, 4-Hβ_{trans} and 4-Hβ_{cis} all gave weak NOEs to the peak at 7.37 ppm, this resonance could probably be assigned to a proton from a nearby amino acid since no protons except 4-Hα proton from the heme can give such a NOE pattern. The unambiguous and complete heme proton assignment was very important because it could

lead to hyperfine resonance assignments of the active site amino acids, and provided the necessary basis for expanding the solution studies of the active site dynamics.
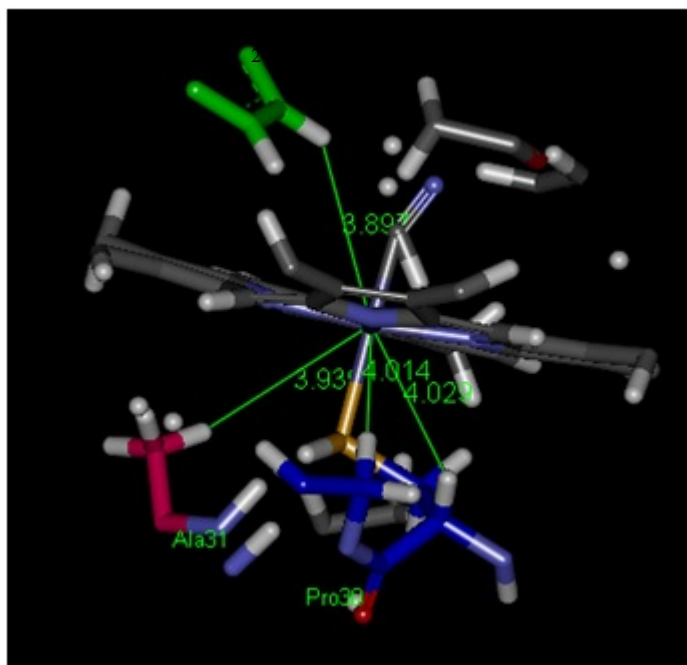
Fig 4.10 Structure of amino acids around the heme and the distance to the central iron are shown (PDB: 1CPO).

4.3.11 UV-Vis spectra of nCPO, 70% dCPO and 90% dCPO (Phe)

The characteristic Soret absorption bands can convey significant information about the active site structure and the coordination state of heme-containding proteins. Fig 4.11 displayed the equilibrium absorption spectra of the ferric species of the native CPO, deuterated CPO and deuterated CPO with a native phenylalanine. The native CPO has strong Soret absorption bands at 398 nanometers. The minor peaks were located at 515, 539, and 650 nanometers. Compared to those of nCPO, we find that there were only minor Soret peak shifts in the spectra of dCPO and dCPO(Phe), and the minor peaks exhibited the same pattern.
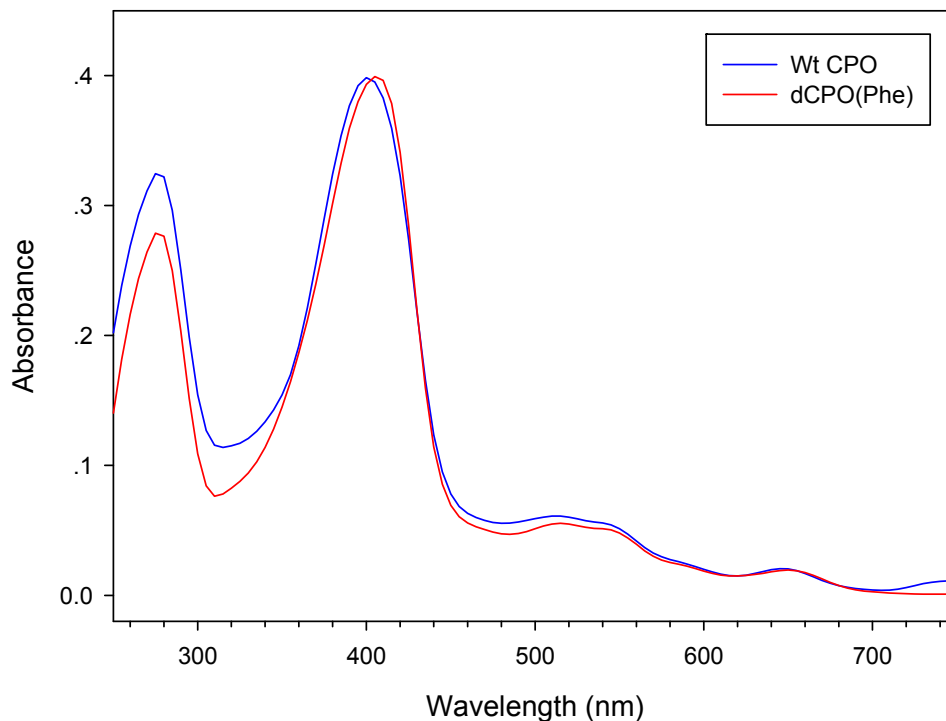
Fig 4.11 Absorption spectra of the purified Wt CPO and dCPO(Phe) in 50 mM potassium phosphate buffer at pH 5.9.

4.3.12 ^{1}H NMR spectra of 90% dCPO(Phe) and Wt CPO

The comparison of ^{1}H NMR spectra of the dCPO-CN and dCPO(Phe)-CN complex was shown in Fig 4.12. The results were plotted so that in each spectrum the protein resonance of methyl groups had the same height. Compared with the nCPO-CN complex, the peak intensities at 11.9 ppm, 10.5 ppm and 9.9 ppm increased remarkably. Since the deuterated CPO was cultured with the excess of Phe at natural hydrogen isotope abundance, the increased peak signals should derive from the Phe 57, Phe 103 and Phe 186 residues, which were close to the heme iron.
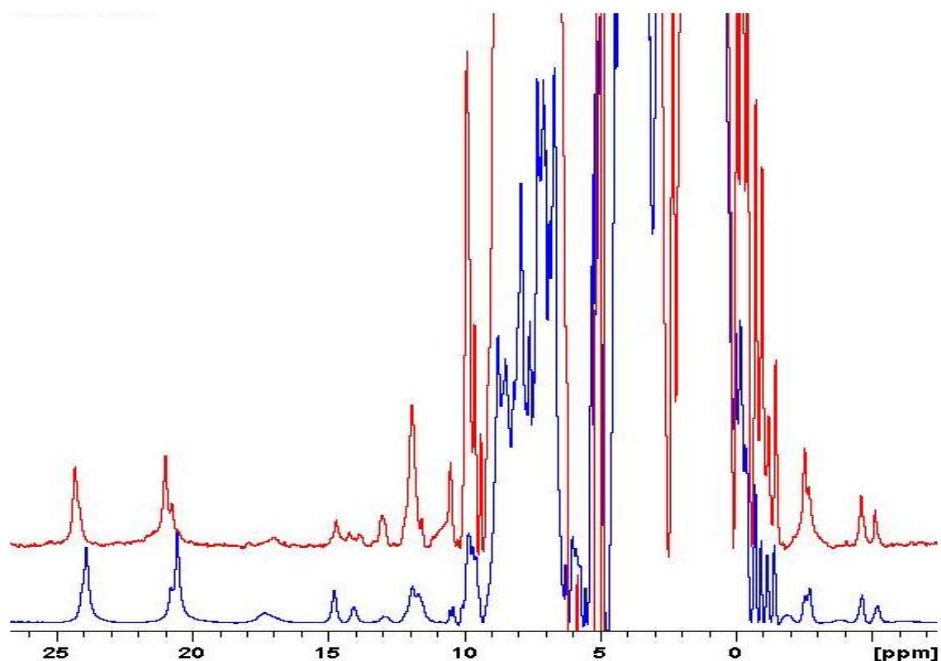
Fig 4.12 600-MHz ^{1}H NMR spectra of the low-spin cyanide complexes of 90% dCPO(Phe) (top trace) and Wt CPO (lower trace) in D_2O. The spectra were collected at 298 K in 50 mM phosphate buffer at pH 5.9.

4.3.13 T_1 measurement

Peak	Shift (ppm)	Estimated T_1 (ms)	Reported T_1 (ms)
A	24.3	30	34
B	21.0	30	32
C	14.7	25	29
D	13.0	30	35
E	11.9	3	n/a
F	10.5	>100	n/a
G	9.9	12	n/a
H	-1.4	30	n/a
I	-2.5	70	70
J	-4.6	80	80
K	-5.1	60	58

Table 4.1 Proton NMR parameters and assignments of paramagnetically shifted resonances in dCPO(Phe)-CN at 298 K, in 50 mM phosphate buffer, pH 5.9.

The chemical shifts and the corresponding T_1 values predicted from T1ir1d programmed experiment were compiled in Table 4.1, along with the reported T_1 data. The resonances I was interested in, located at 11.9 ppm and 9.9 ppm, had not been assigned yet and their T_1 values were not reported before. On the basis of this information, the distance from these two protons to the heme iron could be predicted to complete the proton assignments.

4.3.14 NOE connectivity of dCPO(Phe)-CN
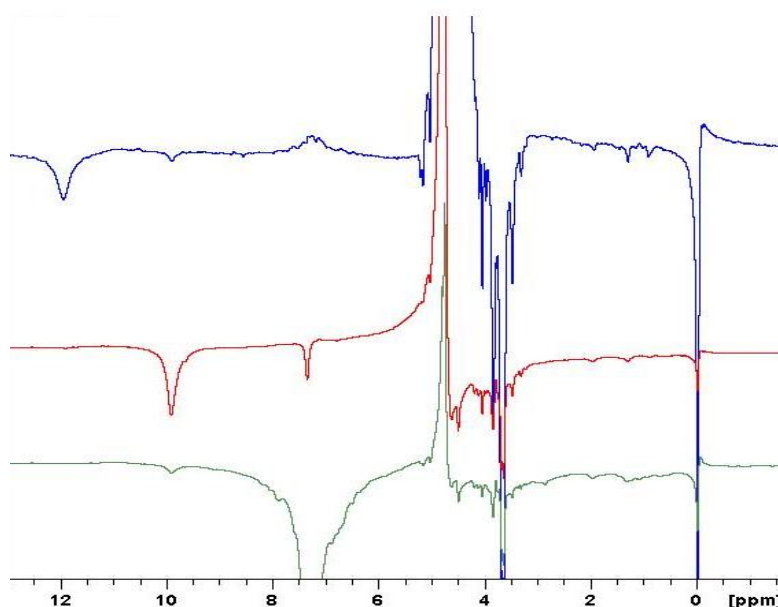
Fig 4.13 600-MHz ^{1}H NMR saturation transfer difference spectra of 90% dCPO(Phe)-CN generated by subtracting the reference spectrum.

The chemical shifts and the corresponding T_1 values predicted from T1ir1d experiment were compiled in Table 4.1, along with the reported T_1 data. The resonances we are interested in, shifts at 11.9 ppm and 9.9 ppm, were not assigned yet and their T_1 values were not reported before. On the basis of this information, we could predict the distance from these two protons to the heme iron and then complete the assignments.

4.3.15 ^{1}H NOESY and COSY spectra of 90% dCPO(Phe)-CN
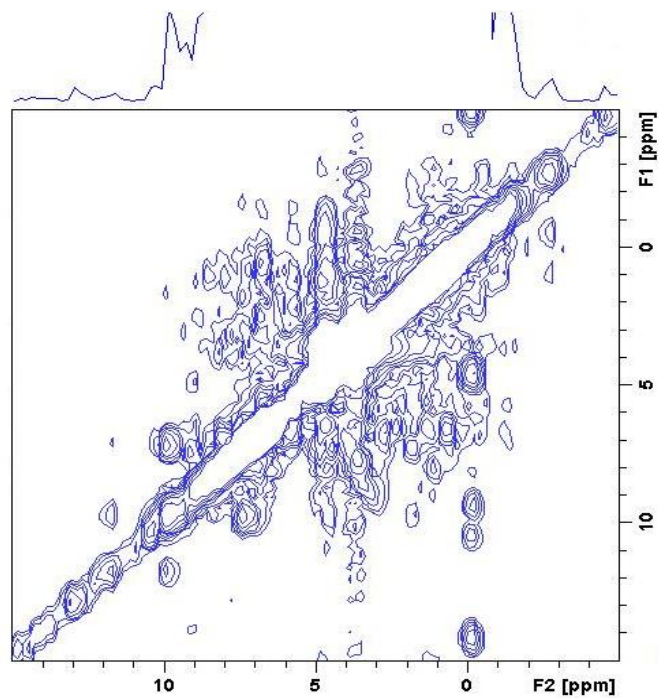
Fig 4.14 600-MHz phase-sensitive ^{1}H spectrum of 0.5mM 90% dCPO(Phe)-CN in 50 mM phosphate buffer, pH 5.9.
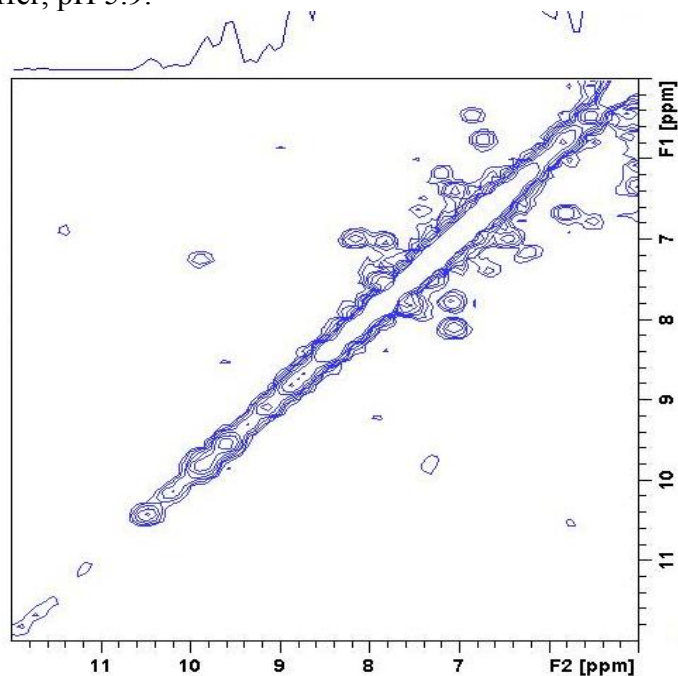
Fig 4.15 600-MHz phase-sensitive ^{1}H COSY spectrum of 0.5 mM 90% dCPO(Phe)-CN in 50 mM phosphate buffer, pH 5.9.

The clear NOESY connectivities and the results from COSY proved the validity of previous NOE resonances observed in one-dimensional NOE experiments and led to the proposed assignments for three nonexchangeable hyperfine shifted protons from the Phe groups in dCPO(Phe)-CN complex. The correlation between 9.9 ppm and 7.2 ppm in the COSY spectra indicated that these resonances were from the same Phe group and the shift at 11.9 ppm belonged to another phenylalanine residue.

4.3.16 Proton assignments of Phe 186 and Phe 103

In CPO's genome, there are 18 Phe. Among them, Phe 57, Phe 103 and Phe 186 are in the close distance to the heme active center. However, Phe 57 is located in the proximal side of heme and does not have the correlation with any other Phe groups, so it could not give the NOESY and COSY spectra as mentioned above. Fig 4.16 showed the locations of Phe 103 and Phe 186. They were close enough to have the NOE effects and both were near the heme center to obtain the chemical shifts inproton NMR spectra.
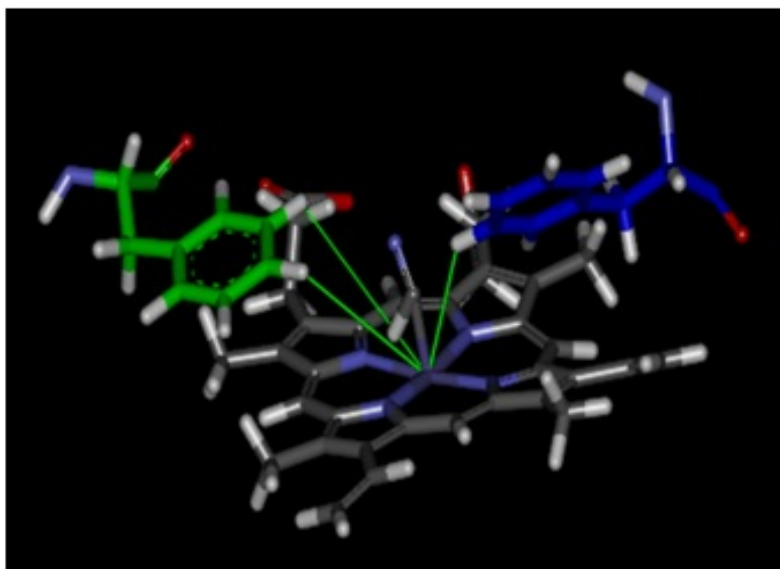
Fig 4.16 Structure of the heme distal pocket in chloroperoxidase showing the position of Phe 186, Phe 103.

Table 4.2 showed the predicted distances that were obtained from the T_1 values for the selected protons according to the relationship $r_i/r_j = [T_{1i}/T_{1j}]^{1/6}$ (Thanabal, De Ropp et al. 1987). The average distance (6.05 Å) of the three protons of the heme 8-CH_3 group to the iron was used as a reference for the predictions. The actual distance of the proton in question to the heme iron was determined from the crystal coordinates of chloroperoxidase (Sundaramoorthy, Terner et al. 1995). Therefore, we could assign the shift at 11.9 ppm to Phe 186 and shifts at 9.9 ppm, 7.2 ppm to phenylalanine 103.

Peak	Shift	T_1	Predicted r	X-ray r	Identity
	ppm	*ms*	Å		
E	11.9	3	4.0	3.9	Hε,Phe[186]
G	9.9	12	5.1	5.1	Hε,Phe[103]
L	7.2	n/a	n/a	5.0	Hδ,Phe[103]

Table 4.2 Distances between the heme iron and the protons of Phe 186 and Phe 103.

4.4 Discussion

Most of the heme protons in CPO have been assigned and the results are consistent with x-ray diffraction studies of the crystal form (Wang 2003). The NOE patterns of dCPO(Phe) are consistent with the results reported before from one dimensional study. The heme methyl resonances at 24.0 and 23.8 ppm give weak NOEs to peaks at 14.1, 12.9 and 11.6 ppm and therefore can be assigned to the 5- or 8-CH_3 group of the two isozymes of CPO. The signals at 20.7 and 20.4 ppm give weak NOEs to resonance at 14.8, -2.7 and -4.4 ppm, and therefore can be assigned to a nearby methyl group of the two isozymes. Since incorporation of natural proton abundance Phe did not change the composition of heme active center, this result is also in perfect agreement with the results obtained from analysis of the Wt CPO structure.

From the 1D proton NMR spectra of dCPO(Phe), apparent increased peak intensity at 11.9, 9.9 and 7.2 ppm indicated that they were from the protons of the Phe amino acids close to the heme iron. By the incorporation of Phe at natural hydrogen isotope abundance, we could assign the protons of Phe 103 and Phe 186 in the distal region of the heme active center. On the basis of the relationship between the $T1$ values of the inequivalent protons in noncoordinating groups and their distances to the paramagnetic center, it was assumed that heme methyl protons had an average distance of 6.1 Å from the heme iron. Therefore, it was reasonable, in the absence of the crystal coordinates of CPO, to assign these signals to the heme mesoprotons, because they were the only remaining protons close enough to the heme iron to experience the sufficient paramagnetic relaxation. In this way, two unknown NMR signals at 9.9 ppm and 7.2 ppm had been successfully assigned to the protons of the Phe 103 residue. The shift at 11.9 ppm was misassigned to CH_2 of Pro 28 in the previous NMR studies. On the basis of the peak intensity and predicted distance, it was considered to be Hε of Phe 186.

The importance of this research is that it is the first time to culture the deuterated heme containing protein in the fungi system with selected amino acids at natural isotope abundance. These results lead to the first unambiguous assignments for most of the hyperfine-shifted resonances of the ferric low-spin dCPO-CN$^-$ complexes. Further studies can be carried out to locate the NMR properties of other important amino acid residues. This can be achieved by replacing these residues with other amino acids, selectively labeling these residues with an NMR active isotope such as ^{13}C or ^{15}N or exchanging the deuterated amino acid with natural isotope abundance.

NMR study of the deuterated heme-containing proteins is a straightforward method that can overcome existing hurdles and allows the complete heme proton assignments. Such an approach is potentially applicable to other hemoproteins.

REFERENCES

Adachi, S., Nagano, S., Ishimori, K., Watanabe, Y., Morishima, I., Egawa, T., Kitagawa, T., and Makino, R. (1993). "Roels of Proximal Ligand in Heme-Proteins - Replacement of Proximal Histidine of Human Myoglobin with Cysteine and Tyrosine by Site-Directed Mutagenesis as Models for P-450, Chloroperoxidase, and Catalase." Biochemistry 32: 241-252.

Allain, E. J., Hager, L. P., Deng, L., and Jacobsen, E. N. (1993). "Highly enantioselective epoxidation of disubstituted alkenes with hydrogen peroxide catalyzed by chloroperoxidase." J. Am. Chem. Soc., 115: 4415-4416.

Antonini, E. a. B., M. (1971). "Hemoglobin and Myoglobin in Their Reactions with Ligands." Elsevier.

Aono, S. O., K., Matsuo, T., and Nakajima, H. (1998). "Redox-controlled ligand exchange of heme in the CO-sensing transcriptional activator CooA." J. Biol. Chem. 273, 25757-25764.

Araiso, T., R. Rutter, M. M. Palcic, L. P. Hager and H. B. Dunford (1981). "Kinetic analysis of compound I formation and the catalatic activity of chloroperoxidase." Can. J. Biochem., 59(4): 233-236.

Auclair, K., Moenne-Loccoz, P., and Ortiz de Montellano, P. R. (2001). "Roles of the Proximal Heme Thiolate Ligand in Cytochrome P450cam." J. Am. Chem. Soc., 123: 4877-4885.

Banci, L., Bertini I., Pease, E. A, Tien, M. and Turano, P. (1992). "H-1-Nmr Investigation of Manganese Peroxidase from Phanerochaete-Chrysosporium - a Comparison with Other Peroxidases." Biochemistry, 31(41): 10009-10017.

Bertini, I., Gray, H. B., Lippard, S. J., and Valentine, J. S. (1994). Bioinorganic Chemistry Univ. Sci. Books.

Boddupalli, S. S., Hasemann, C. A., Ravichandran, K. G., Lu, J. Y., Goldsmith, E. J., Deisenhofer, J., and Peterson, J. A. (1992). "Crystallization and preliminary x-ray diffraction analysis of P450terp and the hemoprotein domain of P450BM-3, enzymes belonging to two distinct classes of the cytochrome P450 superfamily." Proc. Natl. Acad. Sci. USA, 89(12): 5567-5571.

Boffi, A. C., E.; Peterson, E. S.; Wang, J.; Rousseau, D. L.; Friedman, J. M. (1997). "Dynamics of cyanide binding to ferrous Scapharca inaequivalvis homodimeric hemoglobin." Biochemistry, 36, 4510.

Bredt, D. S. H., P.M.; Glatt, C.E.; Lowenstein, O.; Reed, R.R.; and Snyder, S.H. (1991). "Cloned and expressed nitric oxide synthase structurally resembles cytochrome P-450 reductase." Nature, 351, 714-718.

Brown, F. S. a. L. P. H. (1967). "Chloroperoxidase.IV. Evidence for an ionic electrophilic substitution mechanism J. Am. Chem. Soc., 89(3): 719-720.

Capdevila, J., Estabrook, R.W., and Prough, R.A. (1980). "Differences in the mechanism of NADPH and cumene hydroperoxide-supported reactions of cytochrome P-450." Arch. Biochem. Biophys., 200, 186-195.

Casella, L., M. Gullotti, R. Ghezzi, S. Poli, T. Beringhelli, S. Colonna and G. Carrea (1992). "Mechanism of enantioselective oxygenation of sulfides catalyzed by chloroperoxidase and horseradish peroxidase.Spectral studies and characterization of enzyme-substrate complexes." Biochemistry 31(39): 9451-9459.

Casella, L., S. Poli, M. Gullotti, C. Selvaggini, T. Beringhelli and A. Marchesini (1994). "The chloroperoxidase-catalyzed oxidation of phenols.Mechanism, selectivity, and characterization of enzyme-substrate complexes." Biochemistry 33(21): 6377-6386.

Chakraborty, B. N., N. A. Patterson and M. Kapoor (1991). "An electroporation-based system for high-efficiency transformation of germinated conidia of filamentous fungi." Can. J. Microbiol. 37(11): 858-863.

Champion, P. M., Munck, E., Debrunner, P. G., Hollenberg P. F., and Hager, L. P. (1973). "Mossbauer investigations of chloroperoxidase and its halide complexes." Biochemistry 12(3): 426-435.

Choudhury, K., Sundaramoorthy, M., Hickman, A., Yonetani, T., Woehl, E., Dunn, and a. P. M. F., T. L. (1994). "Role of the Proximal Ligand in Peroxidase Catalysis." J. Biol. Chem. 269: 20239-20249.

Cirino, P. C., and Arnold, F. H. (2002). "Regioselectivity and activity of cytochrome P450 BM-3 and mutant F87A in reactions driven by hydrogen peroxide." Adv. Synth. Catal. 344: 932-937.

Conesa, A., van den Hondel, C. A. and Punt, P. J. (2000). "Studies on the production of fungal peroxidases in *Aspergillus niger*." Appl. Environ. Microbiol. 66(7): 3016-3023.

Conesa, A., Weelink, G., van den Hondel, C. A. and Punt, P. J. (2001). "C-terminal propeptide of the *Caldariomyces fumago* chloroperoxidase: an intramolecular chaperone?" FEBS Lett. 503(2): 117-120.

Conesa, A., van De Velde, F., van Rantwijk, F., Sheldon, R. A., van Den Hondel, C. A. and Punt, P. J. (2001). "Expression of the *Caldariomyces fumago* chloroperoxidase in Aspergillus niger and characterization of the recombinant enzyme." J. Biol. Chem. 276(21): 17635-17640.

Conesa, A., Punt, P. J., van Luijk, N., and van den Hondel, C. A. (2001). "The secretion pathway in filamentous fungi: a biotechnological view." Fungal. Genet. Biol. 33(3): 155-171.

Conesa, A., Jeenes, D., Archer, D. B., van den Hondel, C. A., and Punt, P. J. (2002). "Calnexin overexpression increases manganese peroxidase production in *Aspergillus niger*." Appl. Environ. Microbiol. 68(2): 846-851.

Conesa, A., Punt P. J., and van den Hondel, C. A. (2002). "Fungal peroxidases: molecular aspects and applications." J. Biotechnol. 93(2): 143-158.

Corbett, M. D., Chipko B. R., and Batchelor, A. O. (1980). "The action of chloride peroxidase on 4-chloroaniline.N-oxidation and ring halogenation." Biochem. J. 187(3): 893-903.

Cramer, S. P., Dawson, J. H., Hodgson, K. O., and Hager, L. P. (1978). "Studies of the ferric forms of cytochrome P-450 and chloroperoxidase by extended x-ray absotption fine structure. Characterization of the iron-nitrogen and iron-sulfur distances." J. Am. Chem. Soc. 100: 7282-7290.

Daboussi, M. J., Djeballi, A., Gerlinger, C., Blaiseau, P. L., Bouvier, I., Cassan, M., Lebrun, M. H., Parisot, D., and Brygoo, Y. (1989). "Transformation of seven species of filamentous fungi using the nitrate reductase gene of *Aspergillus nidulans*." Curr. Genet. 15(6): 453-456.

Dantas, G. K., Callender, D., Wong, M. and Baker, D. (2003). "A Large Scale Test of Computational Protein Design: Folding and Stability of Nine Completely Redesigned Globular Proteins." J. Mol. Biol. 332(2): 449.

Dawson, J. (1976). "Chloroperoxidase. Evidence for P-450 type heme environment from magnetic circular dichroism spectroscopy." J. Am. Chem. Soc. 98: 3709-3710.

Dawson, J. H., Andersson, L. A. and M. Sono (1982). "Spectroscopic investigations of ferric cytochrome P-450-CAM ligand complexes. Identification of the ligand trans to cysteinate in the native enzyme." J. Biol. Chem. 257(7): 3606-3617.

Dawson, J. H., and Sono, M. (1987). "Cytochrome P-450 and Chloroperoxidase: Thiolate-Ligated Heme Enzymes. Spectroscopic Determination of Their Active Site Structures and Mechanistic Implications of Thiolate Ligation." Chem. Rev. 87: 1255-1276.

Dawson, J. H. (1988). "Probing structure-function relations in hemecontaining oxygenases and preoxidases." Science 240: 433-439.

Debrunner, P., Dexter, A., Schulz, C., Xia, Y.-M., and Hager, L. P. (1996). "Mossbauer and electron paramagnetic resonance studies of chloroperoxidase following mechanism-based inactivation with allylbenzene." Proc. Nati. Acad. Sci. 93: 12791-12798.

Denisov, I. G., Makris, T. M., Sligar, S. G., and Schlichting, I. (2005). "Structure and chemistry of cytochrome P450." Chem. Rev.105: 2253-2277.

Denisov, I. G., Dawson, J. H., Hager, L. P. and Sligar, S. G. (2007). "The ferric-hydroperoxo complex of chloroperoxidase." Biochem. Biophys. Res. Commun. 363(4): 954-958.

Dexter, A. F., Lakner, F. J., Campbell, R. A., and Hager, L. P. (1995). "Highly Enantioselective Epoxidation of 1,1-Disubstituted Alkenes Catalyzed by Chloroperoxidase." J. Am. Chem. Soc. 117: 6412-6413.

Doerge, D. R. (1986). "Oxygenation of organosulfur compounds by peroxidases: evidence of an electron transfer mechanism for lactoperoxidase." Arch. Biochem. Biophys. 244(2): 678-685.

Dolla, A., Florens, L., Bianco, P., Haladjian, J., Voordouw, G., Forest, E., Wall, J., Guerlesquin, F., and Bruschi, M. (1994). "Characterization and oxidoreduction properties of cytochrome c3 after heme axial ligand replacements." J. Biol. Chem. 269(9): 6340-6346.

Dugad, L. B., Wang, X., Wang, C. C., Lukat, G. S., and Goff, H. M. (1992). "Proton nuclear Overhauser effect study of the heme active site structure of chloroperoxidase." Biochemistry 31: 1651-1655.

Dunford, H. B., Lambeir, A. M., Kashem, M. A. and Pickard M. (1987). "On the mechanism of chlorination by chloroperoxidase." Arch. Biochem. Biophys. 252(1): 292-302.

Erman, J. E., Vitello, L. B., Miller, M. A., Shaw, A., Brown, K. A., and Kraut, J. (1993). "Histidine-52 is A Critical Residue for Rapid Formation of Cytochrome-c Peroxidase Compound-I." Biochemistry 32: 9798-9806.

Fang, G. H., Kenigsberg, P., Axley, M. J. , Nuell, M. and Hager, L. P. (1986). "Cloning and sequencing of chloroperoxidase cDNA." Nucleic Acids Res. 14(20): 8061-8071.

Finzel, B. C., Poulos, T. L., and Kraut, J. (1984). "Crystal structure of yeast cytochrome c peroxidase refined at 1.7-A resolution." J. Biol. Chem. 259: 13027-13036.

Foshay, M. C., Vitello, L.B., and Erman, J.E. (2009). "Relocation of the Distal Histidine in Cytochrome c Peroxidase: Properties of CcP(W51H), CcP(W51H/H52W), and CcP(W51H/H52L)." Biochemistry 48: 5417-5425.

Frandsen, T. P., Dupont, C., Lehmbeck, J., Stoffer, B., Sierks, M. R., Honzatko R. B. and Svensson B. (1994). "Site-directed mutagenesis of the catalytic base glutamic acid 400 in glucoamylase from *Aspergillus niger* and of tyrosine 48 and glutamine 401, both hydrogen-bonded to the gamma-carboxylate group of glutamic acid 400." Biochemistry 33(46): 13808-13816.

Frew, J. E. a. P. J. (1984). "Structure and functional properties of peroxidases and catalases." Adv.Inorg.Bio.inorg. 3: 175-212.

G L Kedderis, D. R. K. a. P. F. H. (1980). "N-Demethylation reactions catalyzed by chloroperoxidase." J. Biol. Chem. 255: 10174-10182.

Gajhede, M., Schuller, D. J., Henriksen, A., Smith, A. T., and Poulos, T. L. (1997). "Crystal Structure of Horseradish Peroxidase C at 2.15 Å Resolution." Nat. Struct. Biol. 4: 1032-1038.

Gebicka, L. a. J. D. (2007). "Kinetic studies of the reaction of heme-thiolate enzyme chloroperoxidase with peroxynitrite." J. Inorg. Biochem. 101(1): 159-164.

Geigert, J., Lee, T. D., Dalietos, D. J., Hirano, D. S. and Neidleman S. L.(1986). "Epoxidation of alkenes by chloroperoxidase catalysis." Biochem. Biophys. Res. Commun. 136(2): 778-782.

Gordon, C. L., Khalaj, V., Ram, A. F., Archer, D. B., Brookman, J. L., Trinci, A. P., Jeenes, D. J., Doonan, J. H., Wells, B., Punt, P. J. and van den Hondel, C. A. (2000). "Glucoamylase green fluorescent protein fusions to monitor protein secretion in *Aspergillus niger*." Microbiol. 146(2): 415-426.

Gouka, R. J., Punt, P. J., Hessing J. G., and van den Hondel, C. A. (1996). "Analysis of heterologous protein production in defined recombinant *Aspergillus awamori* strains." Appl. Environ. Microbiol. 62(6): 1951-1957.

Gouka, R. J., Punt, P. J. and van den Hondel, C. A.(1997). "Efficient production of secreted proteins by *Aspergillus*: progress, limitations and prospects." Appl. Microbiol. Biotechnol. 47(1): 1-11.

Green, M. T., Dawson, J. H. and Gray, H. B. (2004). "Oxoiron(IV) in chloroperoxidase compound II is basic: implications for P450 chemistry." Science 304(5677): 1653-1656.

Guengerich, F. P. (1991). "Reactions and Significance of Cytochrome P-450 Enzymes." J. Biol. Chem. 266: 10019-10022.

Hager, L. P., Morris, D. R., Brown, F. S. and Eberwein, H. (1966). "Chloroperoxidase.II. Utilization of halogen anions." J. Biol. Chem. 241(8): 1769-1777.

Hager, L. P., Doubek, D. L., Silverstein, R. M., Hargis, J. H. and Martin, J. C. (1972). "Chloroperoxidase.IX. The structure of compound I." J. Am. Chem. Soc. 94(12): 4364-4366.

Hager, L. P., Lakner, F. J., and Basavapathruni, A. (1998). "Chiral synthons via chloroperoxidase catalysis." J. Mol. Cat. B: Enzymatic 5: 95-101.

Hallenberg, P. F. a. L. P. H. (1978). "Purification of chloroperoxidase from Caldariomyces fumago." Meth. Enzymol. 52: 521-529.

Hanegraaf, P. P., Punt, P. J., van den Hondel, C. A., Dekker, J., Yap, W., van Verseveld, H. W. and Stouthamer, A. H. (1991). "Construction and physiological characterization of glyceraldehyde-3-phosphate dehydrogenase overproducing transformants of *Aspergillus nidulans*." Appl. Microbiol. Biotechnol. 34(6): 765-771.

Hasemann, C. A., Kurumbail, R.G., Boddupalli, S.S., Peterson, J.A. and Deisenhofer, J. (1995). "Structure and function of cytochromes P450: a comparative analysis of three crystal structures." Structure 3: 41-62.

Hewson, W. D. a. L. P. H. (1979). "OXIDATION OF HORSERADISH-PEROXIDASE COMPOUND-II TO COMPOUND-I " J. Biol. Chem. 254(9): 3182-3186.

Hildebrand, D. P., Ferrer, J., Tang, H., Smith, M. and Mauk, A. (1995). "Trans Effects on Cysteine Ligation in the Proximal His93Cys Variant of Horse Heart Myoglobin." Biochemistry 34(36): 11598–11605.

Hofrichter, M. a. R. U. (2006). "Heme-thiolate haloperoxidases: versatile biocatalysts with biotechnological and environmental significance." Appl. Microbiol. Biotechnol. 71(3): 276-288.

Hollenberg, P. F. a. L. P. H. (1973). "The P-450 nature of the carbon monoxide complex of ferrous chloroperoxidase." J. Biol. Chem. 248(7): 2630-2633.

Horner, O., Mouesca, J. M., Solari, P. L., Orio, M., Oddou, J. L., Bonville, P. and Jouve, H. M. (2007). "Spectroscopic description of an unusual protonated ferryl species in the catalase from Proteus mirabilis and density functional theory calculations on related models. Consequences for the ferryl protonation state in catalase, peroxidase and chloroperoxidase." J. Biol. Inorg. Chem. 12(4): 509-525.

Horváth, C. P. B. A. a. L. S. R. (1967). "Fast liquid chromatography. Investigation of operating parameters and the separation of nucleotides on pellicular ion exchangers." Anal. Chem. 39(12): 1422–1428.

Howes, B. D., RodriguezLopez, J. N., Smith, A. T., and Smulevich, G. (1997). "Mutation of distal residues of horseradish peroxidase: Influence on substrate binding and cavity properties." Biochemistry 36: 1532-1543.

Hu, S. H., Hager, L.P. (1999). "Asymmetric epoxidation of functionalized cisolefins catalyzed by chloroperoxidase." Tetrahedron. Lett. 40: 1641-1644.

Hu, S. H., Hager, L.P. (1999). "Highly enantioselective propargylic hydroxylations catalyzed by chloroperoxidase." J. Am. Chem. Soc. 121: 872-873.

Hung, L. B. P., J. F.; Shores, J. C.; Ward, E. H. (1988). "Theoretical and experimental foundation for surface-coverage programming in gas-solid chromatography with an adsorbable carrier gas." J. Am. Chem. Soc. 110(11): 1090-1091.

Igarawshi, J. S., A.; Kitagawa, T.; Yoshimura,T.; Yamauchi,S.; Sagami, I.; Shimizu, T. (2004). "Activation of heme-regulated eukaryotic initiation factor 2 alpha kinase by nitric oxide is induced by the formation of a five-coordinated NO-heme complex." J. Biol. Chem. 279: 15752-15762.

Inoue, H., Hayashi, T., Huang, X. P., Lu, J. F., Athauda, S. B., Kong, K. H., Yamagata, H., Udaka, S. and Takahashi, K. (1996). "Heterologous expression and site-directed mutagenesis studies on the activation mechanism and the roles of the basic residues in the prosegment of aspergillopepsinogen I." Euro. J. biochem. / FEBS 237(3): 719-725.

Ishihara, S. M., K., Sadano, H., Kawabata, S., Gotoh, O. and Omura, T. (1990). "Molecular cloning and sequence analysis of cDNA coding for rat liver hemoprotein H-450." J. Biochemistry 108:899-902.

James, R. Carey, S. K. M., Pfister, T., Garner, D., Kim, H., Abramite, J., Wang, Z., Guo, Z. and Lu, Y. (2004). "A Site-Selective Dual Anchoring Strategy for Artificial Metalloprotein Design." J. Am. Chem. Soc. 126: 10812-10813.

Juge, N., Svensson, B. and Williamson, G. (1998). "Secretion, purification, and characterisation of barley alpha-amylase produced by heterologous gene expression in Aspergillus niger." Appl. Microbiol. Biotechnol. 49(4): 385-392.

Kedderis, G. L., Koop, D. R., Hollenberg, P. F. (1980). "N-Demethylation reactions catalyzed by chloroperoxidase." J. Biol. Chem. 255: 10174-10182.

Kedderis, G. L. a. P. F. H. (1984). "Peroxidase-catalyzed N-demethylation reactions.Substrate deuterium isotope effects." J. Biol. Chem. 259(6): 3663-3668.

Kenigsberg, P., Fang, G. H. and Hager, L. P. (1987). "Post-translational modifications of chloroperoxidase from *Caldariomyces fumago*." Arch. Biochem. Biophys. 254(2): 409-415.

Kim, S. H., Perera, R., Hager, L. P., Dawson J. H. and Hoffman B. M.(2006). "Rapid freeze-quench ENDOR study of chloroperoxidase compound I: the site of the radical." J Am Chem Soc 128(17): 5598-5599.

Kimata, Y., Shimada, H., Hirose, T., Ishimura, Y. (1995). "Role of Thr-252 in cytochrome P450cam: a study with unnatural amino acid mutagenesis." Biochem. Biophys. Res. Commun. 209: 96-102.

Kincaid, S. H. a. J. R. (1993). "Heme active-site structural characterization of chloroperoxidase by resonance Raman spectroscopy." J. Biol. Chem. 268: 6189-6193.

Kobayashi, S., M. Nakano, T. Kimura and A. P. Schaap (1987). "On the mechanism of the peroxidase-catalyzed oxygen-transfer reaction." Biochemistry 26(16): 5019-5022.

Kriechbaum, M., Heilmann, H. J., Wientjes, F. J., Hahn, M., Jany, K. D., Gassen, H. G., Sharif, F.and Alaeddinoglu, G. (1989). "Cloning and DNA sequence analysis of the glucose oxidase gene from Aspergillus niger NRRL-3." FEBS Lett. 255(1): 63-66.

Kuhnel, K., Blankenfeldt, W., Terner, J., Schlichting, I. (2006). "Crystal Structures of Chloroperoxidase with Its Bound Substrates and Complexed with Formate, Acetate, and Nitrate." J. Biol. Chem. 281: 23990-23998.

Lakner, F. J. a. L. P. H. (1996). "Chloroperoxidase as Enantioselective Epoxidation Catalyst: An Efficient Synthesis of (R)-(-)-Mevalonolactone." J. Org. Chem. 61(11): 3923-3925.

Lambeir, A.-M., Dunford, H. (1983). "Kinetics of cyanide binding to chloroperoxidase in the presence of nitrate: detection of the influence of a heme-linked acid group by shift in the appa." J. Inorg. Biochem. 19(4): 291–300.

Lechner, M. C., Ed. (1993). "Cytochrome P-450: Biochemistry, Biophysics, and Molecular Biology." John Libbey Eurotext.

Lewis, D. F. V. (1996). "Cytochromes P450: Structure, Function, and Mechanism." Taylor & Francis.

Li, H. Y., Poulos, T. L. (1994). "Structural variation in heme enzymes: a comparative analysis of peroxidase and P450 crystal structures." Structure 2: 461-464.

Libby, R. D., Thomas, J. A., Kaiser, L. W. and Hager, L. P. (1982). "Chloroperoxidase halogenation reactions. Chemical versus enzymic halogenating intermediates." J. Biol. Chem. 257(9): 5030-5037.

Libby, R. D., Rotberg, N. S., Emerson, J. T., White, T. C., Yen, G. M., Friedman, S. H., Sun, N. S. and Goldowski, R. (1989). "The chloride-activated peroxidation of catechol as a mechanistic probe of chloroperoxidase reactions.Competitive activation as evidence for a catalytic chloride binding site on compound I." J. Biol. Chem. 264(26): 15284-15292.

Libby, R. D., Shedd, A. L., Phipps, A. K., Beachy, T. M. and Gerstberger, S. M. (1992). "Defining the involvement of HOCl or Cl_2 as enzyme-generated intermediates in chloroperoxidase-catalyzed reactions." J. Biol. Chem. 267(3): 1769-1775.

Libby, R. D. a. N. S. R. (1990). "Compound I formation is a partially rate-limiting process in chloroperoxidase-catalyzed bromination reactions." J. Biol. Chem. 265(25): 14808-14811.

Lippard, S. J., and Berg, J.M. (1994). "Principles of Bioinorganic Chemistry." Univ. Sci. Books.

Liu, L., Liu, J., Qiu, R. X., Zhu, X. G., Dong, Z. Y. and Tang, G. M. (2003). "Improving heterologous gene expression in Aspergillus niger by introducing multiple copies of protein-binding sequence containing CCAAT to the promoter." Lett. Appl. Microbiol. 36(6): 358-361.

Liu, Y., Loccoz, P., Hildebrand, D., AWilks, A., Loehr, T., Mauk, A. and Montellano,P. (1999). "Replacement of the Proximal Histidine Iron Ligand by a Cysteine or Tyrosine Converts Heme Oxygenase to an Oxidase." Biochemistry 38(2): 3733–3743.

Lu, Y., Casimiro, D., Bren, K., Richards, J. and Gray, H. (1993). "Structurally engineered cytochromes with unusual ligand-binding properties: expression of Saccharomyces cerevisiae Met-80-->Ala iso-1-cytochrome c." Proc. Natl. Acad. Sci. U S A 90(24): 11456-11459.

Lu, Y., Berry, S. M., and Pfister, T. D. (2001). "Engineering novel metalloproteins: Design of metal-binding sites into native protein scaffolds." Chem. Rev. 101: 3047-3080.

Lu, Y., Yeung, N., Sieracki, N., and Marshall, N. M. (2009). "Design of functional metalloproteins." Nature 460: 855-862.

Makino, C. R., Hager, L. P. (1976). "Oxidation-reduction potential measurements on chloroperoxidase and its complexes." Biochemistry 15(21): 4748-4754.

Malatesta, F., Antonini, G., Sarti, P., and Brunori, M. (1995). "Structure and function of a molecular machine: cytochrome c oxidase." Biophys. Chem. 54: 1-33.

Mansuy, D. (1998). "The great diversity of reactions catalyzed by cytochromes P450." Comp. Biochem. Physiol. Pharmacol. Toxicol. Endocrinol. 121: 5-14.

Martinis, S. A., Blanke, S. R., Hager, L. P., Sligar, S. G., Hoa, G. H. B., Rux, J. J., and J. H. and Dawson (1996). "Probing the heme iron coordination structure of pressure-induced cytochrome P420cam." Biochemistry 35: 14530-14536.

Matsui, T., Nagano, S., Ishimori, K., Watanabe, Y., and Morishima, I. (1996). "Preparation and reactions of myoglobin mutants bearing both proximal cysteine ligand and hydrophobic distal cavity: Protein models for the active site of P-450." Biochemistry 35: 13118-13124.

Matsunaga, I., Sumimoto, T., Ayata, M., Ogura, H. (2002). "Functional modulation of a peroxygenase cytochrome P450: novel insight into the mechanisms of peroxygenase and peroxidase enzymes." FEBS. Lett. 528: 90-94.

Matsunaga, I., and Shir, Y. (2004). "Peroxide-utilizing biocatalysts: structural and functional diversity of heme-containing enzymes." Curr. Opi. Chem. Biol. 8: 127-132.

McCarthy, M. B., White, R.E. (1983). "Functional differences between peroxidase compound I and the cytochrome P-450 reactive oxygen intermediate." J. Biol. Chem. 258 (1), 258-259.

Miller, V. P., Tschirret-Guth R. A., and Montellano, P. R. (1995). "Chloroperoxidase-catalyzed benzylic hydroxylation." Arch. Biochem. Biophys. 319(2): 333-340.

Montellano, O. d., Choe, P., DePillis, G. and Catalano, C. E. (1987). "Structure-mechanism relationships in hemoproteins. Oxygenations catalyzed by chloroperoxidase and horseradish peroxidase." J. Biol. Chem. 262(24): 11641-11646.

Montellano, O. d. (1998). "Heme oxygenase mechanism: Evidence for an electrophilic, ferric peroxide species." Acc. Chem. Res. 31: 543-549.

Mooibroek, H., Kuipers, A. G., Sietsma, J. H., Punt, P. J. and Wessels, J. G. (1990). "Introduction of hygromycin B resistance into *Schizophyllum commune*: preferential methylation of donor DNA." Mol. Gen. Genet. 222(1): 41-48.

Moore, G. R., and GW, P. (1990). "Cytochromes c: Evolutionary, structural and physicochemical aspects." Springer-Verlag, Berlin Heidelberg, New York.

Morris, D. R. a. L. P. H. (1966). "Chloroperoxidase.I. Isolation and properties of the crystalline glycoprotein." J. Biol. Chem. 241(8): 1763-1768.

Nakajima, R., Yamazaki, I. and Griffin, B. W. (1985). "Spectra of chloroperoxidase compounds II and III." Biochem. Biophys. Res. Commun. 128(1): 1-6.

Newcomb, M., Zhang, R., Chandrasena, R. E. P., Halgrimson, J. A., Horner, J. H., Makris, T. M., and Sligar, S. G. (2006). "Cytochrome P450 Compound I." J. Am. Chem. Soc. 128: 4580-4581.

Newmyer, S. L. a. O. d. M., P.R. (1996). "Rescue of the catalytic activity of an H42A mutant of horseradish peroxidase by exogenous imidazoles." J. Biol. Chem. 271: 14891-14896.

Ngiam, C., Jeenes, D. J., Punt, P. J., Van Den Hondel, C. A. and Archer, D. B. (2000). "Characterization of a foldase, protein disulfide isomerase A, in the protein secretory pathway of Aspergillus niger." Appl. Environ. Microbiol. 66(2): 775-782.

Omura, T. (2005). "Heme–thiolate proteins." Biochem. Biophys. Res. Commun. 338: 404-409.

Omura, T. S., H., Hasegawa, T., Yoshida,Y. and Kominami, S. (1984). "Hemoprotein H-450 identified as a form of cytochrome P-450 having an endogenous ligand at the 6th coordination position of the heme." J. Biochem. 96: 1491-1500.

Ortiz de Montellano, P. R. (2005). "Cytochrome P450: structure, mechanism, and biochemistry." Kluwer Academic/Plenum Publishers.

Osborne, R. L., Raner, G. M., Hager, L. P. and Dawson, J. H. (2006). "*C. fumago* chloroperoxidase is also a dehaloperoxidase: oxidative dehalogenation of halophenols." J. Am. Chem. Soc. 128(4): 1036-1037.

Palamakumbura, A. H., Vitello, L. B., and Erman, J. E. (1999). "Oxidation of the His-52 ->Leu Mutant of Cytochrome c Peroxidase by p-Nitroperoxybenzoic Acid: Role of the Distal Histidine in Hydroperoxide Activation." Biochemistry 38: 15653-15658.

Palcic, M. M., Rutter, R., Araiso, T., Hager, L. P. and Dunford, H. B. (1980). "Spectrum of chloroperoxidase compound I." Biochem. Biophys. Res. Commun. 94(4): 1123-1127.

Patterson, W. R., and Poulos, T. L. (1995). "Crystal structure of recombinant pea cytosolic ascorbate peroxidase." Biochemistry 34: 4331-4341.

Pelletier, I., Altenbuchner, J. and Mattes, R. (1995). "A catalytic triad is required by the non-heme haloperoxidases to perform halogenation." Biochem. Biophys. Acta. 1250(2): 149-157.

Penner-Hahn, J. E., McMurry, T. J., Renner, M., Latos-Grazynsky, L., Eble, K. S., Davis, I. M., Balch, A. L., Groves, J. T., Dawson, J. H. and Hodgson, K. O. (1983). "X-ray absorption spectroscopic studies of high valent iron porphyrins. Horseradish peroxidase compounds I and II and synthetic models." J. Biol. Chem. 258(21): 12761-12764.

Penner-Hahn, J. E., Eble, K., McMurry, T. J., Renner, M., Balch, A. L., Groves, J. T., Dawson, J. H. and Hodgson, K. O. (1986). "Structural characterization of horseradish peroxidase using EXAFS spectroscopy. Evidence for Fe=O ligation in compounds I and II." J. Am. Chem. Soc. 108(24): 7819-7825.

Perutz, M. F. (1989). "Myoglobin and haemoglobin: role of distal residues in reactions with haem ligands." Trends. Biochem. Sci. 14: 42-44.

Poulos, T. L., Freer, S. T., Alden, R. A., Edwards, S. L., Skogland, U., Takio, K., Eriksson, B., Xuong, N. H., Yonetani, T., and Kraut, J. (1980). "Crystal-Structure of Cytochrome-c Peroxidase." J. Biol. Chem. 255, 575-580.

Poulos, T. L., Finzel, B. C., Gunsalus, I. C., Wagner, G. C., and Kraut, J. (1985). "The 2.6 A crystal - structure of *Pseudomonas putida* cytochrome P450." J. Biol. Chem. 260: 6122-6130.

Poulos, T. L., Finzel, B. C., and Howard, A. J. (1987). "High-resolution crystal structure of cytochrome p450cam." J. Mol. Biol. 195: 687-700.

Poulos, T. L., Edwards, S. L., Wariishi, H., and Gold, M. G. (1993). "Crystallographic refinement of lignin peroxidase at 2 A." J. Biol. Chem. 268: 4429-4440.

Poulos, T. L. (1996). "The role of the proximal ligand in heme enzymes." J. Biol. Inorg. Chem. 1: 356-359.

Punt, P. J., Oliver, R. P., Dingemanse, M. A., Pouwels, P. H. and van den Hondel, C. A. (1987). "Transformation of *Aspergillus* based on the hygromycin B resistance marker from *Escherichia coli*." Gene 56(1): 117-124.

Punt, P. J., Veldhuisen, G. and van den Hondel, C. A. (1994). "Protein targeting and secretion in filamentous fungi.A progress report." Antonie. Van. Leeuwenhoek. 65(3): 211-216.

Punt, P. J., van Biezen, N., Conesa, A., Albers, A., Mangnus, J. and van den Hondel, C. (2002). "Filamentous fungi as cell factories for heterologous protein production." Trends. Biotechnol. 20(5): 200-206.

Qin, J., La Mar, G. N., Dou, Y., Admiraal, S.and Ikeda-Saito, M. (1994). "1H NMR study of the solution molecular and electronic structure of engineered distal myoglobin His64(E7) Val/Val68(E11) His double mutant. Coordination of His64(E11) at the sixth position in both low-spin and high-spin states." J. Biol. Chem. 269(2): 1083-1090.

Raphael, A. L. a. G., H. B. (1991). "Semisynthesis of Axial-Ligand (Position 80) Mutants of Cytochrome c." J. Am. Chem. Soc. 113: 1038-1040.

Ravichandran, K. G., Boddupalli, S. S., Hasemann, C. A., Peterson, J. A., Deisenhofer, J. (1993). "Crystal structure of hemoprotein domain of P450BM-3, a prototype for microsomal P450's." Science 261: 731-736.

Rubin, B., VanMiddlesworth, J., Thomas, K. and Hager, L. (1982). "Crystallization and preliminary X-ray data for chloroperoxidase." J. Biol. Chem. 257(13): 7768-7769.

Ruiz-Diez, B. "Strategies for the transformation of filamentous fungi." J Appl Microbiol 92(2): 189-195.

Rutter, R., Hager, L. P., Dhonau, H., Hendrich, M., Valentine, M. and Debrunner, P. (1984). "Chloroperoxidase compound I: Electron paramagnetic resonance and Mossbauer studies." Biochemistry 23(26): 6809-6816.

Satterlee, J. D., Erman, J. E., Lamar, G. N., Smith K. M., and Langry, K. C. (1983). "." 105(8): (1983). "Assignment of hyperfine-shifted resonances in low-spin forms of Cytochrome *c* peroxidase by reconstitutions with deuterated hemins." J. Am. Chem. Soc. 105(8): 2099-2104.

Satterlee, J. D., Erman, J. E., Mauro, J. M. and Kraut, J. (1990). "Comparative proton NMR analysis of wild-type Cytochrome *c* peroxidase from yeast, the recombinant enzyme from *Escherichia coli*, and an Asp-235 mutant." Biochemistry 29(37): 8797-8804.

Savenkova, M., Savenkova, J., Satterlee,J., Erman,W. and Helms, G. (2001). "Expression, purification, characterization, and NMR studies of highly deuterated recombinant cytochrome c peroxidase." Biochemistry 40: 12123-12131.

Schmid, G. G. a. M. G. (2001). "Chiral separation by chromatographic and electromigration techniques." Biopharm. Drug Dispos. 22: 291–336.

Scott, R. A., and Mauk, A. G. (1996). "Cytochrome c: A multidisciplinary approach." University Science Books.

Shahangian, S. a. L. P. H. (1981). "The reaction of chloroperoxidase with chlorite and chlorine dioxide." J. Biol. Chem. 256(12): 6034-6040.

Sigel, A., Sigel, H., and Sigel, R. K.O. (2007). "The ubiquitous roles of Cytochrome P450 proteins in Metal Ions in Life Sciences." Metal Ions in Life Sciences.

Sigman, J. A., Pond, A. E., Dawson, J. H., and Lu, Y (1999). "Engineering Cytochrome c peroxidase into Cytochrome P450: A proximal effect on hemethiolate ligation." Biochemistry 38: 11122-11129.

Silverstein, R. M. a. L. P. H. (1974). "The chloroperoxidase-catalyzed oxidation of thiols and disulfides to sulfenyl chlorides." Biochemistry 13(25): 5069-5073.

Silvestrini, M. C., Falcinelli, S., Ciabatti, I., Cutruzzolà, F., and Brunori, M. (1994). "*Pseudomonas aeruginosa* nitrite reductase (or cytochrome oxidase): An overview." Biochimie 76: 641-654.

Sligar, S., Egeberg, K., Sage, T., Morikis, D., and Champion, P. (1987). "Alteration of Heme Axial Ligands by Site Directed Mutagenesis: A Cytochrome Becomes a Catalytic Demethylase." J. Am. Chem. Soc. 109: 7896‑7897.

Snyder, L. R., Kirkland, J. J., and Dolan, J. W. (2009). " Introduction to Modern Liquid Chromatography." John Wiley & Sons, New York.

Sono, M., Dawson, J. H., Hall, K., Hager, L. P (1986). "Ligand and halide binding properties of chloroperoxidase: peroxidase-type active site heme environment with cytochrome P-450 type endogenous axial ligand and spectroscopic properties." Biochemistry 25: 347-356.

Sono, M. R., M. P., Coulter, E. D. and Dawson, J. H. (1996). "Heme-Containing Oxygenases." Chem. Rev. 96: 2841-2887.

Sorrell, T. N., Martin, P. and Bowden, F. (1989). "A novel, functional variant of cytochrome c. Replacement of the histidine ligand with arginine via site-directed mutagenesis." J. Am. Chem. Soc. 111(2): 766–767.

Spencer, A., Morozov-Roche, L. A., Noppe, W., MacKenzie, D. A., Jeenes, D. J., Joniau, M., Dobson, C. M. and Archer, D. B. (1999). "Expression, purification, and characterization of the recombinant calcium-binding equine lysozyme secreted by the filamentous fungus *Aspergillus niger*: comparisons with the production of hen and human lysozymes." Protein Expr. Purif. 16(1): 171-180.

Sriprang, R., Asano, K., Gobsuk, J., Tanapongpipat, S., Champreda, V. and Eurwilaichitr, L. (2006). "Improvement of thermostability of fungal xylanase by using site-directed mutagenesis." J. biotech. 126(4): 454-462.

Stefano C., N. G., Richelmi, L. and Pasta, P. (2000). "Recent biotechnological developments in the use of peroxidases." Tren. Biotech. 17(4): 163–168.

Stone, K. L., Behan, R. K. and Green, M. T. (2006). "Resonance Raman spectroscopy of chloroperoxidase compound II provides direct evidence for the existence of an iron(IV)-hydroxide." Proc. Natl. Acad. Sci. USA 103(33): 12307-12310.

Sun, W., Kadima, T. A., Pickard, M. A. and Dunford, H. B. (1994). "Catalase activity of chloroperoxidase and its interaction with peroxidase activity." Biochem. Cell. Biol. 72(7): 321-331.

Sundaramoorthy, M., Terner, J., and Poulos, T. L. (1995). "The crystal structure of chloroperoxidase: A heme peroxidase-cytochrome P450 functional hybrid." Structure 3(1367-1377).

Sundaramoorthy, M., Terner, J. and Poulos, T. L. (1998). "Stereochemistry of the chloroperoxidase active site: crystallographic and molecular-modeling studies." Chem. Bio. 15(9): 461-473.

Swart, K., Debets, A. J., Bos, C. J., Slakhorst, M., Holub, E. F. and Hoekstra, R. F. (2001). "Genetic analysis in the asexual fungus *Aspergillus niger*." Acta. Biol. Hung. 52(2): 335-343.

Tanaka, M., Ishimori, K., Mukai, M., Kitagawa, T. and Morishima, I. (1997). "Catalytic activities and structural properties of horseradish peroxidase distal His42->Glu or Gln mutant." Biochemistry 36: 9889-9898.

Terner, J., Palaniappan, V., Gold, A., Weiss, R., Fitzgerald, M. M., Sullivan, A. M. and Hosten, C. M. (2006). "Resonance Raman spectroscopy of oxoiron(IV) porphyrin pi-cation radical and oxoiron(IV) hemes in peroxidase intermediates." J. Inorg. Biochem. 100(4): 480-501.

Thanabal, V., Deropp, J. S. and Lamar, G. N. (1987)."." 109(24): (1987). "Identification of the Catalytically Important Amino-Acid Residue Resonances in Ferric Low-Spin Horseradish-Peroxidase with Nuclear Overhauser Effect Measurements." J. Am. Chem. Soc. 109(24): 7516-7525.

Thomas, J. A., Morris, D. R. and Hager, L. P. (1970). "Chloroperoxidase.8. Formation of peroxide and halide complexes and their relation to the mechanism of the halogenation reaction." J. Biol. Chem. 245(12): 3135-3142.

Thomas, J. A., Morris, D. R. and Hager, L. P. (1970). "Chloroperoxidase.VII. Classical peroxidatic, catalatic, and halogenating forms of the enzyme." J. Biol. Chem. 245(12): 3129-3134.

Thomas, J. A. a. L. P. H. (1968). "The peroxidation of molecular iodine to iodate by chloroperoxidase." Biochem. Biophys. Res. Commun. 32(5): 770-775.

Turnbull, I. F., Smith, D. R., Sharp, P. J., Cobon, G. S. and Hynes, M. J. (1990). "Expression and secretion in *Aspergillus nidulans* and *Aspergillus niger* of a cell surface glycoprotein from the cattle tick, Boophilus microplus, by using the fungal amdS promoter system." Appl. Environ. Microbiol. 56(9): 2847-2852.

Udit, A. K., and Gray, H. B. (2005). "Electrochemistry of heme-thiolate proteins." Biochem.Biophys. Res. Commun. 338: 470-476.

Verdoes, J. C., Punt, P. J., Schrickx, J. M., van Verseveld, H. W., Stouthamer, A. H. and van den Hondel, C. A. (1993). "Glucoamylase overexpression in *Aspergillus niger*: molecular genetic analysis of strains containing multiple copies of the glaA gene." Transgenic. Res. 2(2): 84-92.

Verdoes, J. C., van Diepeningen, A. D., Punt, P. J., Debets, A. J., Stouthamer A. H. and van den Hondel, C. A. (1994). "Evaluation of molecular and genetic approaches to generate glucoamylase overproducing strains of *Aspergillus niger*." J. Biotechnol. 36(2): 165-175.

Vetter, S. W., Terentis, A. C., Osborne, R. L., Dawson, J. H., and Goodin, D. B. (2009). "Replacement of the axial histidine heme ligand with cysteine in nitrophorin 1: spectroscopic and crystallographic characterization,." J. Biol. Inorg. Chem. 14: 179-191.

Visser, J., Bussink, H. J. and Witteveen, C. (1995). "Gene expression in filamentous fungi.Expression of pectinases and glucose oxidase in *Aspergillus niger*." Bioprocess Technol. 22: 241-308.

Voigt, C. A. K. S., and Wang, Z. G. (2001). "Rational evolutionary design: the theory of in vitro protein evolution." Adv. Pro. Chem. 55: 79-160.

Wang, W., Lu, J., Yao, P., Xie, Y., and Huang, Z. (2003). "The distinct heme coordination environments and heme-binding stabilities of His39Ser and His39Cys mutants of cytochrome b5." Pro. Engi. 16: 1047-1054.

Wang, X., Tachikawa, H., Yi, X., Manoj, K. M., and Hager, L. P. (2003). "Two dimensional NMR Study of the Heme Active Site Structure of Chloroperoxidase." J. Biol. Chem. 278: 7765-7774.

Wang, X. and. Goff. H. M.(1997). "A nuclear paramagnetic relaxation study of the interaction of the cyclopentanedione substrate with chloroperoxidase." Biochim. Biophys. Acta. 1339(1): 88-96.

Welinder, K. G. (1992). "Superfamily of plant, fungal and bacterial peroxidases." Curr. Opin. Struct. Biol. 2: 388-393.

White, K. A., Marletta, M. A. (1992). "Nitric oxide synthase is a cytochrome P-450 type hemoprotein." Biochemistry 31: 6627-6631.

Williams, R. J. P. (1987). "Missing information in bio-inorganic chemistry." Coord. Chem. Rev. 79: 175-193.

Withers, J. M., Swift, R. J., Wiebe, M. G., Robson, G. D., Punt, P. J., van den Hondel C. A. and Trinci A. P. (1998). "Optimization and stability of glucoamylase production by recombinant strains of *Aspergillus niger* in chemostat culture." Biotechnol. Bioeng. 59(4): 407-418.

Wong, L. L. (1998). "Cytochrome P450 monooxygenases." Curr. Opin. Chem. Biol. 2: 263-268.

Yamada, H., and Yamazaki, I. (1974). "Proton balance in conversions between five oxidation-reduction states of horseradish peroxidase." Arch. Biochem. Biophys. 165: 728-738.

Yi, X., Mroczko, M., Manoj, K.M., Wang, X., Hager, L.P. (1999). "Replacement of the proximal heme thiolate ligand in chloroperoxidase with a histidine residue." Proc. Natl. Acad. Sci. USA 96: 12412-12417.

Yi, X., Conesa, A., Punt, J. P., Hager, L. P. (2003). "Examining the Role of Glutamic Acid 183 in Chloroperoxidase Catalysis." J. Biol. Chem. 278: 13855-13859.

Yoshioka, S., Takahashi, S., Hori, H., Ishimori, K., and Morishima, I. (2001). "Proximal cysteine residue is essential for the enzymatic activities of cytochrome P450cam." Eur. J. Biochem. 268: 252-259.

Zaks, A., and Dodds, D. R. (1995). "Chloroperoxidase-catalyzed asymmetric oxidations: substrate specificity and mechanistic study." J. Am. Chem. Soc. 117: 10419-10424.

Zhang, R., Nagraj, N., Lansakara, P. D., Hager, L. P. and Newcomb, M. (2006). "Kinetics of two-electron oxidations by the compound I derivative of chloroperoxidase, a model for cytochrome P450 oxidants." Org. Lett. 8(13): 2731-2734.

Zhao, C. D. S., Cann, N. M. (2009). "Rational optimization of the Whelk-O1 chiral stationary phase using molecular dynamics simulations." J. Chromatogr. 1216(32): 5968-5978.

Zong, Q., Osmulski, P. A. and Hager, L. P. (1995). "High-pressure-assisted reconstitution of recombinant chloroperoxidase." Biochemistry 34(38): 12420-12425.

APPENDIX A

Figure A1 Amino acid sequence of full-length of Wt CPO.

1   XEPGSGIGYP YDNNTLPYVA PGPTDSRAPC PALNALANHG YIPHDGRAIS

51   RETLQNAFLN HMGIANSVIE LALTNAFVVC EYVTGSDCGD SLVNLTLLAE

101 PHAFEHDHSF SRKDYKQGVA NSNDFIDNRN FDAETFQTSL DVVAGKTHFD

151 YADMNEIRLQ RESLSNELDF PGWFTESKPI QNVESGFIFA LVSDFNLPDN

201 DENPLVRIDW WKYWFTNESF PYHLGWHPPS PAREIEFVTS ASSAVLAASV

251 TSTPSSLPSG   AIGPGAEAVP   LSFASTMTPF LLATNAPYYA QDPTLGPND

Figure A2 DNA sequence of full-length of Wt CPO (1122bp).

1 atgttctcca aggtccttcc cttcgtggga gcggttgccg ccctccctca ctccgtccgt

61 caggagcctg gctccggcat tggctaccca tacgacaaca acaccctgcc atatgtcgcc

121 ccaggtccta ccgactctcg tgctccttgc ccagctctga acgctcttgc caaccacggt

181 tacattcctc acgatggccg tgccatcagc agggagaccc tccagaacgc tttcctcaac

241 cacatgggta ttgccaactc cgtcattgag cttgctctga ccaacgcctt cgtcgtctgc

301 gagtacgtta ctggctccga ctgtggtgac agccttgtca acctgactct gctcgccgag

361 ccccacgctt tcgagcacga ccactccttc tcccgcaagg attacaagca gggtgtcgcc

421 aactccaacg acttcatcga acaggaac ttcgatgccg agaccttcca gacctctctg

481 gatgtcgttg caggcaagac ccacttcgac tatgccgaca tgaacgagat ccgccttcag

541 cgcgagtccc tctccaacga gcttgacttc cccggttggt tcaccgagtc caagccaatc

601 cagaacgtcg agtctggctt catcttcgcc cttgtctctg acttcaacct gcccgacaac

661 gatgagaacc ctctggttcg cattgactgg tggaagtact ggttcaccaa cgagtccttc

721 ccataccacc tcggctggca ccccccgtct ccagccaggg agatcgagtt cgtcacctcc

135

781 gcctcctccg ctgtcctggc tgcctctgtc acctctactc catcttccct tccatccggt

841 gccatcggcc caggtgccga ggctgtccct ctctccttcg cctccaccat gaccccattc

901 ctcctcgcca ccaatgctcc ttactacgcc caggacccaa ctctcggccc caacgacaag

961 cgtgaggctg ccccagctgc caccacctcc atggccgtct tcaagaaccc atacctcgag

1021 gccattggca cccaggacat caagaaccag caggcttacg tcagctccaa ggctgctgcc

1081 atggcctctg ccatggccgc caacaaggcc cgcaaccttt aa   .

Fig A3 Expression vector pCPO3.I-AmdS for co-transformation of *A. niger* strain.

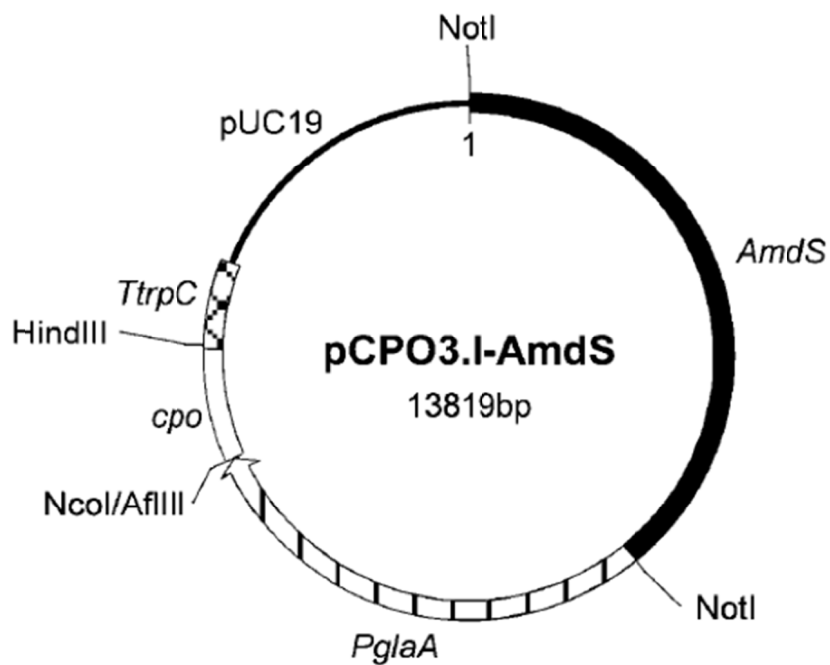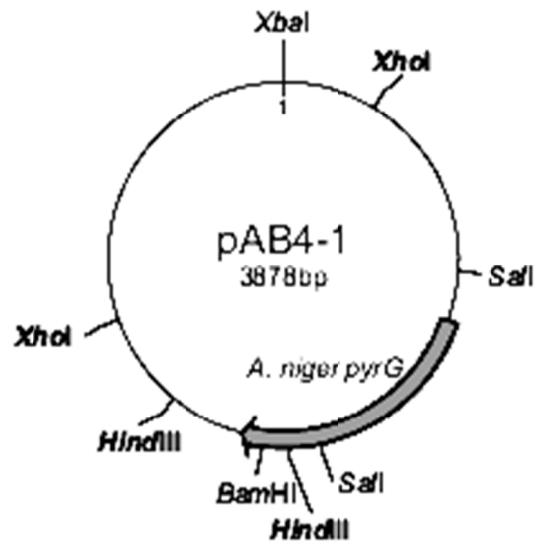**Fig A5 Assistant plasmid pAB4.1 for co-transformation of *A. niger* strain.**

VITA

LIN JIANG

Mar 28, 1983   Born, Shandong, China

2002-2006   Bachelor of Biotechnology,
                                          East China Normal University
2007-   Doctoral Candidate in Chemistry
                                          Florida International University
                                          Miami, Florida

PUBLICATIONS AND PRESENTATIONS

Lin Jiang, Hua Ling and Xiaotang Wang, "Mutation in histidine 105 residue of chloroperoxidase increases the enantioselectivity of bulky styrene derivatives". Abstracts of papers, 244th ACS national meeting, 2012, Philadelphia, PA

Lin Jiang, Zhonghua Wang and Xiaotang Wang, "Expression, purification and characterization of deuterated chloroperoxidase". Abstracts of papers, 243rd ACS national meeting, 2012, San Diego, CA

Lin Jiang, Zheng Wang and Xiaotang Wang, "Asparagine 74 is critical to substrate specificity and ligand stabilization in chloroperoxidase catalysis". Abstracts of papers, 239th ACS national meeting, 2010, San Francisco, CA

Simona Horsa, Lin Jiang, Xiaotang Wang, Jaroslava Miksovska, "Dynamics and energetics associated with ligand photodissociation from Co bound chloroperoxidase." Biophysical Journal, 2009, 96(3), 437a.